12-9-2014 12:00 AM

Poly(Ester Amide) and Poly(Ethyl Glyoxylate) Nanoparticles for Controlled Drug Release

Amira Mohamed Moustafa
The University of Western Ontario

Supervisor
Dr. Elizabeth R. Gillies
The University of Western Ontario

POLY(ESTER AMIDE) AND POLY(ETHYL GLYOXYLATE) NANOPARTICLES FOR
CONTROLLED DRUG RELEASE

(Thesis format: Integrated Article)

by

Amira **Moustafa**

Graduate Program in Chemical and Biochemical Engineering

A thesis submitted in partial fulfillment
of the requirements for the degree of
Masters of Engineering Science

The School of Graduate and Postdoctoral Studies
Western University
London, Ontario, Canada

ABSTRACT

The objective of this research was to develop polymeric nanoparticles (NPs) having improved drug release properties for drug delivery. Poly(ester amide)s (PEAs) are promising biodegradable polymers. PEA NPs were prepared via emulsification-evaporation and salting-out methods and optimized through by varying different processing parameters. Polymer-model drug conjugates based on PEAs containing L-aspartic acid and rhodamine B were synthesized and used for NP preparation. Release behavior was studied and compared to a control system with physically encapsulated rhodamine B. It was shown that the release of rhodamine B from the covalent system did not show the burst effect and exhibited a slower and more sustained profile. A novel PEA-floxuridine conjugate was also prepared and used to synthesize NPs. These NPs exhibited a small burst effect followed by slow drug release. To provide a new stimulus-responsive release mechanism, NPs based on a UV triggerable self-immolative poly(ethyl glyoxylate) PEtG were prepared. PEtG/poly(lactic acid) (PLA) blend NPs were prepared for site-specific and time-controlled drug delivery. PLA NPs were first synthesized by the emulsion-evaporation method and optimized through different experimental conditions. PEtG/PLA NPs were then prepared using the optimized conditions. In this study, letrazole was used as a model drug. These letrazole loaded NPs had a low Z-average diameter of less than 100 nm and high encapsulation efficiency. Increasing burst release was observed with increasing PLA content. Thermal characterization of PEtG/PLA NPs showed phase separation of the two polymers in the NPs. Although the UV irradiated PEtG NPs showed depolymerization upon UV irradiation, letrazole release was not accelerated. The reasons for this lack of triggered release require more investigation and optimization.

Keywords

CO-AUTHORSHIP STATEMENT

The work described in this thesis contains contributions from the author as well as coworkers from Western and supervisor Dr. Elizabeth Gillies. The exact contributions to each project are described below.

Chapter 1 was written by the author and edited by supervisor Dr. Gillies. The literature review illustrated in Chapter 2 was collected and written by the author and edited by supervisor Dr. Gillies.

The work described in Chapter 3 was a project proposed by Dr. Gillies and conducted by collaboration between the author and other members of the Gillies group. The work corresponding to the rhodamine B physically encapsulated in NPs was done by former MESc student Gregory Zilinskas. Dr. Mahmoud Moustafa assisted in the development of synthetic methods for the conjugation of floxuridine and in proof of concept studies of its release. HPLC measurements were performed with the help of the Gillies lab technician, Aneta Borecki. All other experimental work corresponding to synthesis, optimization, characterization, and release experiments was conducted by the author. A draft of a manuscript was written by the author and was edited by Dr. Gillies.

For Chapter 4, the work was a project proposed by Dr. Gillies and conducted through collaboration between the author and Bo Fan from Dr. Gillies group. Poly(ethyl glyoxylate) was synthesized and characterized by Bo Fan. The nanoparticle preparation, optimization, characterization, and release studies were done by the author. This chapter was written by the author and edited by Dr. Gillies.

Chapter 5 was written by the author and edited by supervisor Dr. Gillies.

ACKNOWLEDGMENTS

IN THE NAME OF 'ALLAH'- LORD OF THE WORLDS, THE MOST MERCIFUL AND THE MOST BENEVOLENT

DEDICATION

To my late (deceased) father, Mohamed, for his continuous support

To my mother for her inspiration

To my beloved husband, Ahmed, for his love, patience, and support

And

To my Kids, Fayrouz and Omar, for the best feeling ever they gave to me

Table of Contents

List of Tables

List of Figures

List of Abbreviations

EDC·hcl	(1-ethyl-3-(3-dimethylaminopropyl) carbodiimide)
δ	Chemical shifts
C-S-C	Core shell corona
T_{ds}	Decomposition temperatures
D_2O	Deuterated water
Dox	Doxorubicin
DDS	Drug delivery systems
DLS	Dynamic light scattering
EPR	Enhancement permeability and retention
etg	Ethyl glyoxylate
etgh	Ethyl glyoxylate hydrate
FDA	Food and Drug Administration
FTIR	Fourier transform infrared
T_g	Glass transition temperatures
GSH	Glutathione
GSSG	Glutathione disulfide
GA	Glycolic acid
GAH	Glyoxylic acid hydrate
HMDI	Hexamethylene diisocyanate
hcasmcs	Human coronary artery smooth muscle cell
LA	Lactic acid
LCST	Lower critical solution temperature
T_m	Melting temperatures
MWCO	Molecular weight cutoffs
DIPEA	*N,N*-diisopropylethylamine
DMF	*N,N*-dimethylformamide
dcc	*N,n'*-dicyclohexylcarbodiimide
NC	Nanoconjugates
nps	Nanoparticles
NVOC	Nitroveratryl carbonate

P-gp	P-glycoprotein
Ptxl	Paclitaxel
ppm	Parts per million .
PEO-*b*-ppy	PEO-*co*-polymethacrylate bearing pyrene moiety) .
PLA	poly(lactic acid)
PBS	Phosphate-buffered saline
PHB	Poly(3-hydroxybutyrate)
PDLA	Poly(*D*-lactic acid)
peas	Poly(ester amide)s
petg	Poly(ethyl glyoxylate)
PEO	Poly(ethylene oxide)
PGA	Poly(glycolic acid)
PLLA	Poly(*L*-lactic acid)
PLL	Poly(*L*-lysine)
PLGA	Poly(lactide-*co*-glycolide)
PNIPAAM	Poly(*N*-isopropyl acrylamide
PPO	Poly(propylene oxide),
PCL	Polycaprolactone
PDI	Polydispersity index
ROP	Ring-opening polyaddition
SEM	Scanning electron microscopy
SEC	Size exclusion chromatography
SC	Sodium cholate
SDS	Sodium dodecyl sulfate
SP	Spermine
TEM	Transmission electron microscopy
net$_3$	Triethylamine

Chapter 1 : Introduction

1.1 Introduction

Conventional therapeutics often have undesirable physicochemical and pharmacological properties. Their random distribution leads to side effects and the need for higher doses of the drug to achieve a satisfactory pharmacological response. Additionally, rapid renal clearance as a result of the low molecular weight of some compounds along with other factors such as protein binding, and lipophilicity, result in a requirement for frequent administration and/or a high dose to have a therapeutic effect. To address these intrinsic drawbacks, a widely used approach is to modify the existing therapeutic agents using drug delivery technologies.

Drug delivery systems are designed to improve the pharmacological activity of drugs by enhancing pharmacokinetics such as absorption, distribution, metabolism and excretion. Moreover, these systems offer advantages including their capability to encapsulate poorly soluble drugs and to offer more patient-friendly administration methods. Drug delivery systems are usually high molecular weight carriers and can be processed as nano-and microparticles, micelles, and dendrimers, in which the drug is embedded or covalently bound. Polymer-based systems, especially those composed of biodegradable polymers are amongst most extensively explored in nanosystems for drug delivery.

Nanosystems based on biodegradable polymers seek to improve the drug release profile in a predetermined and controlled manner. Since the degradation rate and the consequent drug release rate can be modulated depending on their chemical compositions, rational design of their chemical structure such as type of covalent bonds between monomers, degree of hydrophilicity, etc. is important to consider. Additionally, these controlled release systems modify the capacity to cross biological carriers, biodistribution, clearance, and stability of the drug by precise control of nanosystems formulation and evaluation of physico-chemical properties e.g. size, surface property, and shape.

1.2 Problem Statement

Many drug delivery systems (DDS) based on physical drug encapsulation have strong limitations including: 1) the poor encapsulation efficiency of hydrophilic drugs which may require the usage of high percentages of the polymeric carrier that might cause toxicity; 2)

the burst effect which results from precipitation of the drug on the outer surface of the particles and a subsequent rapid release after administration and also may cause toxicity; 3) crystallization of poorly soluble drug during preparation of the nanocarriers.

Additionally, DDS based on biodegradable polymeric nanoparticles exhibit a general temporal control over the release process, but typically lack secure encapsulation of the drug before reaching the target site as well as the ability to release the drug rapidly and specifically at the target site. Furthermore, some polymers have been shown to exhibit slow degradation rate and the difficulty to eliminate these polymers from the body after depletion of the drug resulting in several problematic side effects.

1.3 Objectives

The goal of my thesis is to overcome the above limitations and permit polymeric NPs to be used as effective drug delivery systems. Poly(ester amide)s (PEAs) were investigated for NP based DDS since theses polymers are considered as a promising family of biodegradable materials having ester and amide bonds in their backbones. The effects of several experimental valuables were investigated in order to optimize the nanoparticles in terms of their size. PEA-drug conjugates were synthesized by coupling PEAs having pendant carboxylic acid groups first to a dye molecule as a model drug and then to a hydrophilic anti cancer drug floxuridine. NPs based on PEA-floxuridine conjugates were prepared using the optimized conditions. The efficiency of these nanoparticles was investigated in terms of their coupling efficiency with the hydrophilic drug, controlled release profile, and their burst effect.

In addition, initial work was performed towards offering an appropriate NP tool for site-specific and time-controlled drug delivery. The goal of this chapter was to provide a secure encapsulation of the drug before reaching the target site and then use sensitivity towards an external stimulus to increase the release of drug after approaching the target cells or tissues. UV-responsive NPs based on poly(ethyl glyoxylate) (PEtG) and poly(lactic acid) (PLA) blends were synthesized. PEtG is UV-triggerable self-immolative polymer that undergoes end-to-end depolymerization upon UV light exposure. Several experimental parameters were optimized to obtain NP diameters of less than 100 nm. The efficiency of these nanoparticles was investigated in terms of encapsulation efficiency of the hydrophobic anti cancer drug

letrazole. Letrazole release performance was studied in the absence and presence of UV stimulus, and the degradation properties of PEtG NPs upon exposure to UV irradiation was investigated.

1.4 Thesis Organization

This thesis encompasses five chapters and conforms to the "integrated-article" format as outlined in the Thesis Regulation Guide by the School of the Graduate and Postdoctoral Studies (SGPS) of the Western University. After an introduction in the first Chapter, a comprehensive literature review including the background and a thorough assessment of the information on polymeric nanosystems for drug delivery is presented in Chapter 2. Chapter 3 investigates the covalent drug immobilization in poly(ester amide) nanoparticles for controlled drug release. In Chapter 4, nanoparticles based on poly(ethyl glyoxylate) were synthesized with the aim of providing a triggered release mechanism for drug delivery systems. Finally, Chapter 5 summarizes the major findings of this study with recommendations for continuous improvements in nanotechnology and biodegradable polymers for drug delivery.

1.5 Thesis Contributions

This research presents important contributions in the field of biodegradable polymeric NPs used as drug delivery systems to improve the pharmacokinetic and pharmacodynamic profile of therapeutics. PEAs have been investigated as potential candidates for drug delivery system. PEAs containing pedant carboxylic acid functional groups were used to prepare drug delivery NPs. By running a series of optimization scenarios, it was possible to prepare particles having Z-average diameters of less than 200 nm and reasonable polydispersities by emulsification-evaporation and salting-out methods. To investigate the potential use of these functional handles for the drug immobilization of drug molecules, the carboxylic groups in PEA backbone were conjugated to an alcohol functionalized rhodamine B derivative as a model drug via an ester linkage with a coupling efficiency of ~40% prior to nanoparticle preparation. The optimized NPs from the PEA-rhodamine B conjugate and from control NPs in which rhodamine B was physically encapsulated were prepared. Additionally, their release behaviour were compared and the results showed that the covalent conjugate afforded a much slower release than the noncovalent control suggesting that this approach is valuable

for the elimination of the burst release effect. The approach was also extended to covalent immobilization of the hydrophilic anti cancer drug floxuridine in NPs. This system also exhibited a high coupling efficiency of 60% for the hydrophilic drug, a small burst release effect of 5%, and small Z-average diameters of less than 200 nm. This small initial release was followed by a slower and sustained release.

Overall this work suggests the promise of using the optimized PEA NPs for drug delivery applications especially for passive targeting to solid tumors due to the physiological and anatomical modifications of such tissues. Additionally, PEAs provide a better tailor to synthesis polymer-drug conjugates by incorporating α-amino acids with pendant reactive handles. Covalent immobilization of the drug with PEAs achieved a satisfactory drug loading of small and hydrophilic dugs. PEA-drug conjugates were based primarily on hydrolytically unstable ester bonds between the drug and the polymer that ensure control release in a slow and sustained rate with no significant burst effect, which may lead to releasing the drug at the site of action to reduce the drug toxicity.

In order to overcome the problem of nonspecific release of drug throughout the body, which can be expected for most NP systems; in the second part of this study; stimuli responsive NPs were investigated. Drug delivery NPs based on stimuli responsive polymers were prepared using PEtG. PEtG is a new and versatile class of self-immolative linear polymer backbones. A UV cleavable end-cap provides a control and triggerable PEtG that undergoes end-to-end depolymerization upon UV exposure. This study investigated the use of PEtG/PLA blend NPs with PEtG designed to impart stimuli responsive properties to the NPs, for the release of drug to be triggered. It was possible to prepare PEtG/PLA blend NPs having Z-average diameters of less than 100 nm and reasonable polydispersities. These NPs showed good efficiencies to encapsulate the hydrophobic drug letrazole. The results suggested that the burst effect from the NPs depended on the ratio of PLA:PEtG, with more PLA leading to more burst release. NPs based on PEtG might be an appropriate tool for site-specific and time-controlled drug delivery.

Chapter 2 : Literature Review

2.1 Nanotechnology for drug delivery

Nanotechnology has been extensively used in drug delivery. The application of nanotechnology is expected to significantly influence the landscape of biotechnology and pharmaceutical industries. This term is applied to a particle within the range of 1-100 nm in at least one dimension (Farokhzad and Langer, 2009). This interest in nanomedicine is driven by the emerging success of nanoparticle (NP)-based DDS (Davis *et al.*, 2008). Numerous nanocarrier DDS have been developed from various materials, including polymers (micelles, solid nanoparticles, or dendrimers), lipids (dispersion of solid lipids, liposomes), viruses (viral NPs), and conjugated materials (nanotubes) as illustrated in Figure 2-1 (Cho *et al.*, 2008).
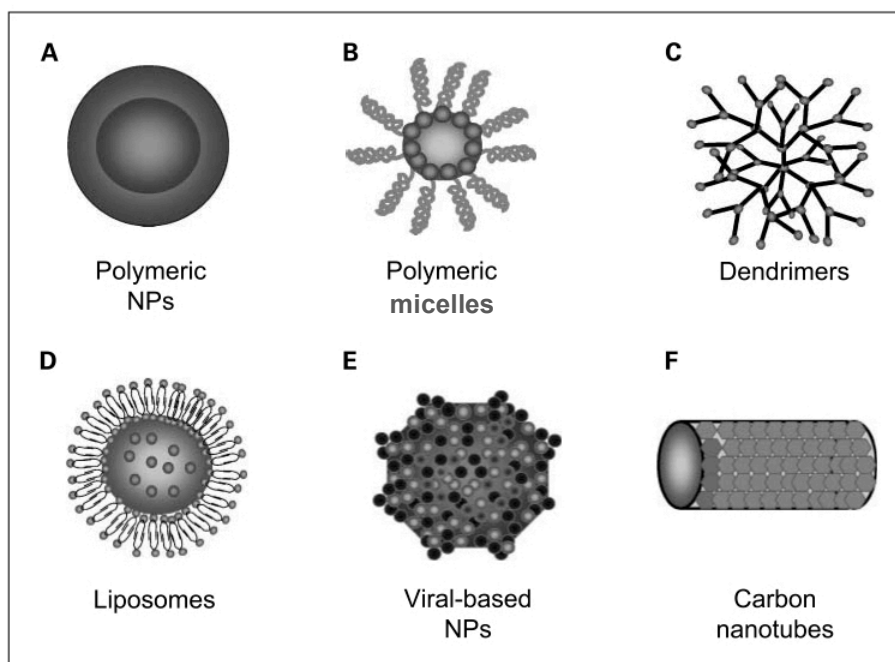
Figure 2-1: Possible nanocarriers for drug delivery. A) Solid polymeric NPs: the drug can be encapsulated or conjugated to the polymeric matrix. B) Polymeric micelles: formed from self-assembly of amphiphilic copolymers forming core shell NPs. C) Dendrimers: highly branched polymers at the nanosized range. D) Liposomes: lipid bilayer nanostructure. E) Viral based NPs: multivalent and self-assembled structures. F) Carbon nanotubes: carbon cylinders from fused benzene rings. (Reprinted with permission from Cho *et al.*, 2008)

Nanoparticle DDS display several advantages over conventional free drugs. For example, the solubility can be a limiting factor for hydrophobic drugs; however, NPs were proven to enhance the dispersibility of different hydrophobic drugs (Torchilin *et al.*, 2003). Also,

depending on the type and composition of NPs, they may be able to considerably decrease the toxicity as compared to free drug (Kim *et al.*, 2006). NPs can provide controlled and/or responsive drug release profiles. The drug can release in a controlled manner over a specific period of time, generally by diffusion (Zhang *et al.*, 2006), which can be exploited in chemotherapy that requires sustained levels of the drug in the cancerous tissue in order to kill the uncontrolled growth of cells. Additionally, several systems have been developed to trigger the drug release upon exposure to specific stimuli such as pH change, temperature, redox potential, and the presence of enzymes (Ahmed *et al.*, 2006; Tirelli, 2006; Ganta *et al.*, 2008; Xu *et al.*, 2008). This can control the release in the target tissue and reduce the toxic side effects in the healthy tissue. NPs have been reported to challenge multidrug resistance mechanisms in cancerous tissue by following a different cellular internalization pathway (Davis eta l., 2008; Dongin *et al.*, 2008). NPs provide protection for the loaded protein and other enzyme-labile molecules from proteolysis and rapid clearance (Simone *et al.*, 2007). Furthermore, owing to their high surface to volume ratio, NPs have the ability to penetrate deeper into tissues and to cross membrane barriers. They are therefore a promising platform for applications such as drug delivery and targeted cancer therapy (Bae *et al.*, 2011; Chanana 2013).

A drug delivery system is a system used to deliver the therapeutic agent to a specific site at an appropriate concentration, and to maintain therapeutic levels for a sufficient period of time. The delivery system is as important as the therapeutic moiety itself. Efforts have been invested to create an integrated system that combines nanotechnology with targeting systems, providing prophylaxis or treatment for numerous diseases. NPs are considered to be one of the most relevant technologies in terms of targeted delivery of many therapeutic agents, including small drug molecules and macromolecules, in attempt to maximize the efficiency of the drug in the target tissue and minimize the toxic side effects. Drug delivery systems, which are composed primarily of lipids and/or polymers, are designed to change and improve the pharmacological properties, such as pharmacokinetics and biodistribution, of the associated drugs.

Two targeting approaches (i.e. passive and active) have been widely applied in drug delivery systems. Passive targeting is the first and most commonly applied approach. It is based on the enhancement permeability and retention (EPR) phenomenon (Iyer *et al.*, 2006; Seki *et al.*;

2009; Fang *et al.*, 2011). In particular, cancerous tissues are characterized by irregular, leaky vascular structure, and large inter-endothelial junctions that allow nanosized systems to selectively reach these tissues. In addition, the poorly developed lymphatic system leads to increased retention of the particles in these tissues. Accordingly, NPs have the potential for significant accumulation in cancerous tissue in comparison with conventional drugs, which can diffuse easily to all tissues. Additionally, similar characteristics have been found in inflammation sites, which provide another application of NPs for diseases such as arthritis (Wang *et al.*, 2007; Liu *et al.*, 2008; Ishihara *et al.*, 2009). Passive targeting is based on the size of the carrier. Many researchers have shown that the pore size of the tumor vasculature ranges from 200 nm - 1.2 um. (Hobbs *et al.*, 1998). Theses pores vary depending on the type and location of the tumor. Thus, a generally recommended size of the NPs designed for passive delivery is less than 200 nm. However, larger particles with hydrophobic surfaces are prone to be recognized by plasma proteins and glycoproteins through process called opsonization. Afterwards, the opsonized particles are attacked by the mononuclear phagocytic system, the reticuloendothelial system. The macrophage cells in the liver (kupffer cells), spleen, and circulating macrophages are responsible for removing these particles and breaking them down (Davis, 1997).

Active targeting is the second approach used in drug delivery. It is based on the fact that the receptors are upregulated on the tumor cells and endothelial cells associated with tumor tissues, which can be chosen for the target system. Thus, specific ligands incorporated on the surfaces of NPs can bind to specific receptors in the target organs. Because the tumor receptors are generally inaccessible in blood vessels, the EPR effect also plays a significant role in receptor targeting. However, targeting groups can also facilitate cell uptake and higher intracellular drug concentrations through receptor-mediated endocytosis of nanoparticle afterwards (Oyewumi *et al.*, 2004). Additionally, vascular targeting can also be employed for therapeutic targeting systems (Schnitzer, 1998).

2.2 Biodegradable polymers for nanoparticle systems

Drug carriers are designed to act as delivery vehicles for drugs through various routes of administration and to overcome deficiencies of treatment with free drugs that lead to poor or failed therapies (Merisko-Liversidge *et al.*, 2003). Since the 1970s, polymers have been

widely developed and recognized for their potential in drug delivery applications, especially after it was demonstrated in 1976 that the release of macromolecules from biodegradable polymers in a sustained manner was possible (Langer and Kolkman, 1976). Polymers offer a long-term and progressive delivery of therapeutic agents (Sanchez *et al.*, 2003). The polymeric dosage forms offer important advantages of delivering the drugs in a sustained manner, thereby avoiding repeated drug administration. Additionally, they allow protection of encapsulated macromolecules, such as proteins and peptides, as these molecules are very sensitive to changes in pH and to enzymes (Jiao *et al.*, 2002). Polymers have emerged as a major and important class of controlled release biomedical systems owing to their ability to regulate the release profile in a predetermined, tunable, and/or responsive manner by manipulating synthesis, physico-chemical, and degradation properties using different techniques (York *et al.*, 2008; Bae and Kataoka, 2009; Dhal *et al.*, 2009). Over the past 4 decades, the technology using controlled release polymers has engaged every field in medicine including cardiology, ophthalmology, neurology, dentistry, immunology, and other fields (Farokhzad and Langer, 2006).

A number of different polymers, both natural and synthetic, have been used in the synthesis of NPs (Marty *et al.*, 1978; Moghimi *et al.*, 2001; Gradishar *et al.*, 2005). However, synthetic polymers have shown the advantage of sustained drug release over a period of days to weeks, compared to natural polymers, which often release drugs very rapidly (Nair and Laurencin, 2007; Sionkowska, 2011). There is a growing interest in controlling the consistency, shape, composition, and size of the NPs to achieve optimal therapeutic effects and to ensure the compliance of nanotechnology with future applications. Consequently, novel production methods and manufacturing techniques have been continuously developed and refined. Drug delivery systems based on polymeric NPs have to undergo development, testing, and evaluation processes in order to meet the requirements of regulatory bodies such as the US Food and Drug Administration (FDA), which is a major hurdle for NP commercialization. A suitable selection of the polymer matrix is necessary to develop a successful delivery system.

The polymers used in biomedical applications can be degradable or non-degradable. The major disadvantage of non-degradable polymers is the difficulty to eliminate these polymers from the body after depletion of the drug. However, degradable polymers undergo degradation in physiological conditions into absorbable building blocks. With these

polymers, it is crucial to ensure that the degradation products are not toxic. The most commonly used synthetic degradable polymers for controlled drug release applications are polyesters, polyanhydrides, polyethers, polyamides, polyorthoesters and polyurethanes. Depending on the method of preparation, the NPs may have the structure of capsules, amphiphilic core/shell (polymeric micelles), solid NPs, or hyperbranched macro-molecules (dendrimers). The following section focuses on PLA as an example aliphatic polyester, and poly(ester amide)s as another synthetic biodegradable polymer used for drug delivery.

2.2.1 Poly(lactic acid) (PLA)

PLA is one of the most widely used biodegradable polymers in drug delivery because it undergoes hydrolysis of the ester backbone in biological fluids into the biodegradable metabolite lactic acid, which is ultimately metabolized into CO_2 and water (Hayashi, 1994; Yang *et al.*, 2004). Protocols have been optimized to synthesize PLA NPs and to incorporate different anti-cancer drugs (Xing *et al.*, 2007), proteins (Gao *et al.*, 2005), hormones (Matsumoto *et al.*, 1999), and anti-restenosis drugs (Fishbein *et al.*, 2000). There are different factors affecting the effective response and release behavior of the PLA nanomedicines including molecular weight of the drug, the drug encapsulation method, particle size, additives to the formulation, and surface modification ((Matsumoto *et al.*, 1999; Storma *et al.*, 1995; Torchilin *et al.*, 1995; Cho *et al.*, 1997; Owens 3rd and Peppas, 2006; Lee *et al.*, 2007). There was a sharp increase in the number of patents in this field from about 90 in the early 1990s to more than 600 in last decade. This increase started with the clinical success and commercialization of Lupron Depot, the first parenteral sustained-release formulation using PLA, which was approved in 1989 (Chaubal, 2002*)*. PLA is a hydrophobic polymer prepared by two distinctive mechanisms: (i) the step-growth polymerization or polycondensation, and (ii) the ring-opening polyaddition (ROP) (chain growth polymerization). The step-growth polymerization mechanism depends on the condensation of lactic acid (Figure 2-2). However, there are drawbacks including the use of high temperatures, long reaction times, difficult control of the stereoregularity, and the generation of water as a byproduct that decrease the conversion and the molecular weight (Enomoto *et al.*, 1994; Ren, 2010).
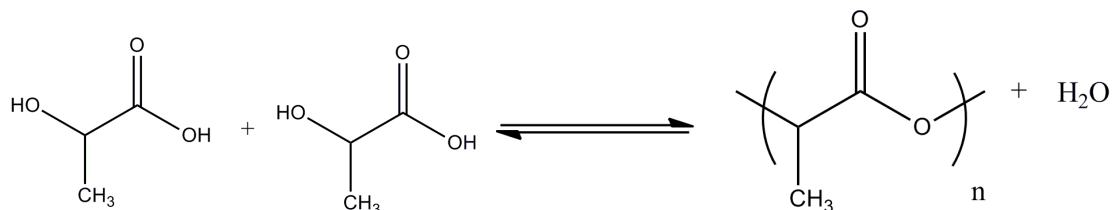
Figure 2-2: The synthesis of PLA from lactic acid monomers through the step growth polymerization.

The polymerization of lactones and lactides by the ring-opening polyaddition mechanism is more favorable and free of these limitations. In this mechanism, tailor-made properties and narrow molecular weight distributions can be easily prepared under mild conditions (Lou *et al.*, 2003; William, 2007). A variety of cationic, anionic, and coordination catalysts can be used in ring opening polymerization (Lecimte and Jérôme, 2005; Penczek *et al.*, 2007).

The ROP proceeds through two major mechanisms depending on the catalyst. In the first mechanism, the metal acts as the catalyst to activate the monomer by complexation with the carbonyl group (Figure 2-3). Polymerization is then initiated by any nucleophile such as water or an alcohol present in the polymerization media, by using a catalyst as Lewis acidic metal fragment (Piedra-Arroni *et al.*, 2011). The second mechanism is a coordination-insertion mechanism. Tin octoate ($Sn(Oct)_2$), tin(II) bis-(2-ethylhexanoate), is the most widely used organometallic initiator for the ring-opening polymerization of aliphatic polyesters, even more than metal free catalytic systems (Stjerndahl *et al.*, 2007). It is accepted as a food additive by the US FDA. Therefore, there are applications that do not need polymer purification, such as packaging. In the second mechanism, tin octoate is converted into tin alkoxide by reaction with alcohols. Reacting tin alkoxide with a second alcohol equivalent produces tin dialkoxide, which acts as the actual initiator (Figure 2-4). Afterwards, tin dialkoxide coordinates with the carbonyl group of the monomer, followed by cleavage of the bond of acyl-oxygen bond. Simultaneous insertion of monomers into the metal alkoxide then takes place. Consequently, the addition of a predetermined amount of alcohol is an effective way to control the molecular weight.
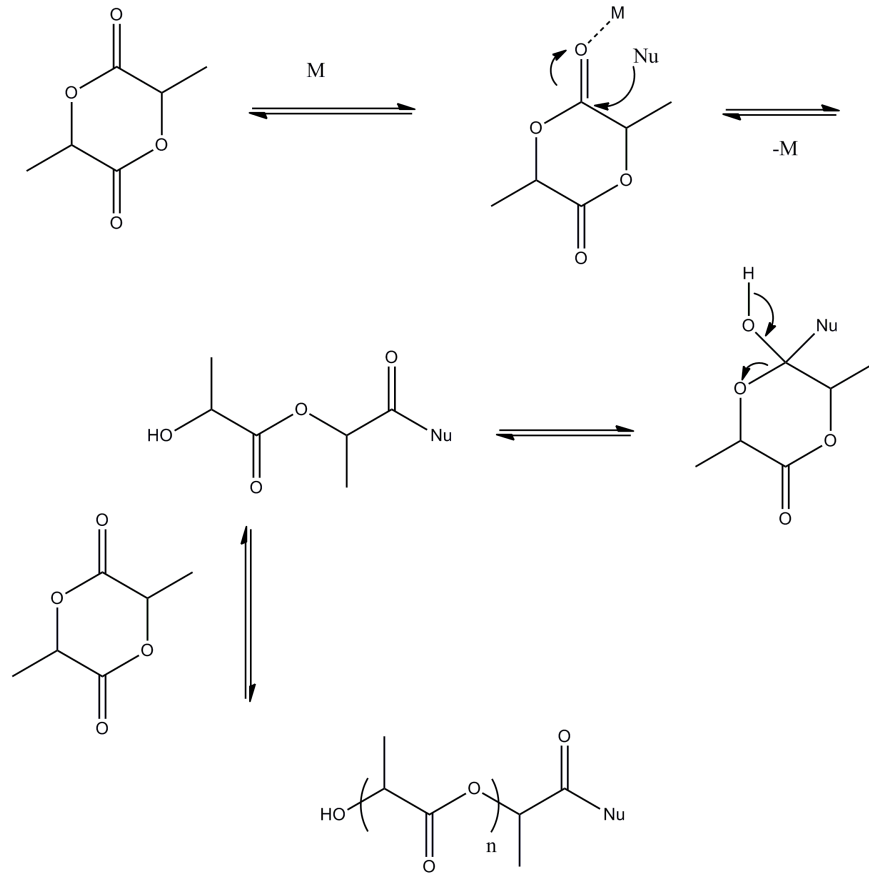
Figure 2-3: Mechanism of PLA synthesis through ring opening polymerization using organometallic catalyst species (M) in presence of nucleophiles (Nu).

PLA can exist in different stereochemical forms, which have different properties. Poly(*D*-lactic acid) (PDLA) and poly(*L*-lactic acid) (PLLA) are semicrystalline materials, exhibiting glass transition temperatures (T_g) of 55-65° C, and melting temperatures (T_m) of 150-175 °C (Rathi *et al.*, 2012; Shao *et al.*, 2012). Racemic (*D,L*)-lactic acid is amorphous due to the random distribution of *D*- and *L*-lactic acid and therefore does not exhibit a T_m. It has a T_g of approximately 55-60°C. Variations in thermal properties impact their chemical and physical properties, providing insight toward relative applicability in different biomedical applications. PDLLA has been shown to exhibit increased degradation rates. It typically starts to show mass loss and fully degrades within 12-16 months, whereas PLLA can take 2-5.6 years. This can be attributed to the crystallinity of PLLA (Chu, 1981; Grijipma *et al.*, 1990; Fukushima *et al.*, 2013).

$$Sn(Oct)_2 \; + \; ROH \; \rightleftharpoons \; Oct\text{-}Sn\text{-}OR \; + \; OctH \qquad (1)$$

$$Oct\text{-}Sn\text{-}OR \; + \; ROH \; \rightleftharpoons \; Sn(OR)_2 \; + \; OctH \qquad (2)$$
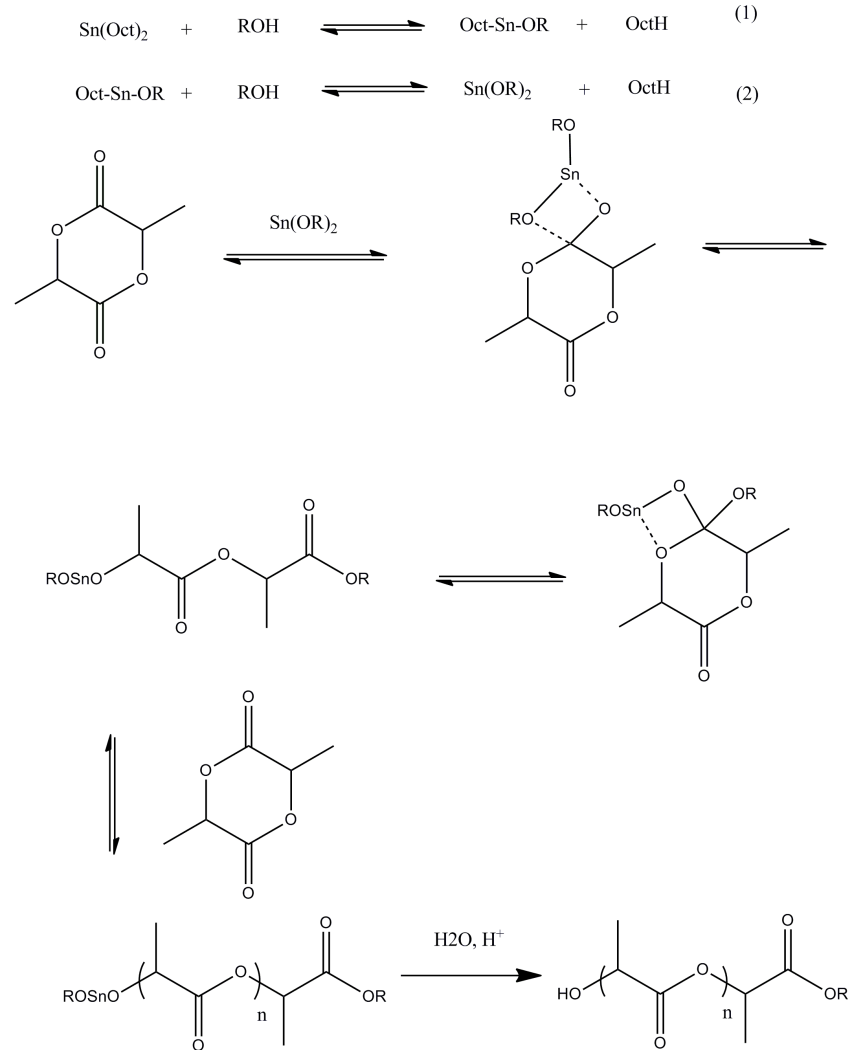
Figure 2-4: Mechanism of PLA synthesis through the ring opening polymerization via coordination insertion mechanism using tin octoate as a catalyst

Due to the slow degradation rate and good tensile strength of the PLLA, it can be used in load bearing applications, including orthopedic fixation devices. The Phantom Soft Thread Soft Tissue Fixation Screw® and Phantom Suture Anchor® (DePuy) are a couple of examples. Additionally, PLLA fibers have been investigated as scaffolding materials for developing ligament replacements to replace non-degradable fibers, such as Dacron (Lu *et al.*, 2005; Cooper *et al.*, 2005). On the other hand, the lower strength and faster degradation rate of PDLLA renders it a preferred candidate for drug delivery vehicles and as low strength scaffolding material for soft tissue regeneration (Nair and Laurencin, 2007).

Extensive research has also focused on the development of copolymers such as poly(lactide-*co*-glycolide) (PLGA) in order to improve the degradation rate. The characteristics of the PLGA are dependent on the composition of the copolymers. For example, poly(*D,L*-lactide-

co-glycolide) with a 50/50 ratio of monomers degrades within 1–2 months, 75/25 lactide:glycolide in 4–5 months and 85/15 in 5–6 months. Additionally, PLGA of 25/75 forms amorphous polymers (Miller *et al.*, 1977).

Polycaprolactone (PCL) is hydrophobic polyester that has also been extensively explored. It is semicrystalline and exhibits a low T_m of 55–60 °C and a T_g of -60 ^{o}C. It is synthesized by the ring opening polymerization of carpolactone. Due to the presence of ester linkages in the backbone, PCL also undergoes hydrolytic degradation, albeit with a slow rate requiring up to 3-4 years to reach completion (Woodruff and Hutmacher, 2010). Thus, it has been investigated in long-term drug delivery devices. Polymeric devices consisting of carpolactone and glycolide are currently used as slowly degrading suture materials (MONACRYL$^®$) (Nair and Laurencin, 2007).

2.2.2 Poly(ester amide)s (PEAs)

Although polyesters such as PLGA, PLA, and PCL constitute the main family of synthetic biodegradable polymers used in a wide range of biomedical applications, some limitations of these polyesters have been reported. For example, PLA and PLGA can undergo bulk degradation, which prevents the degraded chains from escaping to the outer environment, ultimately leading to excessive accumulation of the acidic byproducts and consequently resulting in some cell toxicity and tissue inflammation (Bergsma *et al.*, 1995; Estey *et al.*, 2006; Nair and Laurencin, 2007). Additionally, poor mechanical properties due to weak intermolecular forces and lack of side chain functionalities required for coupling of bioactive molecules have restricted the use of these polymers in medical applications.

Poly(ester amide)s (PEAs) have emerged as promising biodegradable polymers for a wide range of biomedical applications as they have the advantages resulting from both ester and amide bonds in their chemical backbone that promote biodegradability, as well as good thermal and mechanical properties. Additionally, they have so far exhibited good biocompatibility and cell-material interactions (Horwitz *et al*., 2010; Knight *et al*., 2011). The hydrolyzable bonds in their chemical structures are responsible for hydrolytic and enzymatic degradation in a wide range of biological environments, resulting in the release of non-toxic building blocks including amino acids, diols, and dicarboxylic acids (Guo and Chu, 2007; Knigh *et al.*, 2011; Rodriguez-Galan et al, 2011; Sun *et al.*, 2011).

The structure-property relationships of PEAs have been explored, and it has been shown that by rational design of the backbone, the polymer's chemical functionality, degree of crystallinity and degradability, solubility, thermal, and mechanical properties can be readily tailored. PEAs synthesized from a-amino acids, diols, and diacids as shown in Figure 2-5 are of particular interest for our group.
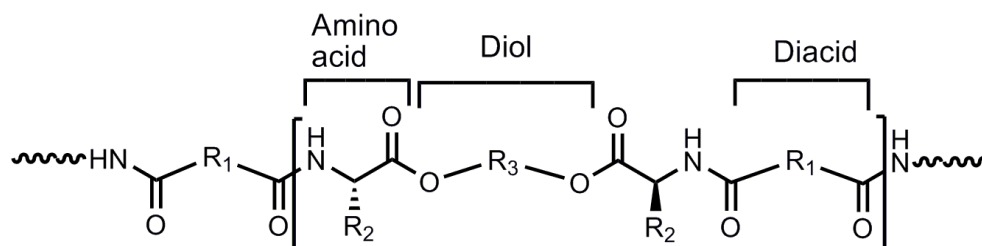
Figure 2-5: General structure of PEA

Soleimani *et al.*, (2014) have prepared various structures of PEAs based on amino acids including *L*-alanine, and *L*-phenylalanine with diols of different structures along with aliphatic and aromatic diacids. It was found that all of the resulting PEAs exhibited high decomposition temperatures (T_{ds}) that exceeded 300 °C, indicating that these polymers can be processed in the melt without degradation. The thermal properties could be tuned by the incorporation of different chemical structures into the PEA backbone. For example, the incorporation of flexible ether bonds in the backbones decreased the T_g compared to the similar PEAs of the same amino acids, diacids, and spacer length of the diol. Increasing the number of methylenes in the diol moiety was another way to lower the T_g in the PEAs of the same structures. Additionally, the chemical structures of amino acids can affect the flexibility of PEAs. For example, the incorporation of *L*-phenylalanine increased the T_g, in comparison with the PEAs with *L*-alanine, due to presence of the rigid phenyl group. PEAs containing stiff units such as terephthalic acid and cyclohexanediol exhibited higher T_gs. In addition to studying structure-property relationships, during the last decade great efforts have been focused to introduce functionalities into the polymer backbone by the incorporation of α-amino acids with carboxyl, hydroxyl, and amine pendant groups. Atkins *et al.*, (2009) has successfully synthesized functionalized PEAs using *L*-aspartic acid and *L*-lysine based monomers. PEAs containing different monomers have been synthesized via two major routes: ring opening polymerization of functionalized lactones and polycondensation of monomers with reactive amine, ester, and hydroxyl end groups. Ring opening polymerizations of morpholine-2,5-diones were usually carried out using tin octoate

[Sn(Oct)$_2$] as a catalyst and adding water or alcohol molecules as initiators. It was hypothesized that the ring opening reaction is initiated by a tin (II) hydroxyl or alkoxide group as shown in Figure 2-6.

ROP, however, has shown some imitations. The morpholine-2,5-diones can coordinate to a metal complex in a non-productive manner as a result of attack of the more nucleophilic oxygen of the amide group. Additionally, the amido N–H group may be involved in a reaction after attack at the ester group, leading to stable chelating ligands. Therefore, polymerization through ROP is terminated by the formation of kinetically inert products (Chisholm *et al.*, 2006). Polycondensation methods are usually utilized to react diamide-diol (I, II), diester-diamine (III) monomers with dicarboxylic acid derivatives, as shown in Figure 2-7. The PEA is prepared via polycondensation methods through two main approaches: interfacial and solution polymerization.
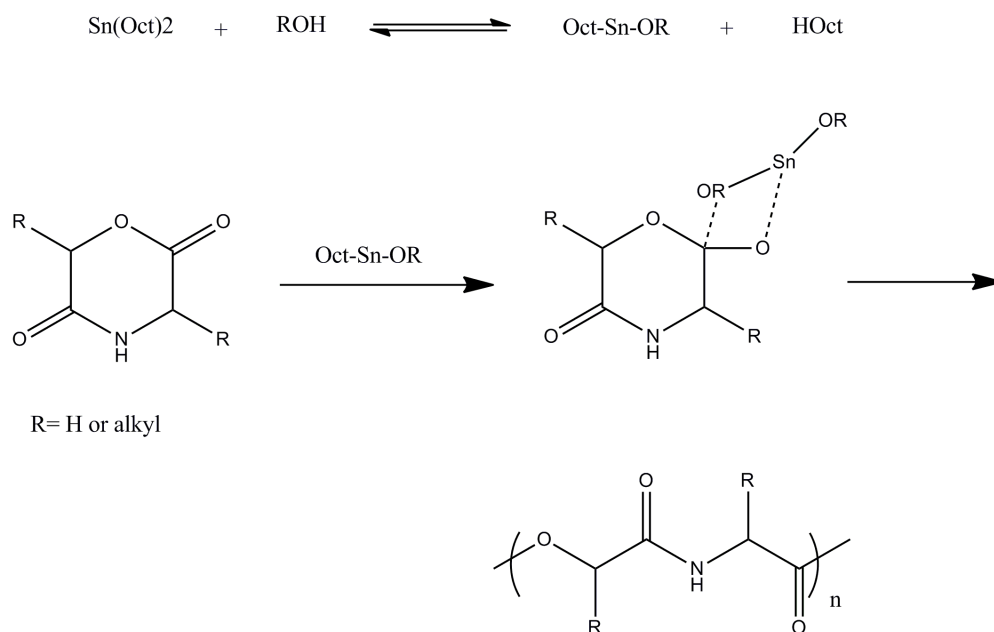
Figure 2-6: Scheme of synthesis of PEA through ring opening mechanism of morpholine-2,5-dione using tin octoate as a catalyst

Interfacial Polymerization. PEAs can be prepared from di-*p*-toluenesulfonic acid salts of bis-(R-amino acid) diesters and diacid chlorides through interfacial polymerization where the polymerization occurs at the interface of Na$_2$CO$_3$ aqueous solutions and water immiscible organic solvents. The method produces high molecular weight polymers, in which the impurities from the monomers remain in the aqueous phase, allowing polymer chain propagation (Knight *et al.*, 2011). Although this method can be performed at low

temperatures with limited side reactions (Paredes et al, 1998), this method has reported several drawbacks of chain-termination and unit-heterogeneity.

Solution Polymerization. The solution polymerization depends mainly on activation of the carboxylic acid by reacting it with a good leaving group to form an activated ester. It is carried out by reacting di-*p*-toluenesulfonic acid salts of bis-(R-amino acid) diesters with di-*p*-nitrophenyl esters of diacids at moderate temperatures of 70 °C in nonprotic solvents. This approach is used in the synthesis of PEAs of different structures by rational selection of diacids or diols, in which either aliphatic or aromatic and saturated or unsaturated backbones with varying lengths of alkylene units can be prepared. Additionally, the solution polymerization method can be carried out without the use of toxic catalysts, which makes it a highly attractive synthetic approach for degradable polymers; however, the resulting polymers require extensive purification to remove the large amounts of side products, such as *p*-nitrophenol.
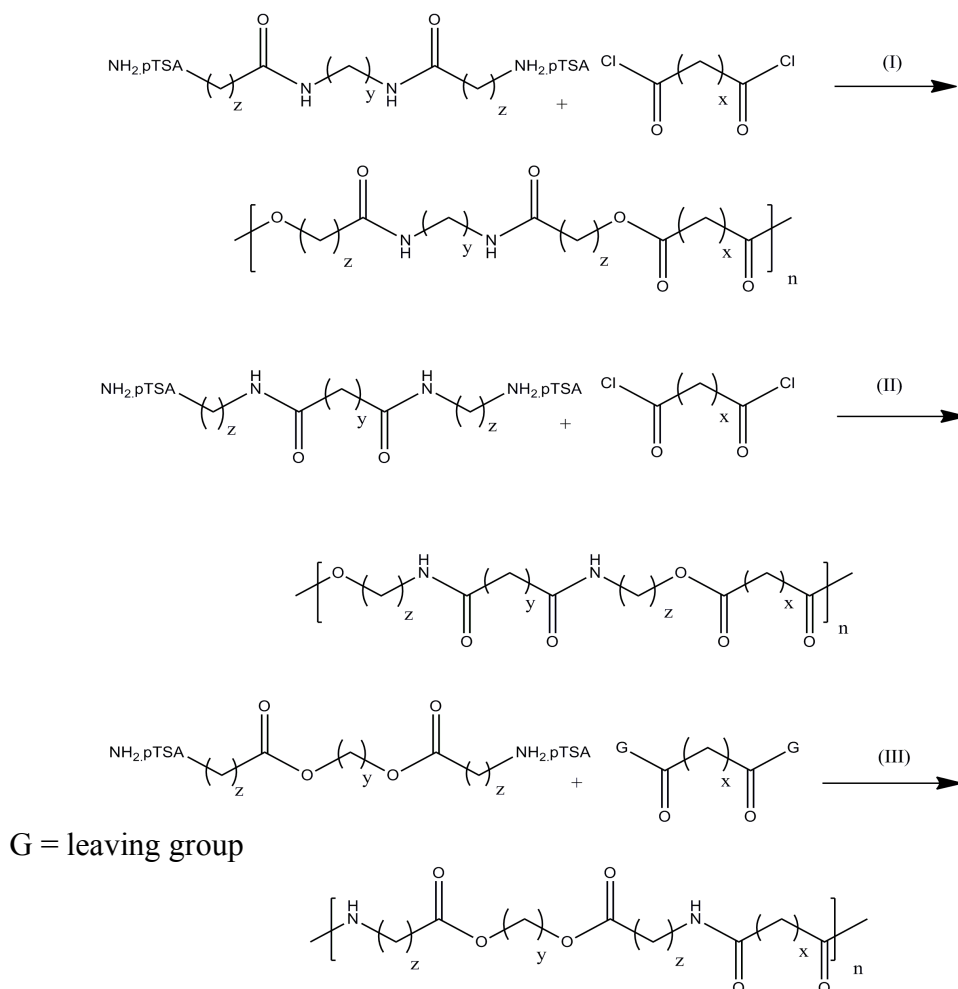
Figure 2-7: Synthesis of PEAs through polycondensation approaches.

PEAs have many advantages for their use in biomedical applications. They are multifunctional biomaterials that are not only biocompatible and biodegradable but are also biomimicking materials since they can be synthesized from natural amino acids. *L*-amino acid containing biodegradable PEAs have been explored for drug delivery, gene delivery, tissue engineering, and medical imaging. For example, Lee *et al.*, (2002) have evaluated PEA coated stents for reducing the neointimal hyperplasia. In this study, a PEA based on L-amino acids (L-leucine and L-lysine), 1,6-hexanediol, and sebacic acid was used. The results suggested that the PEAs have many potential advantages as stent coatings since a positive effect on the vascular healing response was obtained. In addition, PEA coated stents loaded with 50% (wt%) of Tempamine decreased the arterial injury and neointimal hyperplasia in an *in vivo* study (Huang *et al.*, 2006).

PEA microparticles were prepared and optimized via an emulsification evaporation technique based on *L*-phenylalanine-butane-1,4-diester with adipic acid and sebacic acid. The degradation behavior was significantly affected by the enzyme concentration. Paclitaxel loaded microparticles exhibited high encapsulation efficiency (> 95%), showing promise as a carrier for hydrophobic anti cancer drug delivery (Guo and Chu, 2009).

Knight *et al.* 2011 synthesized biodegradable PEAs based on α-amino acids *L*-alanine, *L*-phenylalanine, and *L*-lysine to study human coronary artery smooth muscle cell (HCASMCs) interactions. All of the prepared PEAs exhibited good HCASMC attachment, spreading and proliferation. These results suggested that PEAs could potentially be applicable in vascular tissue engineering applications.

2.3 Polymer-drug conjugates for nanocarriers

Drug loading into polymeric NPs can be achieved through three strategies: (1) covalent attachment of the drug to the polymers through polymer-drug conjugates; (2) adsorption of the drug on the polymeric surface; (3) entrapment of the drug in the polymeric matrix of NPs (Dreis *et al.*, 2007). Accordingly, the drug release profile can be affected by many factors including polymeric matrix degradation, diffusion through the matrix, and erosion of the polymeric surfaces (Peer *et al.*, 2007). Promising results have been reported in the literature regarding the synthesis of nanocarriers and the physical encapsulation of drugs (Elsabahy and Wooley, 2012; Kamaly *et al.*, 2012; Nicolas *et al.*, 2013). However, many delivery systems

based on physical drug encapsulation have strong limitations including: (1) the poor encapsulation efficiency of hydrophilic drugs which may require the usage of high percentages of the polymeric carrier that may cause toxicity; (2) the burst effect which results from precipitation of the drug on the outer surface of the particles and a subsequent rapid release after administration and also may cause toxicity; (3) crystallization of poorly soluble drug during preparation of the nanocarrier. Many attempts have been undertaken in order to solve these problems. For example, the drug can be covalently coupled to the polymer, forming prodrugs that are inactive, but upon cleavage can be converted to the active form. This strategy can overcome the aforementioned limitations. Three main strategies have been followed in order to synthesize polymer-drug conjugates: (i) conjugation of a drug to a monomer before polymerization; (ii) coupling a drug to a synthesized polymer; (iii) use of the drug as an initiator for polymerization.

2.3.1 Conjugation to monomer prior to polymerization

Polymer-drug conjugates were synthesized through a procedure involving grafting a drug on a monomer prior to its polymerization. This technique requires coupling of a drug to a functional group on the monomer. Bertin *et al.*, (2005) reported high-density doxorubicin (Dox)-conjugated polymeric NPs prepared from the coupling of Dox to norbornene monomers through carbamate linkers, and then copolymerizing the functionalized monomer with a water soluble hexa(ethylene oxide)-substituted norbornene monomer using an initiator. The resulting amphiphilic copolymers were then used to prepare core–shell polymeric NPs through the self-assembly, by the addition of water into a DMSO solution containing 0.01% wt% copolymer. The NPs were purified through dialysis against deionized water. The recovered NPs were used for *in vitro* Dox release at two different pH values of 7 and 4. The release profile showed no release for Dox in the neural environment, however, three distinct domains characterized the Dox release in the acidic pH: initial, slow, and plateau, to reach 50% in the first 24 hour as shown in Figure 2-8.
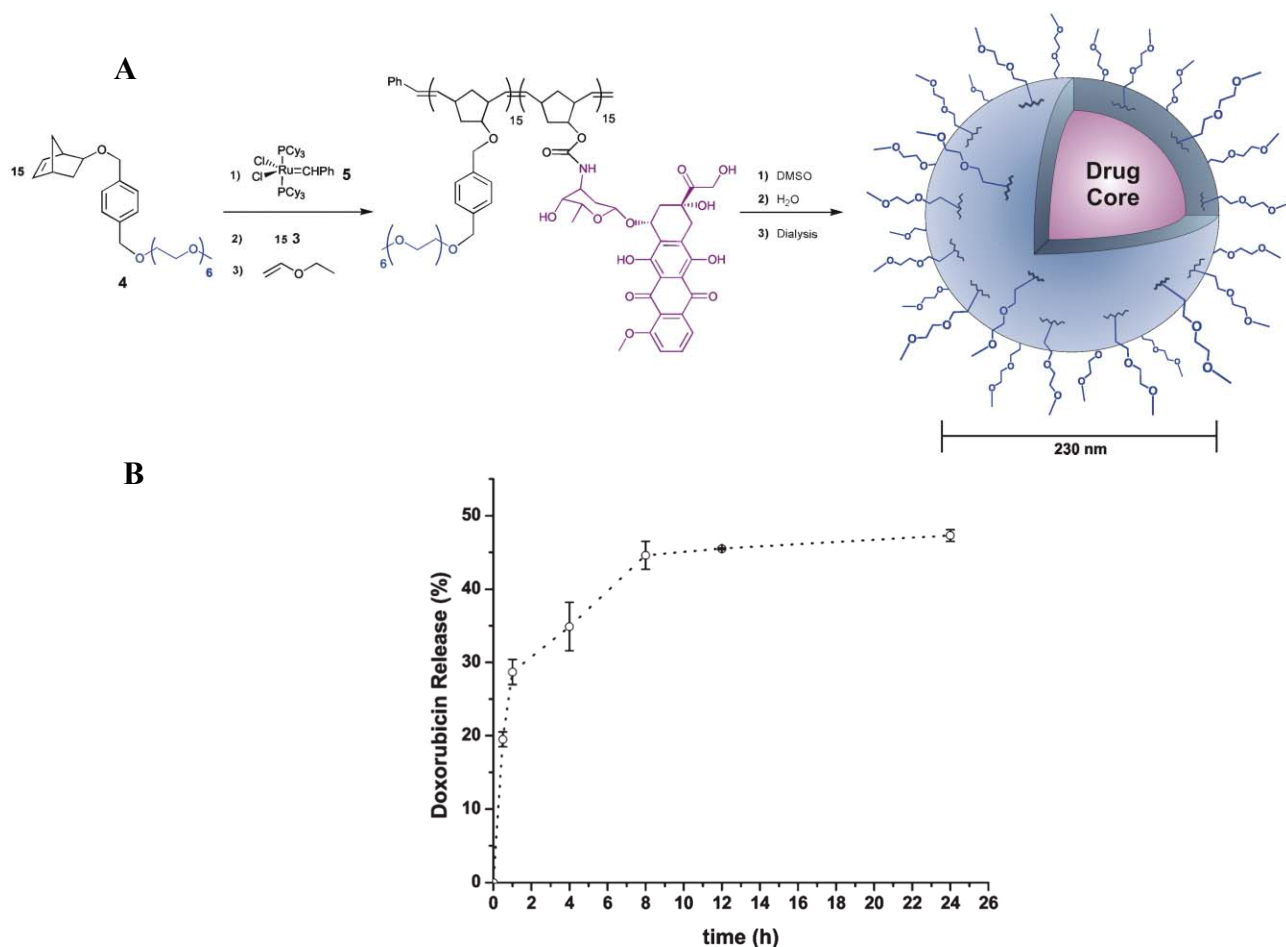
Figure 2-8: A) High-density Dox-conjugated polymeric NPs prepared through coupling the drug to the monomer before polymerization and then performing nanoprecipitation. B) The in vitro release profile of Dox in pH=4. (Reprinted with permission from Bertin *et al.*, 2005)

2.3.2 The drug initiated method

The drug initiated method depends on using the drug as an initiator for polymerization of the required monomer. Tong and Cheng, (2008) demonstrated this concept. They used a hydrophobic anti cancer drug paclitaxel (Ptxl) as an initiator for the polymerization since Ptxl has multiple hydroxyl groups. By reacting Ptxl with 1 equiv [(BDI)MgN-(TMS)$_2$] (BDI =2-((2,6-diisopropyl-phenyl)amino)-4-((2,6-diisopropylphenyl)imino)-2-pentene, TMS=trimethylsilyl), the resulting complex initiated and completed the polymerization of L-lactide within hours at room temperature. [(BDI)MgN-(TMS)$_2$] is an active catalyst developed by Coates and co-workers for the polymerization of LA. Polymers with good drug loading (6-28 wt%) were obtained. The ratio between Ptxl and lactide monomers was the controlling factor for drug loading. The nanoconjugates (NC) were prepared through nanoprecipitation of PLA-Ptxl conjugates, resulting in small NPs less than 100 nm which exhibited controlled release

and the absence of a burst release effect. The Ptxl release kinetics was determined by diffusion as well as the hydrolysis of the ester linkers. The results of MTT assays on PC-3 cancer cells demonstrated that the cytotoxicity was correlated with the drug loading: the higher the drug loading, the lower the IC_{50}. Perfect colloidal stability was obtained after surface modification of NPs with noncovalent addition of PLGA-mPEG to the NC surface instead of covalently conjugating PEG to the NCs as shown in Figure 2-9.
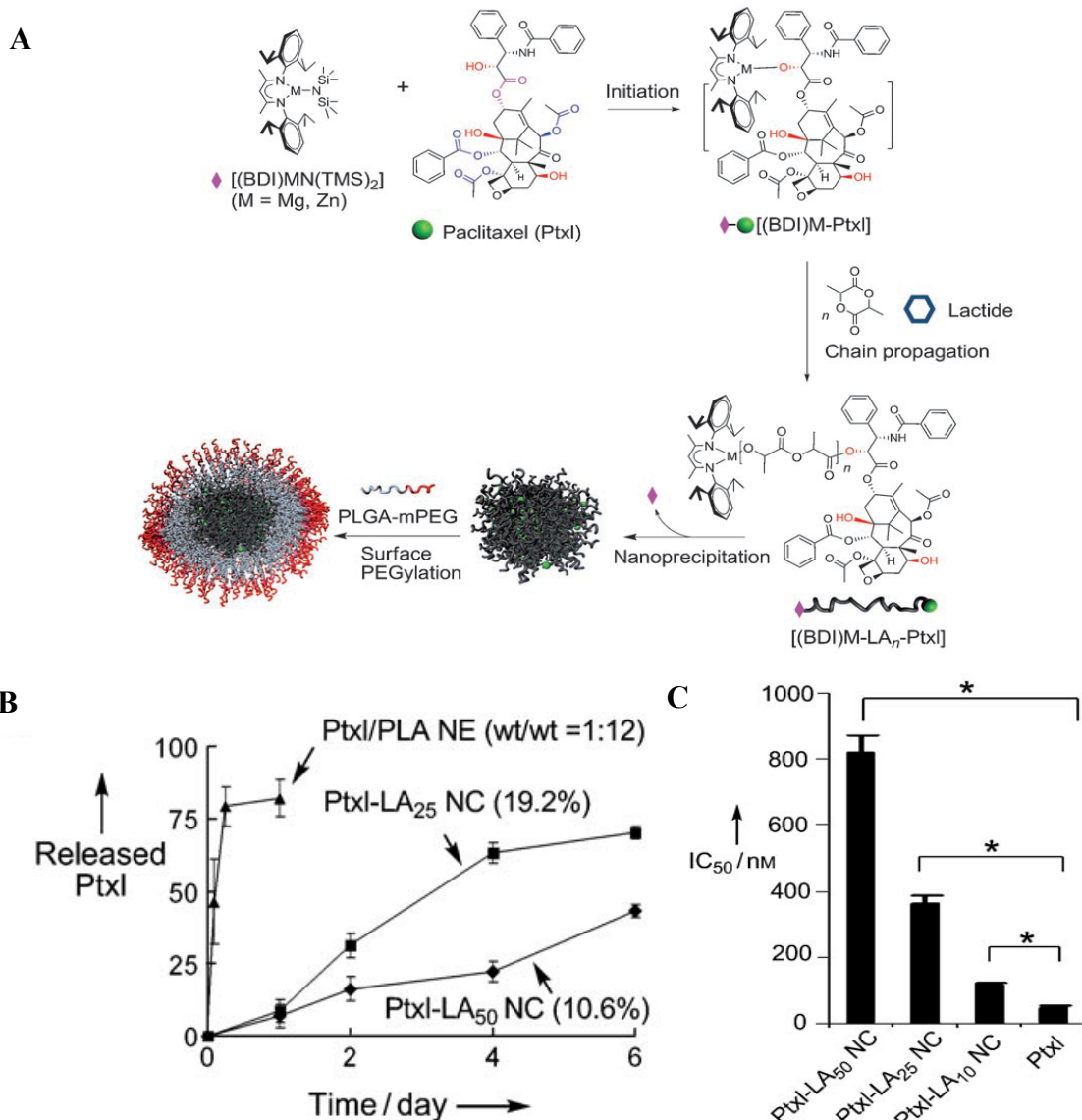
Figure 2-9: Preparation of Ptxl-PLA NCs though Ptxl initiation of PLA polymerization, followed by nanoprecipitation and noncovalent surface modification with PLGA-mPEG. (Reprinted with permission from Tong and Cheng, 2008)

2.3.3 Conjugation to polymers

In this approach, the drug is conjugated to a polymer scaffold and the nanosystem can be

formulated from the functionalized polymer through different techniques. Notably, Xiong and Lavasanifar, (2012) grafted siRNA and Dox onto RGD-functionalized PEO-b-PCL copolymers in order to synthesize integrated multifunctional micellar nanocarriers for targeted drug delivery. The attachment of Dox through a hydrazone linkage provides pH-triggered drug release.

Micellar systems based on acetal-poly(ethylene oxide)-b-PCL (acetal-PEO-b-PCL) copolymers with Dox (acetal-PEO-b-P(CL-hyd-Dox)) and spermine (SP) (acetal-PEO-b-P(CL-g-SP)) conjugated to the PCL block were prepared. These micellar systems were prepared by incubation of siRNA with acetal-PEO-b-P(CL-g-SP) in a buffer solution in order to form a complex. Secondly, TAT and RGD targeting ligands TAT-PEO-b-P(CL-g-SP), RGD4C-PEO-b-P(CL-Hyd-Dox), or both of them were added to the polymer/siRNA complex to prepare TAT and RGD shell-functionalized micelles containing siRNA and Dox in the core of the micellar system as shown in Figure 2-10.
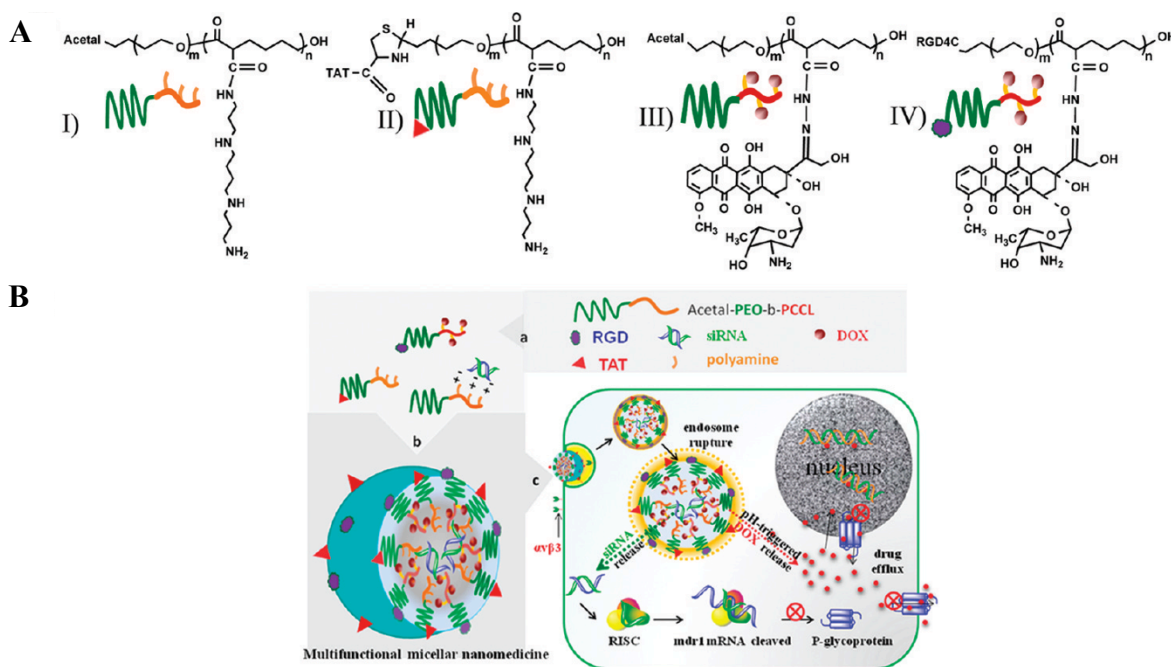
Figure 2-10: A) Schematic composition of acetal-and TAT-PEO-b-(CL-g-SP) for I and II, acetal and RGD4C-PEO-b-P(CL-Hyd-DOX) for III and IV. Permission(Reprinted with permission from Xiong and Lavasanifar, 2012)

This sequence was followed in order to avoid binding of siRNA to the positive charges of TAT and RGD in the micelle surface. The Dox loading was ~6.0 % of the weight of the polymer. The prepared micelles were of an average size of 100 nm. Also, these micelles

demonstrated improvement in cellular uptake, Dox penetration into nuclei, and efficiency of Dox and siRNA against overexpression of P-glycoprotein (P-gp) transporter protein on the cancer cells, which is responsible for multidrug resistance.

2.4 Stimuli-responsive polymers for nanosystems

The ultimate aim of a drug delivery system is to provide a secure environment to encapsulate the drugs without leakage before reaching the target organ, but to release the drugs after entering the target tissues. To achieve these requirements, stimuli-responsive materials have captured the attention of many researchers. The release characteristics are programmed by incorporating a means to build sensitivity to internal or external, chemical or physical stimuli, particularly in the area of polymers. These materials can undergo significant changes in their chemical and physical properties in response to variations in the environment.

There are two major classes that can be distinguished in terms of stimuli-responsive nanomaterials: endogenous and exogenous. Some endogenous stimuli include pH and enzymes, while exogenous stimuli could be light, temperature, magnetic fields, or even mechanical stress. However, endogenous triggers such as pH may vary from person to person, which makes systems based on these stimuli challenging in terms of applicability. Exogenous stimuli are thus more promising in this regard. There are many examples involving the use of stimuli-responsive nanocarriers in drug delivery (Cabane *et al.*, 2012; Alvarez-Lorenzo and Concheiro, 2014; Cheng *et al.*, 2014).

2.4.1 Endogenous stimuli-responsive polymers

a) pH-responsive nanosystems

Variation in the pH of different tissues and cells has been exploited for developing pH-responsive polymers. Cancerous tissues are characterized by low pH as a result of accumulation of lactic acid, the byproduct of glycolysis metabolism, leading to lowering of the pH of the extracellular matrix (Cairns *et al.*, 2011). Additionally, the lower pHs of endosomes (5–6) and lysosomes (4–5) have been used for developing pH-responsive DDS which are designed to only release the payloads after endocytosis (Ulbrich and Subr, 2004)

Polymers with amine groups are one category of pH-responsive polymers, based on the protonation-induced change in polymer hydrophobicity. Yao *et al.*, (2011) synthesized a core

shell corona (C-S-C) system using triblock copolymers of PEO-block-poly(dimethylaminoe-thyl methacrylate)-block-PCL (PEG-PDMA-PCL) as a pH sensitive nanocarrier for intracellular delivery. PCL is hydrophobic and formed the core to accommodate hydrophobic drugs. PDMA moieties formed the shell and served to impart pH-responsive release. PEO moieties form the corona and stabilize the nanostructure to provide long circulation times *in vivo* as shown in Figure 2-11. The release behavior, hydrodynamic diameter, and the TEM images were assessed to determine pH-responsive micellization behavior at three different pH levels of 3.0, 5.5, and 7.4. The results revealed that the release rate and micelle size increased with a decrease in pH from 7.5 to 3.0. It was also observed that an increase in electrostatic repulsion between protonated amine groups on PDMA blocks was accompanied by an increase in hydrodynamic diameter of the micelles upon a decrease in pH from 7.4 to 5.0 of the media. A higher degrees of ionization of amine groups, increases in electrostatic repulsion among the polymer chains led to a higher solubility in aqueous solution and faster release rate due to good contact of the PCL core with the buffer solution. Suppression of the growth of SKOV-3 cells was observed after incubation of Dox-loaded PEG-PDMA-PCL micelles in an MTT cytotoxicity assay, showing that this pH-responsive carrier is a good candidate for intracellular delivery.
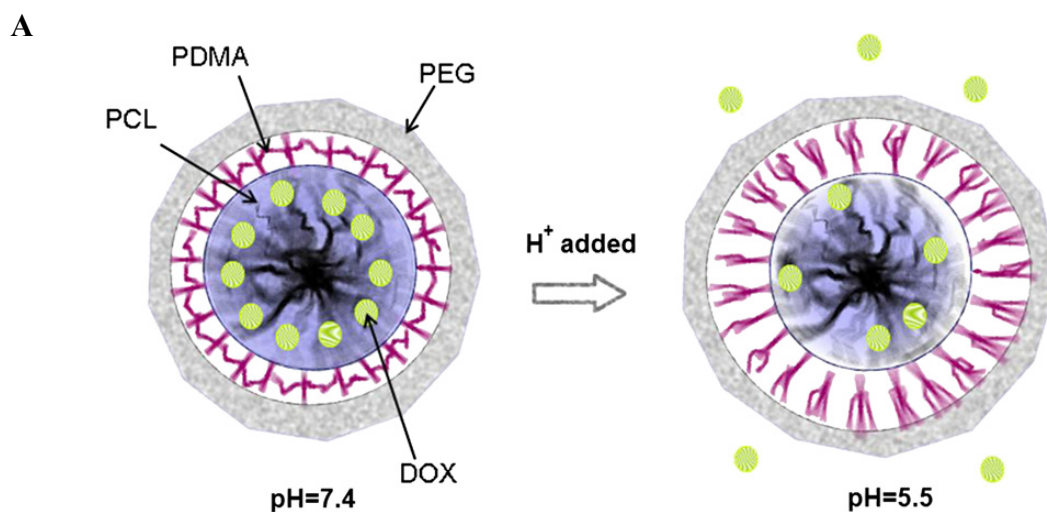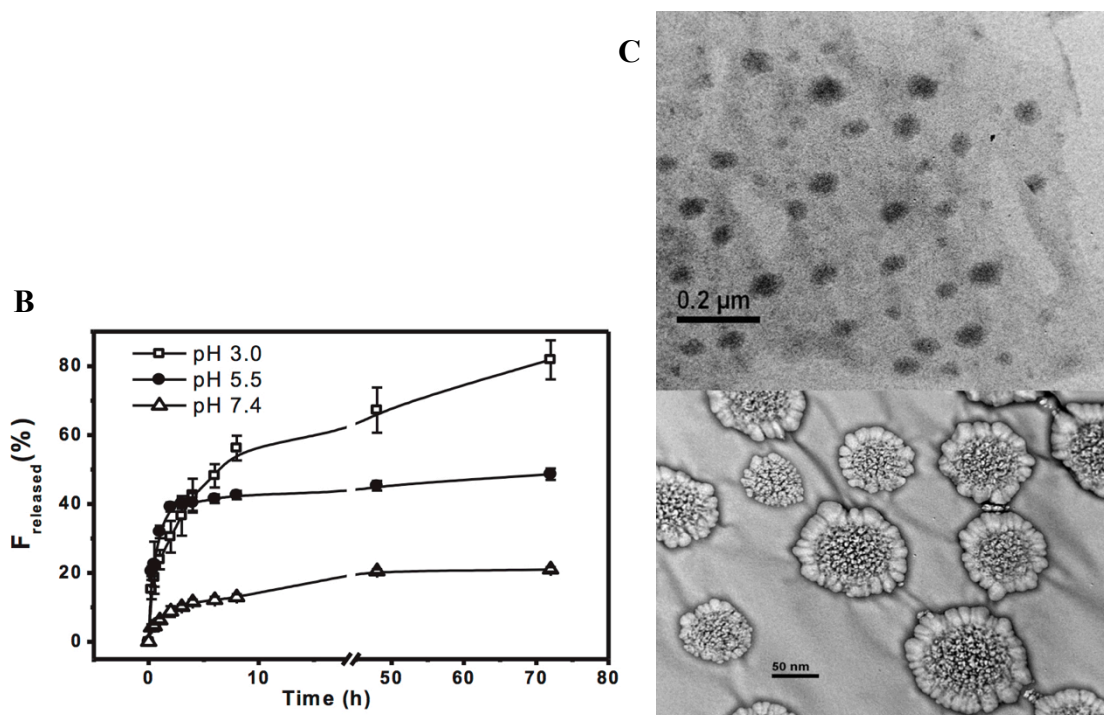
Figure 2-11: A) Structure of Dox-loaded PEO-PDMA-PCL micelles and pH-responsive drug release. B) TEM images of the micellar system at different magnification in neutral aqueous media. C) *In vitro* **release behavior of Dox at pH 3.0, 5.5, and 7.4 in buffer solution. (Reprinted with permission from Yao** *et al.***, 2011)**

b) Redox-responsive nanosystems

The presence of glutathione (GSH), along with glutathione disulfide (GSSG) plays a major role in redox homeostasis. Additionally, intracellular compartments of cells are much more reductive than the extracellular matrix due to the fact that the concentration of GSH in intracellular compartments is 100 – 1000 times higher than in the extracellular matrixes (Cheng *et al.*, 2011). GSH has significant effects on many cellular functions including protein function, gene expression, and programmed cell death (Kroemer *et al.*, 1998; Cadenas and Davies, 2000; Schafer and Buettner, 2001; Estrela *et al.*, 2006). Moreover, the high GSH level is related to many human diseases like cancer, liver disease, neurodegenerative disease, and diabetes (Estrela *et al.*, 2006); Djuric *et al.*, 1990; Balendiran *et al.*, 2004; Franco *et al.*, 2007; Valko *et al.*, 2007). High levels of GSH also play an important role in multi-drug and radiation resistance (Estrela *et al.*, 2006; Balendiran *et al.*, 2004; Stavrovskaya *et al.*, 2000). These significant differences in the redox environment have been exploited for developing redox-responsive drug delivery systems. One important approach is to incorporate disulfide bonds within the systems via different methods.

Ryn *et al.*, (2010) synthesized redox-sensitive micelles from amphiphilic polymers obtained by grafting of different alkyl chains (hydrophobic) to hydrophilic chains of triethylene glycol monomers through disulfide bonds, and then encapsulated rile red as a hydrophobic dye. The release of the dye from the NPs resulted from the conversion of macromolecular nanoassemblies to hydrophilic and hydrophobic components by cleavage of the disulfide bonds upon treatment with GSH. The disassembly and release rate of the dye were dependent on the time and GSH concentrations as illustrated in Figure 2-12. Moreover, Dox-encapsulated micelles were prepared and used for an MTT assay. It was found that the cell viability was dependent on the concentration of GSH and that this affected the cytotoxicity to MCF-7 cells. Figure 2-12(Figure 2-12). Therefore, drug delivery based on GSH responsive nanocarriers can facilitate the controlled release of the drug interacellularly and chemotherapeutic agents after cleavage of disulfide bonds.
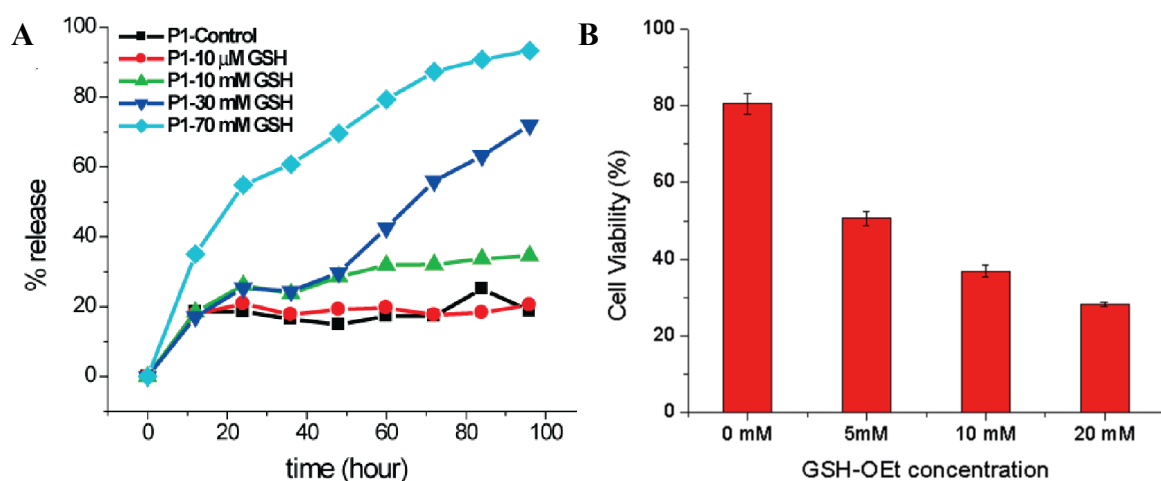
Figure 2-12: a) Nile red release profile at different GSH concentrations. b) MCF-7 cell viability after 72 h glutathione monoethyl ester (GSH-OEt) concentrations. (Reprinted with permission from Ryn *et al.*, 2010)

2.4.2 Exogenous stimuli-responsive polymers

a) Thermo-responsive nanosystems

Thermo-responsive polymers can undergo phase transitions upon a change in temperature. Different techniques have been used to generate the change in temperature, including applying magnetic fields to iron oxide systems, direct heat treatment, and applying light on gold particle-containing systems. Poly(*N*-isopropyl acrylamide (PNIPAAM) is an example of the thermoresponsive polymers that has a lower critical solution temperature (LCST) of around 31–32 °C (Meyer *et al*. 2001; Curcio *et al*. 2010; Zhang *et al*. 2012), where it

becomes water soluble when the temperature is below LCST and water insoluble above the LCST (Fujishige *et al*. 1989). Stover *et al*., (2008) utilized this criterion to improve the solubility of ceramide through the preparation of ceramide loaded thermo-responsive NPs composed of PNIPAAM, PLA, and poly(*L*-lysine) (PLL) dendrons as demonstrated in the Figure 2-13. Ceramide is a bioactive sphingolipid that has shown potential to induce cell growth arrest and/or apoptosis in various cancer cells, but which has an extremely hydrophobic character (Radian, 2001). Incorporation of PLLA provides the NPs with the hydrophobic part that is responsible for drug encapsulation, in addition to sustained release of the encapsulated drug upon gradual degradation. The integration of the PLL as a cationic and hydrophilic moiety is to enhance the drug delivery through the electrostatic interaction with polyanionic phospholipids in the cell membrane.
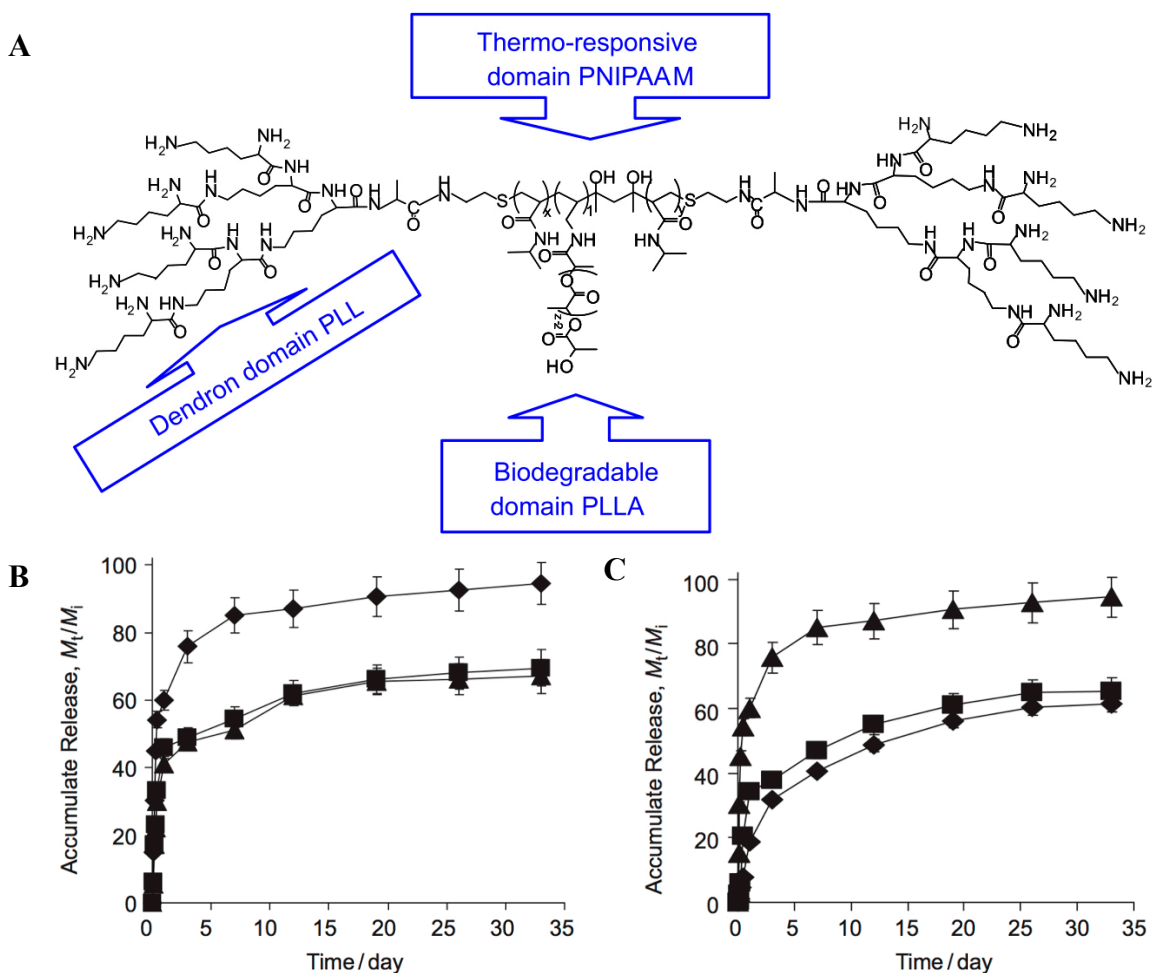
Figure 2-13: A) Composition of linear-dendritic polymer composed of thermoresponsive and biodegradable polymers. B) Accumulated release of ceramide from linear-dendritic NPs at different temperatures of 25 °C (w), 37 °C (n), and 45 °C. C) The accumulated release of ceramide at different SDS concentrations of 0.5%, 0.3%(n), and 0.1%(w) (w/v). (Reprinted with permission from Stover *et al.*, 2008)

The incorporation of hydrophobic ceramide into the NPs decreased the LCST from 30 to 28 °C. The release kinetics were strongly dependent on the temperature, with the ceramide release being faster at 25 °C (below LCST) than at 37 and 45°C (above the LCST). That can be explained by that the NPs would be more hydrophilic at 25°C and more hydrophobic at 37 and 40 °C. Additionally, the *in vitro* release pattern depended on the sodium dodecyl sulfate (SDS) concentration. SDS was expected to form micelles to solubilize the released ceramide as shown in Figure 2-13. These PNIPAAM based NPs have shown great potential for improvement of ceramide uptake while protecting it from degradation until reaching the target solid tumor tissue.

b) Photo-responsive nanosystems

Of the exogenous stimuli-responsive nanosystems, those triggered by light have attracted enormous interest. Light represents a non-invasive trigger used in drug delivery systems, that allows controlled release over space and time. Several achievements of light-triggered nanomaterials were reported in recent review papers (Sortino, 2012; Bansal and Zhang, 2014). Many strategies have been applied to the synthesis photo-responsive nanomedicines. These strategies include light induced breaking of nanocarriers, which was reported by Jiang *et al.*, (2005). Pyrenylmethyl esters, a hydrophobic photolabile chromophore, were used to synthesize nile red-encapsulating micelles from the block copolymer of PEO-*co*-polymethacrylate bearing pyrene moiety) (PEO-*b*-PPy). Upon UV light exposure, the micellar system underwent photosolvolysis as a result of the detachment of pyrene moieties (the hydrophobic block) from the polymer, leading to changes in hydrophilic/hydrophobic balance. The previous result was confirmed by investigation of the release behavior of nile red, a hydrophobic dye. Figure 2-14 shows the drastic changes in the fluorescence emission of the dye before and after UV irradiation, where nile red became insoluble in water after irradiation. This nanosystem therefore provides a possible approach for triggering and controlling the release a drug at specific target.
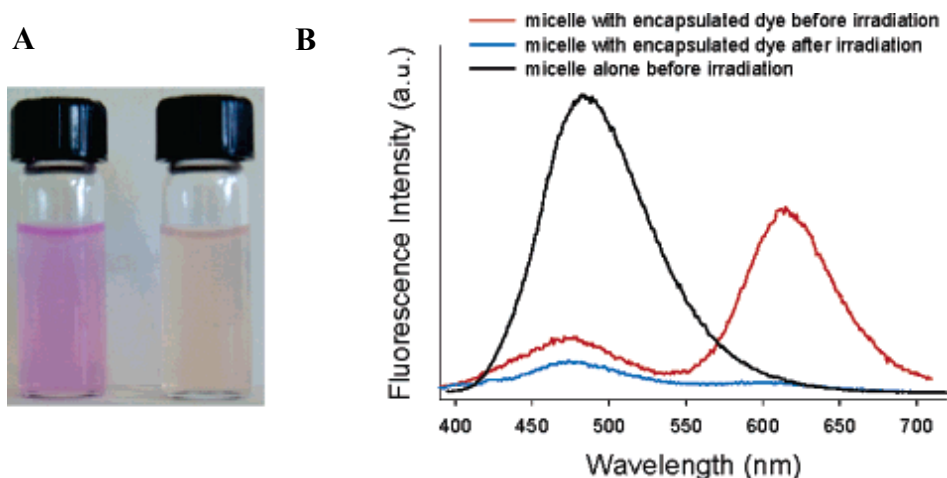
Figure 2-14: a) Nile red loaded PEO-b-PPy micellar solution before (left) and after (right) UV irradiation. b) The fluorescence emission spectra of irradiated and non-irradiated Nile red loaded micellar solution and non-loaded micellar solution as a control experiment. (Reprinted with permission from Jiang *et al.*, 2005)

2.4.3 Self-immolative polymers for nanocarriers

Self-immolative polymers represent an area of tremendous growth and promise in the area of stimuli-responsive materials. These polymers are designed to undergo a head-to-tail depolymerization through a cascade of intramolecular reactions upon removal of the triggering end group. (Sagi *et al*., 2008; Esser-Kahn *et al*., 2010; Wong *et al*., 2012). Poly(ethyl glyoxylate) (PEtG) is an example of a polymer that undergoes a cascade of reactions leading to complete disintegration of the polymer.(Fan *et al.*, 2014) Ethyl glyoxylate hydrate (EtGH), followed by ethanol and glyoxylic acid hydrate (GAH) are the degradation products of PEtG and are acceptable in medical, pharmaceutical and environmental applications (Belloncle *et al*., 2012).

PEtG has been synthesized by anionic polymerization of ethyl glyoxylate (EtG) (Burel *et al.*, 2003). Since EtG readily oligomerizes in contact with moisture, a distillation step is necessary prior to any polymerization to obtain high molecular weight polymers. PEtG, like other polyacetals, exhibits a low ceiling temperature at which the rate of polymerization and depolymerization are equal. Therefore, the polymerization process is carried out at low temperature. Most importantly, end capping is necessary to obtain thermally stable polymers. The end capping of polyglyoxylates by etherification or esterification in diluted media or at room temperature cannot prevent the spontaneous depolymerization (Brachais at al., 1998), however, end capping with isocyanates improved the stability of the final polymers (Brachais

et al., 1997). Burel *et al.*, (2003) synthesized PEtG with phenyl isocyanate end caps that exhibited enhanced thermal stability (>200°C), compared to uncapped PEtG. In vitro PEtG degradation was studied and the results showed that PEtG is stable and the degradation started after ~7 days. Afterwards, the fast depolymerization (unzipping) occured as a result of hydrolysis of the side ester groups and formation of free carboxylic acids that in turn were responsible for chain scission and hydrolysis of side ester groups (Belloncle *et al.*, 2008). Kim *et al.*, (2010) synthesized and characterized pH-sensitive PEtG based block copolymers for controlled drug delivery. Hexamethylene diisocyanate (HMDI) was used to react with PEtG through carbamate bonds to form stable end-capped PEtG. The remaining isocyanate groups were activated to couple with PEO to achieve biodegradable triblock copolymers. These amphiphilic copolymers were used to synthesize Ptxl loaded micelles to investigate pH-dependent polymer degradation and *in vitro* drug release. PTX release from the polymeric micelles was different at pH values of 5.0, 6.5, and 7.4 as a result of pH dependent polymer degradation; higher release was obtained from more acidic environment.

Recently our group has developed polyglyoxylates as a potentially versatile new class of self-immolative linear polymers, which have ability to degrade selectively through an end-to-end depolymerization mechanism (Figure 2-15). Fan *et al.*, (2014) successfully incorporated a 6-nitroveratryl carbonate (NVOC) end-cap onto PEtG. NVOC is a photolabile organic molecule that undergoes photolysis upon exposure to UV irradiation of low energy under normal conditions, allowing triggered depolymerization of PEtG.
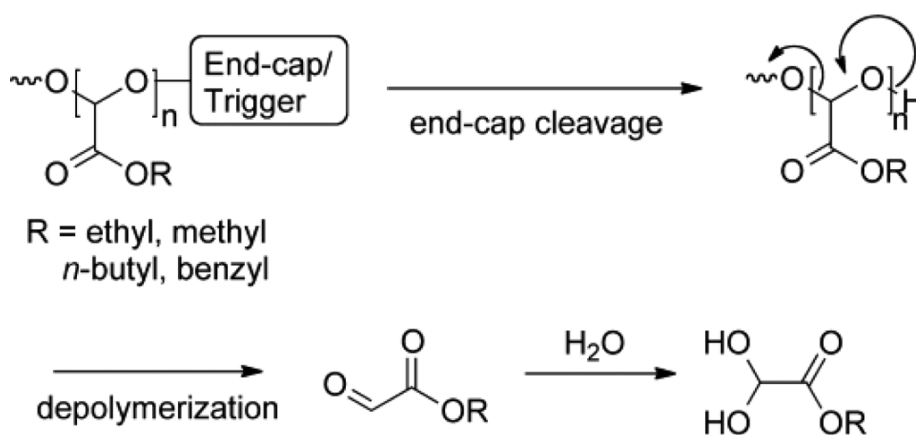
Figure 2-15: Scheme of depolymerization of polyglyoxylates after end cap cleavage.

The degradation behavior of stimuli-responsive PEtG was investigated at different time

points using NMR spectroscopy. It was found that 40 minute UV exposure was enough for complete cleavage of the NVOC group. As a result of cleavage of the end cap, 50% of the PEtG had depolymerized into EtGH within 3 h, then up to 70% within 24 h. Meanwhile, the non-irradiated end capped PEtG did not show any degradation in solution after 7 days. In a study of the mass loss of a film of end capped PEtG, the results suggested that the degradation over the first 12 days happened via a surface erosion mechanism that was associated with a gradual decrease in the mass of the PEtG film. A variety of homopolymers and copolymers with EtG were developed through simple synthetic processed and characterized, providing materials with a range of characteristics. Additionally, using a multifunctional end cap, polyglyoxylate block copolymers were synthesized. These copolymers self-assembled into micelles in aqueous solution. Rapid degradation of 90% of the PEtG block copolymers was observed just after irradiation with UV light. This work suggests that UV-responsive polyglyoxylates can be promising drug carriers.

2.5 References

[1]   Ahmed, F.; Pakunlu, R.I.; Srinivas, G.; Brannan, A.; Bates, F.; Klein, M.L.; Minko, T.; Discher, D.E., (2006). "Shrinkage of a Rapidly Growing Tumor by Drug-Loaded Polymersomes: pH-Triggered Release through Copolymer Degradation", Molecular Pharmaceutics, 3, 340-350.

[2]   Alvarez-Lorenzo C.; Concheiro, A., (2014). "Smart drug delivery systems: from fundamentals to the clinic", Chemical Communications, 50, 7743-7765.

[3]   Atkins, K.; Lopez, D.; Knight, D.; Mequanint, K.; Gillies, E., (2009). " A versatile approach for the syntheses of poly(ester amide)s with pendant functional groups", Journal of Polymer Science: Part A: Polymer Chemistry, 47, 3757-3772.

[4]   Bae, K. H.; Chung, H. J.; Park, T. G., (2011). "Nanomaterials for cancer therapy and imaging", Molecules and Cells, 31, 295−302.

[5]   Bae, Y.; Kataoka, K., (2009). "Intelligent polymeric micelles from functional poly(ethylene glycol)-poly(amino acid) block copolymers", Advanced Drug Delivery Reviews, 61, 768–784.

[6]   Balendiran, G.K.; Dabur, R.; Fraser, D., (2004). "The role of glutathione in cancer", Cell Biochemistry and Function, 22, 343–352.

[7]   Bansal, A.; Zhang, Y., (2014). "Photocontrolled Nanoparticle Delivery Systems for Biomedical Applications: Review", Acc. Chem. Res., cc. Chem. Res., 47 (10), 3052-3060

[8]   Belloncle, B.; Bunel, C.; Menu-Bouaouiche, L.; Lesouhaitier, O.;Burel, F. J., (2012). "Study of the Degradation of Poly(ethyl glyoxylate): Biodegradation, Toxicity and Ecotoxicity Assays, Journal of Polymers and Environment, 20, 726-731.

[9]   Belloncle, B.; Burel, F.; Oulyadi, H.; Bunel, C., (2008). "Study of the in vitro degradation of poly(ethyl glyoxylate)", Polymer Degradation and Stability, 93, 1151–1157.

[10] Bergsma, J. E.; Debruijn, W. C.; Rozema, F. R.; Bos, R. R. M.; Boering, G. 1995 Late degradation tissue response to poly(L-lactide) bone plates and screws, Biomaterials, 16, 25.

[11] Bertin, P. A.; Smith, D.; Nguyen, S. T., (2005). "High-density doxorubicin-conjugated polymeric nanoparticles via ring-opening metathesis polymerization", Chemical Communication, 3793-3795.

[12] Brachais, C.H., Ph.D., Thesis Rouen University, France: num: 1995ROUES043; 1995.

[13] Brachais, C.H.; Huguet, J.; Bunel, C., 1997. "Synthesis, characterization and stabilization of poly(methyl glyoxylate)", Polymer 38, 4959–4964.

[14] Brachais, C.H.; Huguet, J.; Bunel, C.; Brachais, L., 1998b. "In vitro degradation of poly(methyl glyoxylate) in water", Polymer 39, 883–890.

[15] Burel, F.; Rossignol, L.; Pontvianne, P.; Hartman, J.; Couesnon, N.; Bunel, C., 2003. "Synthesis and characterization of poly (ethyl glyoxylate) − a new potentially biodegradable polymer", e-Polymers, no. 031.

[16] Cabane, E.; Zhang, X.; Langowska, K.; Palivan, C. G.; Meier, W., (2012). "Stimuli-

Responsive Polymers and Their Applications in Nanomedicine", Biointerphases 7:9.

[17] Cadenas, E.; Davies, K.J.A., (2000). "Mitochondrial free radical generation, oxidative stress, and aging", Free Radical Biology & Medicine, 29, 222–230.

[18] Cairns, R.A.; Harris, I.S.; Mak, T.W., (2011). "Regulation of cancer cell metabolism", Nature Reviews Cancer,11, 85–95.

[19] Chanana,M.; Rivera_Gil,P.; Correa-Duarte,M.A.; Liz-Marzań, L. M.; Parak, W. J., (2013). "Physicochemical Properties of Protein-Coated Gold Nanoparticles in Biological Fluids and Cells before and after Proteolytic Digestion", Angewandte Chemie International Edition, 52, 4179−4183.

[20] Chaubal, M., (2002)."Polylactides/glycolides — excipients for injectable drug", Drug Deliv. Technol. 2 (n°5)

[21] Cheng, R.; Feng, F.; Meng, F.; Deng, C.; Feijen, J.; Zhong, Z., (2011). "Glutathione-responsive nano-vehicles as a promising platform for targeted intracellular drug and gene delivery", Controlled Release, 152, 2–12.

[22] Cheng, W.; Gu, L.; Ren, W.; Liu, Y., (2014). "Stimuli-responsive polymers for anti-cancer drug delivery", Materials Science and Engineering C, articles in press.

[23] Chisholm, M.H.; Galucci, J.; Krempner, C.; Wiggenhorn, C., (2006). "Comments on the ring-opening polymerization of morpholine-2,5-dione derivatives by various metal catalysts and characterization of the products formed in the reactions involving R(2)SnX(2), Where X = OPr(i) and NMe(2) and R = Bu(n), Ph and p-Me(2)NC(6)H(4)", Dalton Transactions, 6, 846-851.

[24] Cho, C.S.; Jeong, Y.I.; Ishihara , T.; Takei, R.; Park, J.U.; Park, K.H.; Maruyama, A.; Akaike, T., (1997). "Simple preparation of nanoparticles coated with carbohydrate-carrying polymers", Biomaterials, 18, 323–326.

[25] Cho, K.; Wang, X.; Nie, S.; Chen, Z.; Shin, D. M., (2008). "Therapeutic Nanoparticles for Drug Delivery in Cancer, Cancer Nanotherapeutics for Drug Delivery", Clinical Cancer Research, 14,1310-1316.

[26] Chu, C. C. J. (1981). "Hydrolytic degradation of polyglycolic acid: Tensile strength and crystallinity study", Journal of Applied Polymer Science, 26, 1727-l 734.

[27] Cooper, J.A.; Lu, H.H.; Ko, F.K.; Freeman, J.W.; Laurencin, C.T., (2005). "Fiber-based tissue-engineered scaffold for ligament replacement: design considerations and in vitro evaluation", Biomaterials, 26,1523–32.

[28] Curcio, M.; Gianfranco Spizzirri, U.; Iemma, F.; Puoci, F.; Cirillo, G.; Parisi, O.I.; Picci, N., (2010). "Grafted thermo-responsive gelatin microspheres as delivery systems in triggered drug release", European Journal of Pharmaceutics and Biopharmaceutics, 76, 48–55.

[29] Davis, M. E.; Chen, Z. G.; Shin, D. M., (2008)." Nanoparticle therapeutics: an emerging treatment modality for cancer", Nature Reviews Drug Discovery, 7, 771–782.

[30] Davis, S. S., (1997). "Biomedical applications of nanotechnology -implications for drug targeting and gene therapy", Journal of Trends in Biotechnology, 15, 217-224.
Dhal, P. K.; Polomoscanik, S. C.; Avila, L. Z.; Holmes-Farley, S. R.; Miller, R. J.,

(2009). "Functional polymers as therapeutic agents: Concept to market place", Advanced Drug Delivery Reviews, 61, 1121–1130

[31] Djuric, Z.; Malviya, V.K.; Deppe, G.; Malone, J.; McGunagle, D.L.; Heilbrun, L.K.; Reading, B.A.; Lawrence, W.D., (1990). "Detoxifying enzymes in human ovarian tissues: comparison of normal and tumor tissues and effects of chemotherapy", Journal of Cancer Research and Clinical Oncology, 116, 379–383.

[32] Dongin, K.; Seong, E. L.; Taek, K. O.; Gao, Z. G.; Han, Y. B., (2008). "Doxorubicin-Loaded Polymeric Micelle Overcomes Multidrug Resistance of Cancer by Double-Targeting Folate Receptor and Early Endosomal pH", Small, 4, 2043-2050.

[33] Dreis, S.; Rothweiler, F.; Michaelis, M.; Cinatl, J.; Kreuter, J.; Langer, K., (2007). "Preparation, characterisation and maintenance of drug efficacy of doxorubicin-loaded human serum albumin (HSA) nanoparticles", International Journal of Pharmaceutics, 341, 207–214.

[34] Elsabahy, M.; Wooley, K. L., (2012). "Design of polymeric nanoparticles for biomedical delivery applications: Review", Chemical Society Reviews, 41, 2545.

[35] Enomoto, K.; Ajioka, M.; Yamaguchi, A., (1994). "Polyhydroxycarboxylic acid and preparation process thereof, US Patent 5310865".

[36] Esser-Kahn, A. P.; Sottos, N. R.; White,S. R.; Moore, J. S., (2010). "Programmable Microcapsules from Self-Immolative Polymers", Journal of the American Chemical Society, 132, 10266–10268.

[37] Estey, T.; Kang, J.; Schwendeman, S. P.; Carpenter, J. F., (2006). "BSA degradation under acidic conditions: a model for protein instability during release from PLGA delivery systems", Journal of Pharmaceutical Sciences, 95, 1626-1639.

[38] Estrela, J.M.; Ortega, A.; Obrador, E., (2006). " Glutathione in cancer biology and therapy", Journal of Critical Reviews in Clinical Laboratory Sciences, 43, 143–181. European Polymer Journal, 49, 706-717.

[39] Fan, B.; John F. Trant, Andrew D. Wong, and Elizabeth R. Gillies, (2014). "Polyglyoxylates: A Versatile Class of Triggerable Self-Immolative Polymers from Readily Accessible Monomers", Journal of American Chemical Society, 136, 10116−10123.

[40] Fang, J.; Nakamura, H.; Maeda, H., (2011). "The EPR effect: Unique features of tumor blood vessels for drug delivery, factors involved, and limitations and augmentation of the effect", Advanced Drug Delivery Reviews, 63, 136-151.

[41] Farokhzad, O. C.; Langer, R., (2006). "Nanomedicine: Developing smarter therapeutic and diagnostic modalities", Advanced Drug Delivery Reviews, 58, 1456–1459.

[42] Farokhzad, O.C.; Langer, R.;(2009). "Impact of Nanotechnology on Drug Delivery". ACS Nano, 3, 16-20.

[43] Fishbein, I.; Chorny,M.; Rabinovich, L.; Banai, S.; Gati, I., (2000). "Nanoparticulate delivery system of a tyrphostin for the treatment of restenosis", Controlled Release 65 (1–2) 221–229.

[44] Franco, R.; Schoneveld, O.J.; Pappa, A.; Panayiotidis, M.I., (2007). "The central role of glutathione in the pathophysiology of human diseases", Archives of Physiology and

Biochemistry, 113, 234–258.

[45] Fujishige, S.; Kubota, K.; Ando, I.; (1989). "Phase transition of aqueous solutions of poly(N-isopropylacrylamide) and poly(N-isopropylmethacrylamide)", Journal of Physical Chemistry, 93, 3311–3313.

[46] Fukushima, K.; Feijoo, L. J.; Yang, M.-C., (2013). "Comparison of abiotic and biotic degradation of PDLLA, PCL and partially miscible PDLLA/PCL blend", European Polymer Journal, 49 (3), 706-717

[47] Ganta, S.; Devalapally, H.; Shahiwala, A.; Amiji, M., (2008). "A review of stimuli-responsive nanocarriers for drug and gene delivery", Controlled Release, 126, 187-204.

[48] Gao, H.; Wang, Y.N.; Fan, Y.G.; Ma, J.B., (2005). "Synthesis of a biodegradable tadpole-shaped polymer via the coupling reaction of polylactide onto mono(6-(2-aminoethyl)amino-6-deoxy)-beta-cyclodextrin and its properties as the new carrier of protein delivery system", Controlled Release 107 (1) 158–173.

[49] Gradishar, W. J.; Tjulandin, S.; Davidson, N., (2005). "Phase III trial of nanoparticle albumin-bound paclitaxel compared with polyethylated castor oil-based paclitaxel in women with breast cancer". Journal of Clinical Oncology, 23, 7794-7803.

[50] Grijpma, D.W.; Nijenhuis, A.J.; Pennings, A.J., (1990). "Synthesis and hydrolytic degradation behaviour of high-molecular-weight l-lactide and glycolide copolymers", Polymer, 31, 2201–2206.

[51] Guo, K.; Chu, C. C., (2009). "Biodegradable and Injectable Paclitaxel-Loaded Poly(ester amide)s Microspheres: Fabrication and Characterization", Journal of Biomedical Materials Research Part B: Applied Biomaterials, 89, 491–500.

[52] Guo, R.; Chu, C.-C., (2007). " Biodegradation of unsaturated poly(ester-amide)s and their hydrogels", Biomaterials, 28, 3284-3294.

[53] Hayashi, T., (1994), "Biodegradable polymers for biomedical uses", Progress in Polymer Science, 19, 663-702.

[54] Hobbs, S.K.; Monsky, W.L.; Yuan, F.; Roberts, W.G.; Griffith, L.; Torchilin, V.P.; Jain, R.K.; (1998). "Regulation of transport pathways in tumor vessels: Role of tumor type and microenvironment", Proceedings of the National Academy of Sciences of the United States of America, 95, 4607-4612.

[55] Horwitz, J. A.; Shum, K. M.; Bodle, J. C.; Deng, M.X.; Chu, C.-C.; Reinhart-King, C. A., (2010). "Biological performance of biodegradable amino acid-based poly(ester amide)s: Endothelial cell adhesion and inflammation in vitro", Journal of Biomedical Materials Research, 95, 371–380.

[56] Huang, Y.; Wang, L.; Li, S.; Liu, X.; Lee, K.; Verbeken, E.; Werf, F.V.; de Scheerder, I., (2006). "Stent-based tempamine delivery on neointimal formation in a porcine coronary model", Acute Cardiac Care, 8, 210-216.

[57] Ishihara, T.; Kubota, T.; Choi, T.; Higaki, M., (2009). "Treatment of Experimental Arthritis with Stealth-Type Polymeric Nanoparticles Encapsulating Betamethasone Phosphate", Journal of Pharmacology and Experimental Therapeutics, 329, 412-417.

[58] Iyer, A. K.; Khaled, G.; Fang, J.; Maeda, H., (2006), "Exploiting the enhanced permeabilityand retention effect for tumor targeting", Drug Discovery Today, 11, 812-

818.

[59] Jiang, J.; Tong, X.; Zhao, Y., (2005). "A new design for light-breakable polymer micelles". Journal of Am. Chem. Soc., 127, 8290−8291.

[60] Jiao,Y.; Ubrich, N.; Marchand-Arvier, M.; Vigneron, C.; Hoffman, M.; Lecompte, T.; Main-cent, P.; (2002). "In vitro and *in vivo* evaluation of oral heparin-loaded polymeric nanoparticles in rabbits", Circulation, 105, 230–235.

[61] Kamaly, N.; Xiao, Z.; Valencia, P. M.; Radovic-Moreno, A. F.; Farokhzad, O. C.; (2012). "Targeted polymeric therapeutic nanoparticles: design, development and clinical translation: Review Chemical Society Reviews, 41, 2971.

[62] Kim, J.-H.; Kim, Y.-S.; Kim, S.; Park, J.H.; Kim, K.; Choi, K.; Chung, H.; Jeong S.Y.; Park, R.-W.; Kim, I.-S.; Kwon, I.C., (2006). "Hydrophobically modified glycol chitosan nanoparticles as carriers for paclitaxel", Controlled Release, 111, 228-234.

[63] Kim, J.-K.; Garripelli, V. K.; Jeong, U.-H.; Park, J.-S.; Repka, M. A.; Jo, S.,g., (2010). "Novel pH-sensitive polyacetal-based block copolymers for controlled drug delivery", International Journal of Pharmaceutics, 401, 79–86.

[64] Knight, D. K.; Gillies, E. R.; Mequanint, K., (2011). "Strategies in Functional Poly(ester amide) Syntheses to Study Human Coronary Artery Smooth Muscle Cell Interactions", Biomacromolecules, 12, 2475–2487.

[65] Langer, R.; Folkman, J., (1976). " Polymers for the sustained release of proteins and other macromolecules", Nature, 263, 797–800.

[66] Lecomte, P.; Jérôme, R.; (2005). "New developments in the synthesis of aliphaticpolyesters by ring-opening polymerization", Biodegradable Polymers for Polymer Industrial Applications, 77−106.

[67] Lee, S. H.; Szinai, I.; Carpenter, K.; Katsarava, R.; Jokhadze, G.; Chu, C.-C.; Huang, Y.; Verbeken, E.; Bramwell, O.; De Scheerder, I.; Hong, M. K., (2002). "In-vivo biocompatibility evaluation of stents coated with a new biodegradable elastomeric and functional polymer", Coronary Artery Disease, 13, 237-241.

[68] Lee, S.H.; Zhang, Z.; Feng, S.S., (2007). "Nanoparticles of poly(lactide)-tocopheryl polyethylene glycol succinate (PLA-TPGS) copolymers for protein drug delivery", Biomaterials, 28, 2041–2050.

[69] Liu, X.M.; Quan, L.D.; Tian, J.; Alnouti, Y., Fu, K., Thiele, G.M.; Wang, D., (2008). "Synthesis and evaluation of a well-defined HPMA copolymer-dexamethasone conjugate for effective treatment of rheumatoid arthritis", Pharmaceutical Research, 25, 2910-2919.

[70] Lou, X.; Detrembleur, C.; Jérôme, R., (2003)." Novel aliphatic polyesters based on functional cyclic (di)esters", Macromolecular Rapid Communications24, 161−172.

[71] Lu, H.H.; Cooper, J.A.; Manuel, S.; Freeman, J.W.; Attawia, M.A.; Ko, F.K., (2005). "Anterior cruciate ligament regeneration using braided biodegradable scaffolds: in vitro optimization studies", Biomaterials, 26, 4805–16.

[72] Marty, J. J.; Oppenheim, R. C.; Speiser, P., (1978). "Nanoparticles--a new colloidal drug delivery system", Pharmaceutica Acta Helvetiae, 53, 17-23.

[73] Matsumoto, J.; Nakada,Y.; Sakurai, K.; Nakamura,T.; Takahashi, Y., (1999).

"Preparation of nanoparticles consisted of poly(l-lactide)–poly(ethylene glycol)–poly(l-lactide) and their evaluation in vitro", International Journal of Pharmaceutics. 185, 93–101.

[74] Merisko-Liversidge, E.; Liversidge, G. G.; Cooper, R E., (2003) "Nanosizing: a formulation approach for poorly water-soluble compounds", European Journal of Pharmaceutical Sciences, 18, 113–120.

[75] Meyer, D.E.; Shin, B.C.; Kong, G.A.; Dewhirst, M.W.; Chilkoti, A., (2001). "Drug targeting using thermally responsive polymers and local hyperthermia", Journal of Control Release, 74, 213–224.

[76] Miller, R.A.; Brady, J.M.; Cutright, D.E., (1977). "Degradation rates of oral resorbable implants (polylactates and polyglycolates: rate modification with changes in PLA/PGA copolymer ratios", Journal of Biomedical Materials Research, 11, 711–9.

[77] Moghimi, S.M.; Hunter, A.C.; Murray, J.C., (2001). "Long-circulating and target specific nanoparticles: theory to practice", Pharmacological Reviews, 53, 283–318.

[78] Nair, L. S.; Laurencin, C. T., (2007). "Biodegradable polymers as biomaterials", Progress in Polymer Science, 32, 762-798.

[79] Nicolas, J.; Mura, S.; Brambilla, D.; Mackiewicz, N.; Couvreur, P., (2013). "Design, functionalization strategies and biomedical applications of targeted biodegradable/biocompatible polymer-based nanocarriers for drug delivery: Review", Chemical Society Reviews, 42, 1147.

[80] Owens 3rd, D.E.; Peppas, N.A.; (2006). "Opsonization, biodistribution, and pharmacoki netics of polymeric nanoparticles", International Journal of Pharmaceutics, 307, 93–102.

[81] Oyewumi, M.O.; Yokel, R.A.; Jay, M.; Coakley, T.; Mumper, R.J., (2004). "Comparison of cell uptake, biodistribution and tumor retention of folate-coated and PEG-coated gadolinium nanoparticles in tumor-bearing mice", Controlled Release, 95, 613-626.

[82] Paredes, N.; Rodriguez-Galan, A.; Puiggali, J., (1998). "Synthesis and Characterization of a Family of Biodegradable Poly(ester amide)s Derived from Glycine", Polymer Science Part A: Polymer Chemistry 36, 1271–1282.

[83] Peer, d.; Karp, j. M.; Hong, S.; Farokhzad, O. C.; Margalit, R.; Langer, R., (2007). "Nanocarriers as an emerging platform for cancer therapy", Nature nanotechnology, 2.

[84] Penczek, S.; Cypryk, M.; Duda, A.; Kubisa, P.; Slomkowski, S., (2007). "Livingring-opening polymerisations of heterocyclic monomers", Progress in Polymer Science, 32, 247–282.

[85] Piedra-Arroni, E.; Brignou, P.; Amgoune, A.; Guillaume, S. M.; Carpentier, J.-F.; Bourissou, D., (2011). "A dual organic/organometallic approach for catalytic ring-opening polymerization", Chemical Communications, 47, 9828–9830.

[86] Radin, N.S., (2001). "Killing cancer cells by poly-drug elevation of ceramide levels: a hypothesis whose time has come?", European Journal of Biochemistry, 268, 193–204.

[87] Rathi, S. R.; Coughlin, E. B.; Hsu, S. L.; Golub, C. S.; Ling, G. H.; Tzivanis, M., (2012). "Effect of midblock on the morphology and properties of blends of ABA

triblock copolymers of PDLA-mid-block-PDLA with PLLA", Polymer, 53, 3008-3016.

[88] Ren, J., (2010). "Synthesis and Manufacture of PLA", Biodegradable Poly(Lactic Acid): Synthesis, Modification, Processing and Applications, Springer, 15-37.

[89] Rodriguez-Galan, R.; Franco, A.; Puiggali, L.; Degradable J., (2011). "Poly(ester amide)s for biomedical applications: Review", Polymers, 3, 65-99.

[90] Ryu, J.H.; Roy, R.; Ventura, J.; Thayumanavan, S., (2010). "Redox-sensitive disassembly of amphiphilic copolymer based micelles", Langmuir, 26, 7086–7092.

[91] Sagi, A.; Weinstain, R.; Karton, N.; Shabat, D., (2008). "Self-Immolative Polymers", Journal of the American Chemical Society, 130, 5434–5435.

[92] Sanchez, A.; Tobio, M.; Gonzalez, L.; Fabra, A.; Alonso, M.J., (2003). "Biodegradable micro-and nanoparticles as long-term delivery vehicles for interferon-alpha", European Journal of Pharmaceutical Sciences, 18, 221–229.

[93] Schafer, F.Q.; Buettner, G.R., (2001). "Redox environment of the cell as viewed through the redox state of the glutathione disulfide/glutathione couple", Free Radical Biology & Medicine, 30, 1191–1212.

[94] Schnitzer, J.E., (1998). "Vascular Targeting as a Strategy for Cancer Therapy", New England Journal of Medicine, 339, 472-474.

[95] Seki, T.; Fang, J.; Maeda, H., (2009). "Tumor-targeted macromolecular drug delivery based on the enhanced permeability and retention effect in solid tumor", In Pharmaceutical Perspectives of Cancer Therapeutics, Lu, Y.; Mahato, R. I., Springer US, 93-120.

[96] Shao, J.; Sun, J.; Bian, X.; Cui, Y.; Li, G.; Chen, X., (2012). "Investigation of Poly(lactide) Stereocomplexes: 3-Armed Poly(l-lactide) Blended with Linear and 3-Armed Enantiomers", Journal of Physical Chemistry B, 116, 9983-9991.

[97] Simone, E.A.; Dziubla, T.D.; Colon-Gonzalez, F.; Discher, D.E.; Muzykantov, V.R., (2007). "Effect of polymer amphiphilicity on loading of a therapeutic enzyme into protective filamentous and spherical polymer nanocarriers", Biomacromolecules, 8, 3914-3921.

[98] Sionkowska, A., (2011). "Current research on the blends of natural and synthetic polymers as new biomaterials: Review", Progress in Polymer Science, 36, 1254-1276.

[99] Soleimani, A.; Drappel, S.; Carlini, R.; Goredema, A.; Gillies, E., (2014). "Structure–Property Relationships for a Series of Poly(ester amide)s Containing Amino Acids", Journal of Industrial and Engineering Chemistry, 53, 1452–1460.

[100] Sortino, S., (2012). "Photoactivated nanomaterials for biomedical release applications: Review", Journal of Mater. Chem., 22, 301−318.

[101] Stavrovskaya, A.A., (2000). "Cellular mechanisms of multidrug resistance of tumor cells", Biochemistry Moscow, 65, 95–106.

[102] Stjerndahl, A.; Wistrand, A.F.; Albertsson, A.C., (2007). "Industrial utilization of tin-Initiated resorbable polymers: synthesis on a large scale with a low amount of initiator, Biomacromolecules", 8, 937–940.

[103] Storma, G.; Belliota, S.O.; Lasicc, T.D.D.; (1995). "Surface modification of nanoparticles to oppose uptake by the mononuclear phagocyte system", Advanced

Drug Delivery Reviews, 17, 31-48.

[104] Stover, T.C.; Kim, Y.S.; Lowe, T.L.; Kester, M., (2008). "Thermoresponsive and biodegradable linear-dendritic nanoparticles for targeted and sustained release of a pro-apoptotic drug", Biomaterials, 29, 359–369.

[105] Sun, H.; Meng, F.; Dias, A.; Hendriks, M.; Feijen, J.; Zhong, Z., (2011). "α-Amino acid containing degradable polymers as functional biomaterials: Rational design, synthetic pathway, and biomedical applications:Review", Biomacromolecules, 12,1937-1955.

[106] Tian, D.; Dubois, P.; Grandfils, G.; Jérôme, J. (1997). "Ring-Opening Polymerization of 1,4,8-Trioxaspiro[4.6]-9-undecanone: A New Route to Aliphatic Polyesters Bearing Functional Pendent Groups", Macromolecules, 30, 406-409.

[107] Tirelli, N., (2006). "(Bio)Responsive nanoparticles", Journal of Current Opinion in Colloid & Interface Science,11, 210-216.

[108] Tong, R.; Cheng, J., (2008). "Paclitaxel-Initiated, Controlled Polymerization of Lactide for the Formulation of Polymeric Nanoparticulate Delivery", Journal of Angewandte Chemie International Edition, 47, 4830 –4834.

[109] Torchilin, V.P.; Lukyanov, A.N.; Gao, Z.; Papahadjopoulos-Sternberg, B., (2003). "Immunomicelles: Targeted pharmaceutical carriers for poorly soluble drugs", Proceedings of the National Academy of Sciences of the United States of America, 100, 6039-6044.

[110] Torchilin, V.P.; Trubetskoy, V.S., (1995). "Which polymers can make nanoparticulate drug carriers long-circulating?", Advanced Drug Delivery Reviews, 16, 144-155.

[111] Ulbrich, K.; Subr, V., (2004). "Polymeric anti cancer drugs with pH-controlled activation", Journal of Advanced Drug Delivery Reviews, 56, 1023–1050.

[112] Valko, M.; Leibfritz, D.; Moncol, J.; Cronin, M.T.D.; Mazur, M.; Telser, J., (2007). "Free radicals and antioxidants in normal physiological functions and human disease", The International Journal of Biochemistry & Cell Biology, 39, 44–84.

[113] Wang, D.; Miller, S.; Liu, X.-M.; Anderson, B.; Wang, X.S.; Goldring, S., (2007). "Novel dexamethasone-HPMA copolymer conjugate and its potential application in treatment of rheumatoid arthritis". Arthritis Research & Therapy, 9, R2.

[114] Williams, C.K., (2007). " Synthesis of functionalized biodegradable polyesters", Chemical Society Reviews, 36 1573–1580.

[115] Wong, A. D.; DeWit, M. A.; Gillies, E. R., (2012) "Amplified release through the stimulus triggered degradation of self-immolative oligomers, dendrimers, and linear polymers", Advanced Drug Delivery Reviews, 64, 1031–1045.

[116] Woodruff, M.A.; Hutmacher, D.W., (2010). "The return of a forgotten polymer—Polycaprolactone in the 21st century", Progress in Polymer Science, 35, 1217-1256.

[117] Xing, J.; Zhang, D.; Tan, T., (2007). "Studies on the oridonin-loaded poly(d,l-lactic acid) nanoparticles in vitro and *in vivo*:, International Journal of Biological Macromolecules, 40, 153–158.

[118] Xiong, X. B.; Lavasanifar, A., (2011). "Traceable Multifunctional Micellar Nanocarriers for Cancer-Targeted Co-delivery of MDR-1 siRNA and Doxorubicin",

ACSNANo, 5, 5202–5213.

[119] Xu, H.; Deng, Y.; Chen, D.; Hong, W.; Lu, Y.; Dong, X., (2008). "Esterase-catalyzed dePEGylation of pH-sensitive vesicles modified with cleavable PEG-lipid derivatives", Controlled Release, 130, 238-245.

[120] Yang, J.; Webb, A. R.; Ameer, G. A., (2004). "Novel Citric Acid Based Biodegradable Elastomers for Tissue Engineering", Advanced Materials, 16, 471–566.

[121] Yao, J.; Ruan, Y.; Zhai, T.; Guan, J.; Tang, G.; Li, H.; Dai, S., (2011). "ABC block copolymer as "smart"pH-responsive carrier for intracellular delivery of hydrophobic drugs", Polymer ,52,3396–3404.

[122] York, W. A.; Kirkland, E. S.; McCormick, L. C., (2008). "Advances in the synthesis of amphiphilic block copolymers via RAFT polymerization: Stimuli-responsive drug and gene delivery", Advanced Drug Delivery Reviews, 60, 1018–1036.

[123] Zhang, H.; Yan, Q.; Kang, Y.; Zhou, L.; Zhou, H.; Yuan, J.; Wu, S., (2012). "Fabrication of thermo-responsive hydrogels from star-shaped copolymer with a biocompatible β-cyclodextrin core", Polymer (United Kingdom), 53, 3719–3725.

[124] Zhang, Z.; Grijpma, D.W.; Feijen, J., (2006). "Poly(trimethylene carbonate) and monomethoxy poly(ethylene glycol)-block-poly(trimethylene carbonate) nanoparticles for the controlled release of dexamethasone", Controlled Release, 111, 263-270.

Chapter 3 Covalent Drug Immobilization in Poly(Ester Amide) Nanoparticles for Controlled Drug Release

3.1 Introduction

In recent years, there has been an increasing interest in using nanotechnology for the delivery of small molecule drugs as well as macromolecular drugs such as peptides, proteins, and nucleic acids (Moghimi *et al.*, 2001). Therapeutic NPs offer many potential advantages including enhanced therapeutic efficacy of the drug by increasing its concentration at the site of action, improved transport across biological barriers such as cell membranes, the ability to deliver a drug and imaging agent simultaneously, and improved pharmacological and pharmaceutical characteristics relative to the free drug (Farokhzad and Langer, 2009; Burgess *et al.*, 2010). NPs based on biodegradable polymers have been demonstrated to be an important class of controlled release systems because of their physiochemical properties, degradation, and biocompatibility (York *et al.*, 2008; Bae and Kataoka, 2009; Dhal *et al.*, 2009). In addition, they are able to overcome the limitations associated with liposomes, including low drug loadings, problematic phospholipid oxidation and low shelf stability (Drummond *et al.*, 1999; Davis, 2009; Shai *et al.*, 2011). Polymeric NPs can provide high drug loading capacities and can also employ controlled and triggered release profiles (Caldorera-Moore *et al.*, 2011). Polymeric NPs have been investigated in many different fields of medicine including pulmonary disease, pain, neurology, and cardiology (Farokhzad and Langer, 2006). The most commonly used polymers for controlled release applications are the family of linear aliphatic polyesters including PLGA, PLA, and PGA (Acharya and Sahoo, 2011) due to their favourable characteristics of biodegradability and biocompatibility (Anderson and Shive, 1997).

In addition to aliphatic polyesters, PEAs have emerged as a promising family of biodegradable materials (Guo and Chu, 2007). The ester linkages throughout the backbone can be degraded through enzymatic or non-enzymatic hydrolysis, while the amide bonds can be degraded enzymatically (Jokhadze *et al.*, 2007). In addition, the amides impart good thermal and mechanical properties. There are several different backbone structures for PEAs, but PEAs containing α-amino acids are of particular interest because of their biomimetic nature, as α-amino acids are the main constituents of proteins. In addition, the ability to

incorporate amino acids such as L-lysine and L-aspartic acid, which have pendant functional groups, was recently demonstrated through the use of protecting group strategies (Atkins *et al.*, 2009), and offers the possibility to functionalize these pendant groups on the polymer after protecting group removal. PEAs containing α-amino acids have recently been investigated in vascular tissue engineering (Knight *et al.*, 2011) and in vascular grafts (Horwitz *et al.*, 2010). In these applications, they have been shown to be well tolerated by cells, non-immunogenic and to support cell growth. Guo and Chu, (2009) successfully fabricated PEA microspheres in good yield and with narrow size distribution and used them to encapsulate the anti cancer drug Pxtl. However, these microparticles, with diameters of slightly less than 1 μm, would be too large to circulate in the vasculature as they would be rapidly taken up by the reticuloendothelial system. This would limit their use to localized administration.

With the aim of addressing the limitations of the micrometer-sized PEA particles described above, this chapter describes the development of procedures to prepare PEA particles with diameters less than 200 nm. Such particles have the potential to deliver drugs intravascularly, providing targeting of diseased sites such as tumours through the EPR effect. It has also been demonstrated in some cases that only submicrometer-sized particles were taken up as in Hepa 1-6, HepG2, and KLN 205 (Zauner *et al.*, 2001). Additionally, some studies have demonstrated that the range of 100 nm nanoparticle showed 6 times greater uptake than 10 μm particles and 2.5 times greater uptake than 1 μm particles (Desai *et al.*, 1996). In addition, to address the burst release problem associated with many nanoparticle-based delivery systems, where a large fraction of the drug is rapidly released upon immersion of the nanoparticle in a buffer system, we utilize the group's PEAs having pendant carboxylic acid groups to covalently conjugate first a dye molecule as a model drug, and then the anti cancer drug molecule floxuridine. The effect of this covalent conjugation on the drug's release rate is investigated.

3.2 Materials and Methods

All materials were purchased from commercial suppliers and used as received unless otherwise noted. Poly(vinyl alcohol) (PVA) with a molar mass of 31 kg/mol and a hydrolysis degree of 86.7-88.7 mol% (PVA 4-88), was purchased from Sigma-Aldrich. Floxuridine (5-

fluoro-2'-deoxyuridine) was purchased from Alfa Aesar. Solvents were purchased from Caledon. CH_2Cl_2, triethylamine (NEt_3), and *N,N*-diisopropylethylamine (DIPEA) were distilled from CaH_2 immediately before use. Anhydrous *N,N*-dimethylformamide (DMF) was obtained from solvent purification system using aluminium hydroxide columns. Dialyses were performed using Spectra/Por regenerated cellulose membranes with 1, 3.5 and 50 kg/mol molecular weight cutoffs (MWCO). ^{1}H NMR spectra were obtained on a Varian Inova 400 spectrometer (Varian Canada Inc., Mississaga, ON.). Chemical shifts were reported in parts per million, and calibrated against residual solvent signals of $(CD_3)_2SO$ (Chemical shifts (δ) 2.0 and 39.52 ppm) or $CDCl_3$ (δ 7.27). All coupling constants (*J*) were reported in Hz. Fourier transform infrared (FTIR) spectra were attained on KBr disks using a Bruker Tensor 27 instrument. UV-visible absorption spectroscopy was performed using a Varian Cary 300 Bio spectrophotometer. Size exclusion chromatography (SEC) was performed at 85 ℃ in DMF with 0.1 M LiBr and 1% (v/v) NEt_3. The calibration was prepared using polystyrene standards. Deionized water was obtained from a Millipore purification system.

3.2.1 Physiochemical Characterization of the NPs

a) Particle diameter

Nanoparticle diameter was determined by dynamic light scattering (DLS) using a Zetasizer Nano ZS instrument (Malvern Instruments) at a concentration of 0.05 mg/mL in deionized water. The analysis was performed at 25 ℃. Values reported are the mean diameter and Z-average with the standard deviation, along with polydispersity. Each measurement was performed in triplicate and measured after filtration (using 0.2 µm syringe filter).

b) Zeta potential

The zeta potentials of the particles were determined by using a Zetasizer Nano ZS instrument (Malvern Instruments). Measurements were performed in deionized water at neutral pH. Each measurement was performed in triplicate.

c) Transmission electron microscopy

A suspension of NPs (0.01 mL, 0.05 mg/mL) was deposited onto a Formvar/carbon grid and left for 2 minutes, then the excess liquid was blotted off using a piece of filter paper. TEM

images were obtained using a Philips CM10 microscope operating at 80 KV with a 40 μm aperture.

d) Scanning electron microscopy

Morphological evaluation of the NPs was performed using scanning electron microscopy (SEM) (SmartSEM microscope, supra 55vp, Carl Zeiss SMT LTD). The freeze-dried NPs were dispersed in water and mounted over metallic studs, then coated with osmium oxide using a sputter coater. Images were taken at various magnification ranges in order to study nanoparticle morphology.

3.2.2 Optimization of nanoparticle preparation

a) Synthesis of PEA 1 without pendant functional groups

PEA **1** was prepared via a solution polycondensation method as previously reported by our group (Atkins *et al.*, 2009). The molar mass characteristics for this batch as determined from SEC are as follows: $M_n = 20$ kg/mol; $M_w = 25$ kg/ mol; PDI= 1.3.

b) Preparation of PEA NPs

PVA was selected as the emulsifying agent. The influence of other parameters such as organic solvent:water ratio, concentration of PEA in the organic phase, concentration of PVA in aqueous phase, and the use of concentrated salt on particle diameter were evaluated and these parameters are summarized in Table 3-1, Table 3-2, Table 3-3, and Table 3-4. The following different nanoparticle preparation methods were used, followed by a common purification procedure described below. Each preparation was performed in triplicate.

Emulsification-evaporation: 5 mg of PEA was dissolved in 1 mL of chloroform, and then poured into 5 mL of water containing PVA at concentrations of 2, 10, 14, 18, or 40 mg/mL). The two-phase solution was subjected to sonication for 2 minutes: 30 seconds on and 10 seconds off (Branson 450 digital sonifier using an amplitude of 25%,). The resulting emulsion was stirred for 3 hours to evaporate the organic solvent.

Emulsification-evaporation using MgCl$_2$ Salt (Salting-out): 3 mL of water containing PVA at concentrations of 2, 10, 14, 18, and 40 mg/mL and 2 mL of 30 wt. % MgCl$_2$ were

poured into 1 mL of CHCl$_3$ containing 5 mg of PEA. The two-phase solution was subjected to the same sonication and evaporation procedure described above.

Nanoparticle Purification: Following the evaporation procedure, the nanoparticle suspension was transferred to a 50 kg/mol MWCO dialysis membrane and dialyzed against water for 24 hours with 3-4 changes of the water. The purified NPs were then lyophilized at 0.060 mBar and -80º C for 24 hours (Labconco Lyophilizer)).

3.2.3 Synthesis of a PEA with pendant functional moiety (2)

PEA **2** containing 10 mol% of aspartic acid monomer was prepared via a solution polycondensation method as previously reported by our group (Atkins *et al.*, 2009). The molar mass characteristics for this batch (in its protected form) as determined from SEC are as follows:. M$_n$ = 9.2 kg/mol; M$_w$ = 14 kg/mol; PDI= 1.5.

3.2.4 Preparation and study of rhodamine-containing NPs – a comparison of the noncovalent and covalent system

a) Synthesis of NPs with noncovalently incorporated rhodamine B

These NPs were prepared by the emulsification-evaporation method described above using 18 mg/mL PVA except that 2.5 mg of rhodamine B was added to the CHCl$_3$ phase. The particles were purified as described above.

b) Synthesis of a rhodamine-PEA conjugate 4

PEA **2** (0.056 g, 0.024 mmol of COOH groups, 1.0 equiv.) and rhodamine B 4-(3-hydroxypropyl) piperazine amide **3** (0.034 g, 0.061 mmol, 2.5 equiv. relative to the number of pendant carboxylic acids) (Nguyen and Francis, 2003) were dissolved in 1 mL of anhydrous CH$_2$Cl$_2$. *N,N'*-Dicyclohexylcarbodiimide (DCC) (0.013 g, 0.061 mmol, 2.5 equiv. relative to the number of pendant carboxylic acids), DMAP (0.0006 g, 0.005 mmol, 0.2 equiv. relative to the number of pendant carboxylic acids), and DPTS (0.0014 g, 0.005mmol, 0.2 equiv. relative to the number of pendant carboxylic acid) were added under nitrogen and the reaction mixture was covered by aluminum foil to prevent photo-bleaching and stirred for 24 hours. The unreacted rhodamine and byproducts were removed by dialysis against DMF for 24 hours using a 3.5 kg/mol MWCO dialysis membrane with 3 changes of the dialysate

during this time period. The solvent was removed *in vacuo* to provide 0.064 g (71 % yield) of the conjugate **4** as a deep pink solid. The coupling efficiency was measured by UV-visible spectroscopy in DMF (relative to a calibration curve of rhodamine piperazine amide) to be ~40%, corresponding to 10 wt% of rhodamine in the polymer. FTIR (KBr pellet, cm^{-1}): 3313 (N-H stretch, amide), 3070 (C-H stretch, aromatic), 3026 (C-H stretch, aromatic), 2962 (C-H stretch, aliphatic), 2891 (C-H stretch, aliphatic), 1741 (C=O stretch, ester), 1652 (C=O stretch, amide), 1635(C=O stretch, tertiary amide in Rhodamine derivative), 1542 (N-H bend, C-H stretch, amide), 1498 (C=C stretch, aromatic), 1446 (CH$_2$ stretch, aliphatic), 1184 (C-O stretch, ester).

c) Preparation of NPs from the PEA conjugate

These NPs were prepared by the emulsification-evaporation method described above using 18 mg/mL PVA. The particles were purified as described above.

d) Release experiment for NPs containing noncovalently encapsulated and covalently-conjugated rhodamine

Lyophilized NPs were suspended in 3 mL deionized water and injected into a Slide-A-Lyzer dialysis cassette with a MWCO of 3.5 kg/mol. The dialysis cassette was suspended in 150 mL of 7.4 phosphate-buffered saline (PBS) and stirred at 37 °C. Aluminum foil was used to protect the system from light. The amount of released rhodamine in the dialysate was measured by UV-vis spectroscopy at 565 nm. For the NPs with noncovalent rhodamine, the 150 mL of PBS was replaced with the same amount of fresh PBS every 24 hours for 9 days and UV-vis measurements were performed at each of these time points. For the nanoparticle with covalently incorporated rhodamine, measurements were taken and the PBS was replaced every 24 hours for the first 7 days and then every 48 hours for the next 23 days.

3.2.5 Preparation and study of PEA NPs containing covalently immobilized floxuridine

a) Synthesis of a PEA-floxuridine conjugate 6

PEA **2** (0.28 g, 0.122 mmol of COOH groups, 1 equiv.), floxuridine **5** (0.06 g, 0.24 mmol, 2 equiv. relative to the number of pendant carboxylic acids), DIPEA (0.024 g, 0.18 mmol, 1.5 equiv. relative to the number of pendant carboxylic acids), EDC·HCl (0.08 g, 0.49 mmol, 4

equiv. relative to the number of pendant carboxylic acids), and DMAP (0.008 g, 0.006 mmol, 0.05 equiv. relative to the number of pendant carboxylic acids) were dissolved in 1 mL of anhydrous DMF. The reaction mixture was stirred for 24 hours at room temperature, and then purified using a 3.5 kg/mol MWCO dialysis membrane against DMF for 24 hours with multiple dialysate changes to remove unreacted floxuridine, reagents, and byproducts. The solvent was removed *in vacuo* to provide the conjugate **6** as a white solid (0.18 g, 41% yield). The coupling efficiency was 60% as determined by NMR spectroscopy, corresponding to 3.3 wt% of floxuridine on the polymer. ^{1}H NMR (400 MHz, DMSO-d_6,): δ 11.81-11.76 (m, 0.13 H), 9.85 (m, 0.05), 8.29-8.27 (m, 2.26 H), 8.16 (m, 0.1 H), 7.20-7.14 (m, 11.84 H), 6.08-6.07 (m, 0.15 H), 4.40-4.34 (m, 2.13 H), 3.97-3.87 (m, 5.01 H), 2.92-2.83 (m, 4.96 H), 2.21 (m, 4.49 H), 2.07-2.04 (m, 0.26 H), 1.33 (m, 4.32 H). FTIR (KBR pellet, cm^{-1}): 3334 (N-H stretch, amide), 3072 (C-H stretch, aromatic), 3038 (C-H stretch, aromatic), 2964 (C-H stretch, aliphatic), 2894 (C-H stretch, aliphatic), 1741 (C=O stretch, ester), 1658 (C=O stretch, amide), 1542 (N-H bend, C-H stretch, amide), 1508 (C=C stretch, aromatic), 1452 (CH_2 stretch, aliphatic), 1199 (C-O stretch, ester). SEC: M_n= 13 kg/ mol; M_w = 22 kg/mol; PDI= 1.7.

b) Preparation of NPs from the PEA-floxuridine conjugate

These NPs were prepared by the emulsification-evaporation method described above using 18 mg/mL PVA. The particles were purified as described above.

c) Release experiment for NPs from the PEA-floxuridine conjugate

40 mg of lyophilized NPs containing 1.29 mg of floxuridine were dissolved in deionized water (5 mL) and then the suspension was transferred to a 1 kg/mol MWCO dialysis membrane. The dialysis membrane was placed in 100 mL of PBS at 37 °C and stirred. Samples of the dialysate were collected every 6 hours for the first 24 hours and then every 24 hours for the next 13 days. At each time point the complete volume of PBS dialysate was replaced. The amount of released floxuridine was detected by HPLC. The experiment was performed in triplicate. The HPLC instrument comprised a Waters 2695 Separations Module, a Photodiode Array Detector (Waters 2998) and a Jupiter C18 5 μm (4.6 x 250mm) column connected to a C18 guard column. The PDA detector was used to monitor floxuridine at 265nm. Floxuridine separation was obtained using a gradient method with Solvent A being

water and Solvent B being acetonitrile with 1% TFA flowing at 1 mL/min. The gradient method involved Solvent A 100% decreasing to 44% over 25 minutes and then increasing back to 100% over the next 5 minutes. The column was then equilibrated for 5 minutes before the next run. The retention time of floxuridine was 6.97 min.

3.3 Result and Discussion

3.3.1 Optimization of nanoparticle preparation

While micrometer-sized PEA NPs were previously prepared (Guo and Chu, 2009), it was necessary to optimize conditions for the preparation of nanometer-sized particles. It was anticipated to be more difficult to prepare NPs in comparison to microparticles due to their larger surface:volume ratio. For the optimization of this protocol, PEA **1** (Figure 3-1), composed of phenylalanine, butanediol, and succinic acid, was selected as it would form the backbone for the desired drug conjugates and is easy and inexpensive to prepare. It was prepared by the previously reported procedure (Atkins *et al.*, 2009). An emulsification-evaporation method was selected because it uses water as the nonsolvent which simplifies and improves process economics, consequently facilitating the washing step and minimizing particle agglomeration (Aftabrouchard and Dorlker, 1992). Chloroform was chosen as the organic phase as it is a water immiscible solvent in which the PEA is soluble. This method involves two steps. The first step is the emulsification of the polymer solution into the aqueous layer, forming suspended nanodroplets. The second is evaporation of the organic solvent, inducing the formation of suspended solid NPs. A survey of different surfactants was performed in preliminary work, and PVA was chosen as the emulsifier since it has been commonly used in pharmaceutical preparations and has previously been shown to provide small, uniform, and dispersable particles in aqueous medium (Julienne *et al*., 1992). It is noteworthy to mention that Tween 20 was also explored but led to coagulation and significantly larger particles. At this stage, there were four other parameters to study in order to optimize the particle diameter: organic:water ratio, concentration of PEA in the organic layer, amount of surfactant used in aqueous layer, and the effect of high concentrations of salts in the salting-out method.
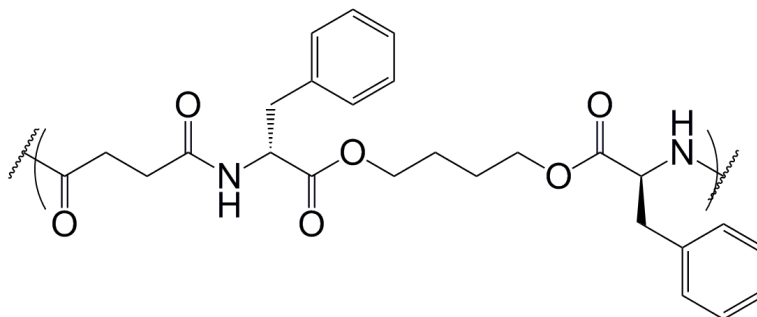
Figure 3-1: Chemical structure of PEA 1.

a) Effect of organic:aqueous ratio

First, the ratio between the organic and aqueous layer was studied. Fixing the amount of PEA constant, 5 mg of PEA **1** was dissolved in 0.5, 1, 2, or 3 mL of $CHCl_3$ and this organic phase was added to 5 mL of 18 mg/mL PVA in water solution. As shown in Table 3-1, the results showed that the ratio of 1:5 $CHCl_3$:water was the best in terms of providing the smallest particle diameter, with a Z-average diameter of 147 ± 5 nm. Larger diameters were obtained with other ratios. The polydispersity index (PDI) is acceptable at 0.15. Thus, this ratio was used to further optimization of NPs.

Table 3-1: Influence of different ratios between the organic and aqueous layer on diameter and diameter distribution of NPs prepared by emulsification-evaporation method using the same concentration of PVA of 18 mg/mL. This data resulted from three determinations from three different batches after filtration (using 0.2 μm syringe filter).

Ratio of $CHCl_3$:H_2O (mL:mL)	Z-average diameter[*] (nm)	PDI[*]	Mean diameter[*] (nm)
0.5: 5	235± 5	0.14±0.02	275±9
1: 5	147±5	0.15±0.01	173±6
2: 5	185±7	0.16±0.01	222±11
3:5	238±24	0.11±0.02	268±8

[*]Average ± SD

b) Effect of the concentration of PEA in organic layer

The effect of PEA concentration in $CHCl_3$ was investigated using concentrations ranging from 5 to 10 mg/mL. In general, an increase in the concentration of PEA led to an increase in the Z-average and mean diameter. As illustrated in Table 3-2, increasing the concentrations from 5 to 10 mg/mL increased the Z-average from 147 ± 5 to 275 ± 18 nm. This increase can be explained by the fact that at higher concentration a single droplet of organic phase would contain more polymer chains.

Table 3-2: Influence of different concentrations of PEA in the organic layer on the diameter and diameter distribution of NPs prepared by an emulsification-evaporation method using the concentration of PVA of 18 mg/mL. This data resulted from three determinations from three different batches after filtration (using 0.2μm syringe filter).

Concentration of PEA mg/mL	Z-average diameter[*] (nm)	PDI[*]	Mean diameter[*] (nm)
5	147±5	0.15±0.01	173±6
7	264±5	0.11±0.09	301±21
9	268±24	0.05±0.05	307±30
10	275±18	0.11±0.02	318±40

[*]Average ± SD

c) Effect of PVA concentration in the aqueous layer

Using a fixed concentration of 5 mg/mL of PEA in 1 mL of $CHCl_3$ and 5 mL of water optimized above, the influence of PVA concentration on nanoparticle diameter was also investigated. As illustrated in Table 3-3, as the concentration of PVA in the aqueous phase increased from 2 mg/mL to 18 mg/mL, the particle diameter decreased from 351 to 160 nm. At higher concentrations, no further decrease in diameter was observed. That can be explained by the fact that at 2 mg/mL, there was insufficient PVA to stabilize small droplets due to their high surface:volume ratio. However, at concentrations of 14 to 18 mg/mL of PVA, there was sufficient PVA to stabilize the small droplet and the NPs diameter decreased to 160 and to 177 nm, respectively. After using a 0.2 μm syringe filter, the particle diameter could be further reduced to 147 nm, without significant loss of material, as measured by DLS (Figure 3-2 and Figure 3-3). At higher PVA concentrations of 40 mg/mL, the Z-average diameters increased significantly again. This could be explained by a higher PVA concentration leading to increased PVA density at emulsion droplets, which in turn increased the thickness of PVA layer around the droplets. It was explained that the hydrophobic part of PVA is anchored into the polymeric droplets while the hydrophilic part is oriented into external aqueous phase. There it resists shear and imparts mechanical stability to the emulsion droplets, in addition to inducing steric effects that contributes to repulsion between droplets (Galindo-Rodriguez et al, 2004).

Table 3-3: Influence of PVA concentration nanoparticle diameter and diameter distribution prepared by emulsification-evaporation method. This data resulted from three determinations from three different batches.

PVA mg/mL	Without filtration			With filtration		
	Z-average diameter* (nm)	PDI*	Mean diameter* (nm)	Z-average* (nm)	PDI*	Mean diameter* (nm)
2	351±33	0.27±0.04	327±37	175±24	0.05±0.04	188±7
10	251±12	0.06±0.03	262±11	183±10	0.12±0.06	180±18
14	177±2	0.13±0.03	204±10	163±3	0.1±0.02	180±3
18	160±5	0.14±0.02	187±4	148±5	0.1±0.01	167±3
40	314±10	0.07±0.01	338±11	180±12	0.08±0.01	198±9

*Average ± SD

A

B
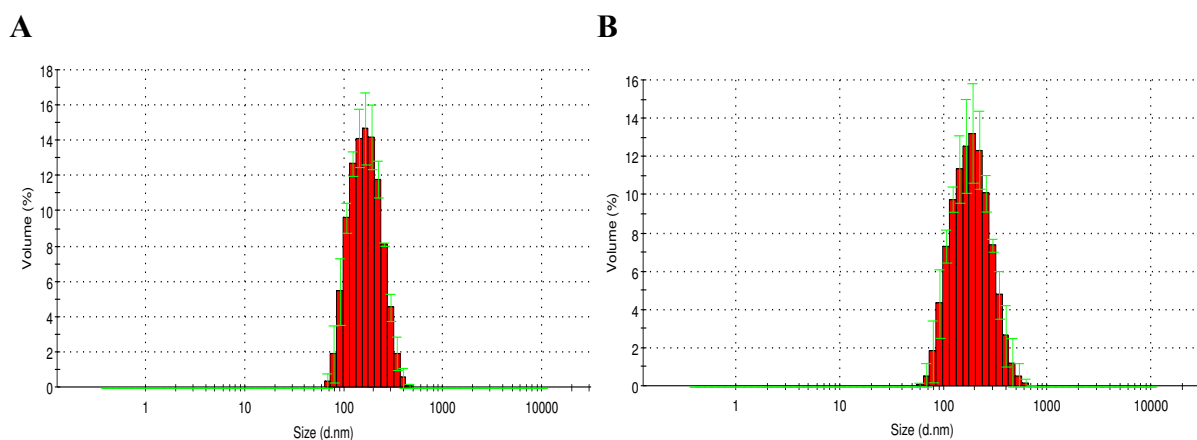
Figure 3-2: Particle diameter distribution of PEA NPs formed using 5 mL 14 mg/mL PVA in water and 1 mL of CHCl₃ containing 5 mg of PEA 1 via an emulsification-evaporation technique: (a) with filtration (using 0.2μm syringe filter). Z-average: 163±3 nm, and (b) Without filtration. Z-average: 177±2 nm.

A

B
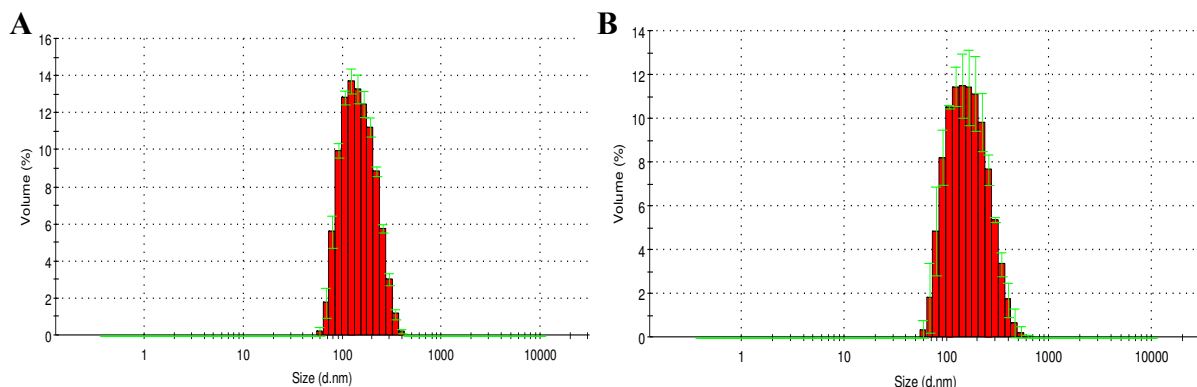
Figure 3-3: Particle diameter distribution of PEA nanoparticle formed from 5 mL aqueous solution of 18 g/L PVA (equals 90 mg PVA in 5 mL water) with 1 mL CHCl₃ containing 5 mg of base polymer via emulsification-evaporation technique, (a) with filtration (using 0.2μm syringe filter). Z-average: 148±5 nm, and (b) without filtration. Z-average: 160±5 nm.

d) Effect of using concentrated salt in the preparation

The influence of using of concentrated $MgCl_2$ in a technique called "salting-out" (Allémann *et al.*, 1993) with different concentrations of PVA was also studied and the results were compared with the above results using the standard emulsion-evaporation technique. As shown in Table 3-4, as the concentration of PVA increased from 2 to 18 mg/mL, the Z-average diameter decreased from 303±5 to 147±5 nm and the mean diameter decreased from 379±12 to 173±6 nm. Afterwards, by increasing the concentration to 40 mg/mL of PVA, the Z-average and mean diameter rose up to 379±10 and 414±48 nm respectively. Thus, overall the Z-average and the mean diameter values were smaller in presence of $MgCl_2$ solution at the range of 2 to 18 mg/mL of PVA. This suggests that this technique, used with 14-18 mg/mL PVA is the optimal procedure for nanoparticle preparation as shown in Figure 3-4 and Figure 3-5. However, at 40 mg/mL PVA solution, the Z-average and mean diameters were higher than the results from absence of the salt. These differences could be explained by the fact that the presence of concentrated $MgCl_2$ in the aqueous phase resulted in a decrease in solubility of PVA in this phase. This would induce more PVA to be present in or at the interface of the organic phase. In this study, a ratio of 1:5 $CHCl_3$:H_2O, concentration of 5 mg/mL of PEA in $CHCL_3$, concentration of 14-18 mg/mL of PVA, and sonication of 2 minutes were the optimized conditions to synthesis PEA NPs of less than 200 nm particle diameter via emulsification-evaporation and salting-out methods. Theses experimental conditions were used for all of the experiment.

Table 3-4: Influence of different concentration of PVA on diameter and diameter distribution of NPs prepared by salting-out method. This data resulted from three determinations from three different batches.

	Without filtration			With filtration		
PVAL g/L	Z-average diameter* (nm)	PDI*	Mean diameter* (nm)	Z-average* (nm)	PDI*	Mean diameter* (nm)
2	303±5	0.206±0.02	379±12	176±5	0.175±0.01	217±3.2
10	160±8	0.123±0.04	178±10	147±2	0.09±0.01	164±4
14	155±7	0.125±0.01	179±9	145±7	0.15±0.05	175±23
18	147±5	0.15±0.01	173±6	133±3	0.11±0.03	151±8
40	379±10	0.1±0.1	414±48	223±47	0.14±0.002	259±54

*Average ± SD
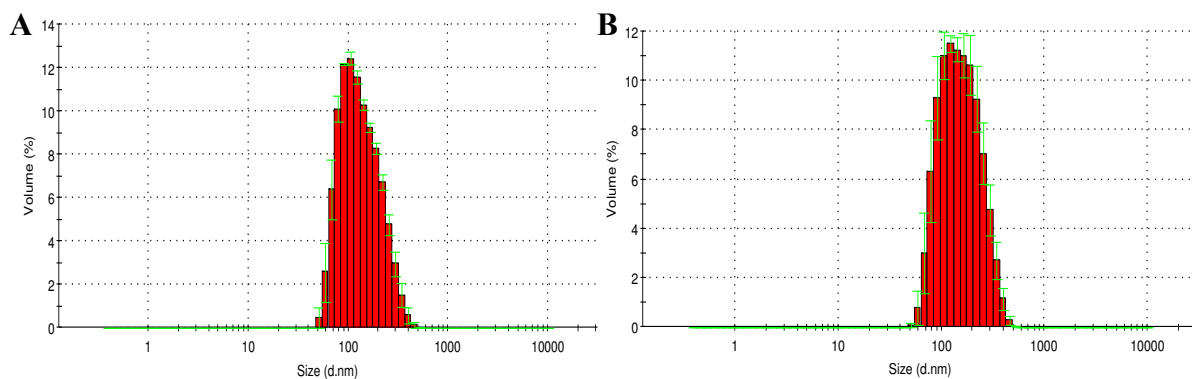
Figure 3-4: Particle diameter distribution of PEA nanoparticle formed from 3 mL aqueous solution of 14 g/L PVA (equals 70mg PVA in 5 mL water) with 1 mL CHCl₃ containing 5 mg of base polymer via salting-out technique, (a) with filtration (using 0.2µm syringe filter). Z-average: 145±7 nm, and (b) without filtration. Z-average: 155±7 nm.
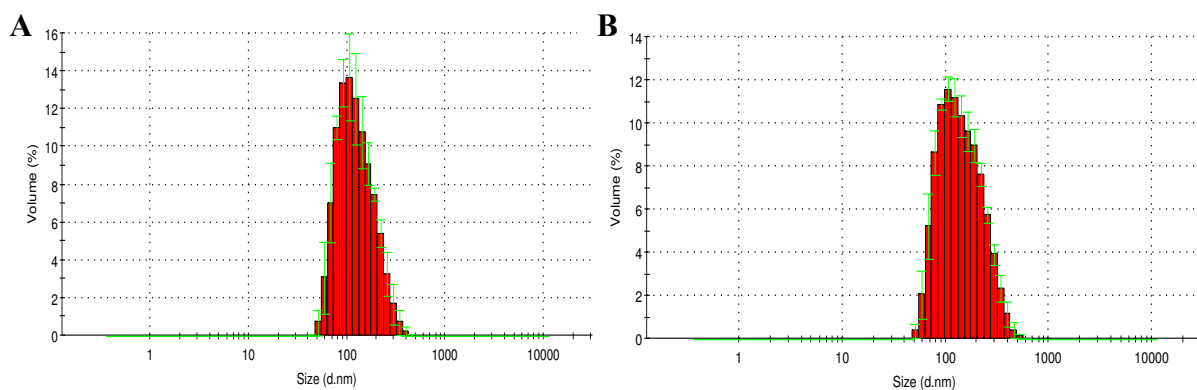
Figure 3-5: Particle diameter distribution of PEA nanoparticle formed from 3 mL aqueous solution of 18 g/L PVA (equals 90 mg PVA in 5 mL water) with 1 mL CHCl₃ containing 5 mg of base polymer via salting-out technique, (a) with filtration (using 0.2µm syringe filter). Z-average: 133±3 nm, and (b) without filtration. Z-average: 147±5 nm.

e) Zeta potential

Another important characteristic of the NPs is the zeta potential. The zeta potential value indicates the total charge on the surface of the particles. Moreover, the nanoparticle containing suspension is stabilized by electrostatic repulsion between particles, which is important to prevent aggregation. As shown in Table 3-5, when PVA was used in the synthesis of the NPs, the zeta potential was always slightly negative regardless of whether the standard emulsion-evaporation or salting-out procedure was used. This can be attributed to the presence of a large number of surface hydroxyl groups from the PVA on the NPs. Even if a very small fraction of these hydroxyls is deprotonated, the particles would exhibit a negative zeta potential. Within the experimental errors on the measurements, there are no trends in zeta potential with the amount of PVA used in the preparation and no differences in

the procedures with and without salt, suggesting that all NPs were likely coated fully with PVA.

Table 3-5: Influence of PVA concentrations on zeta potential using both emulsification-evaporation and using salting-out methods. This data resulted from three determinations from three different batches.

Concentration of PVA (mg/mL)	Emulsification-evaporation	Using MgCl₂
	Zeta potential* (mV)	Zeta potential* (mV)
2	-4±5	-3.5±5
10	-6±4	-8±5.7
14	-5±4	-7±5
18	-5± 4	-6.5±3
40	-2.5±4	-2±4

*Average ± SD

f) Nanoparticle imaging

Both SEM and TEM imaging were performed to further characterize selected particles. As shown in Figure 3-6, Figure 3-7, Figure 3-8, and Figure 3-9, these images confirmed that the particles were indeed spherical and that the sizes were in approximate agreement with those measured by DLS. The images show some dispersity in sizes, but most diameters were below 200 nm.
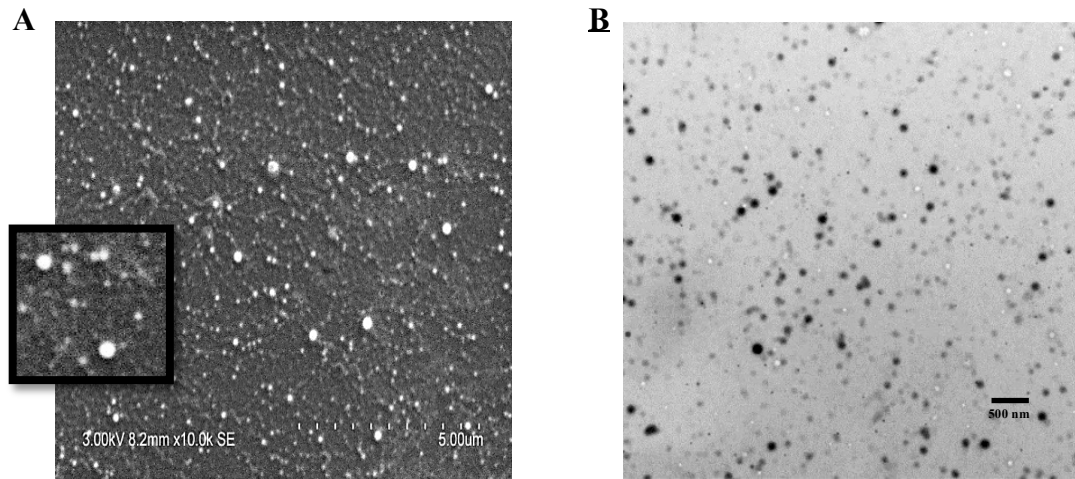
Figure 3-6: NPs prepared by emulsification-evaporation method technique using 14 g/L PVA, A) SEM images, and B) TEM image.
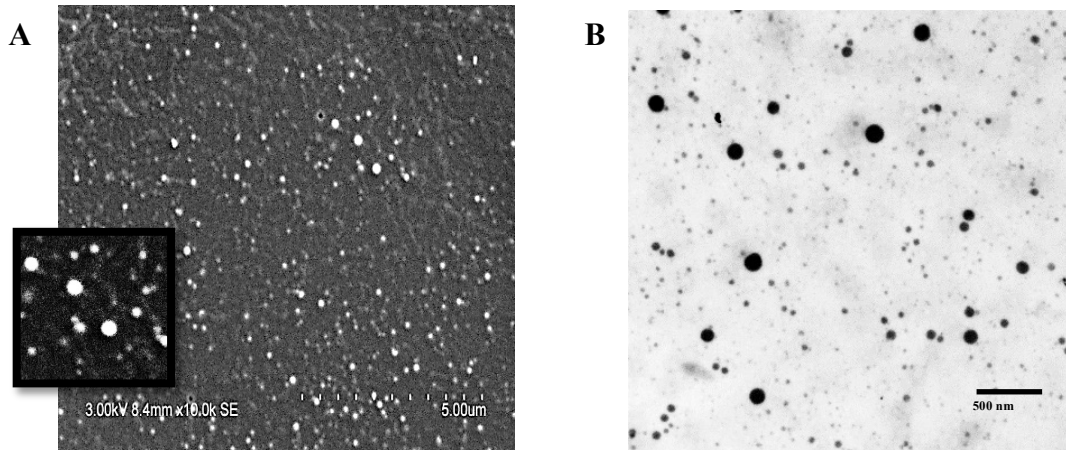
Figure 3-7: NPs prepared by emulsification-evaporation method technique using 18 g/L PVA, A) SEM images, and B) TEM image.
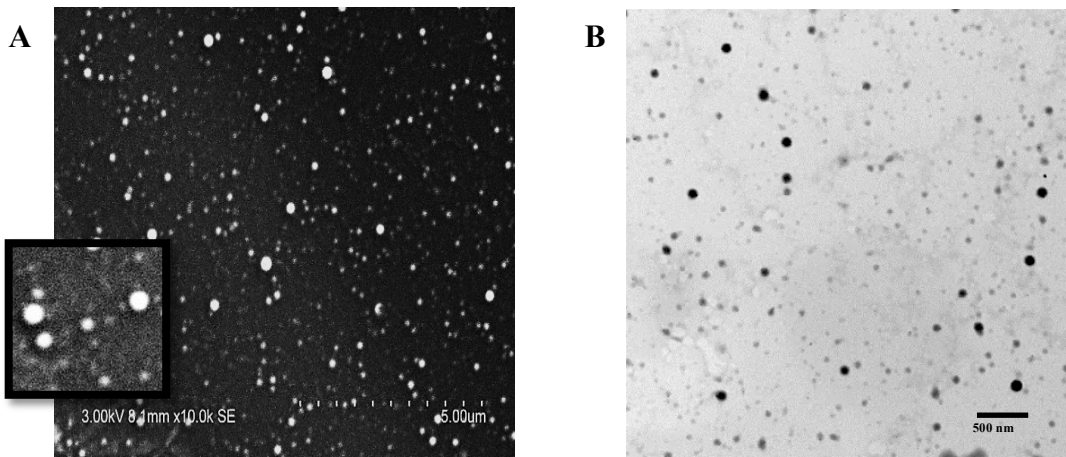
Figure 3-8: NPs prepared by salting-out technique using 14 g/L PVA, A) SEM images, and B) TEM image.
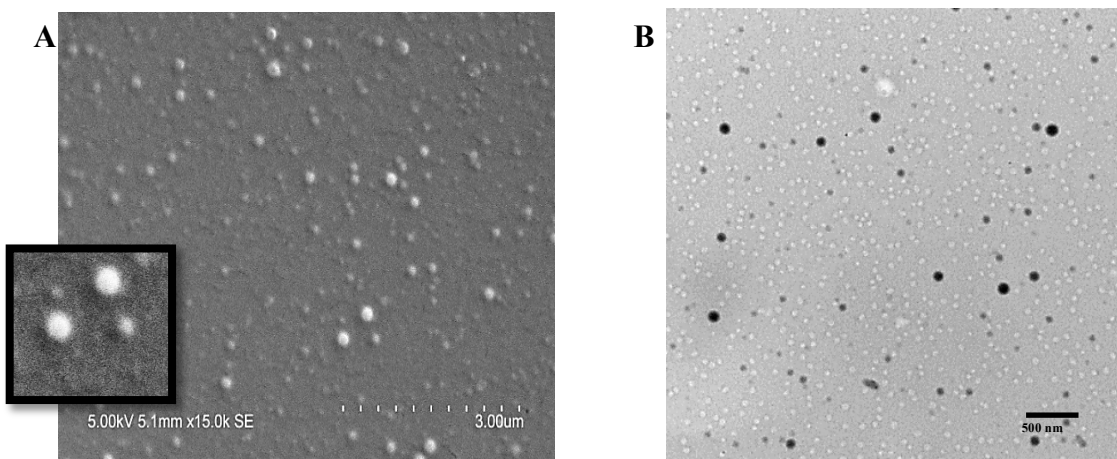
Figure 3-9: NPs prepared by salting-out technique using 18 mg/mL PVA, A) SEM image, and B) TEM image.

3.3.2 Preparation of PEA NPs Containing Rhodamine

PEA **2** (Figure 3-10) was synthesized as previously reported by our group. Its pendant carboxylic acid groups allow for the conjugation of drug molecules or other moieties by ester or amide linkages. For initial work, rhodamine B 4-(3-hydroxypropyl) piperazine amide (**3**), as a model drug was coupled as shown in Figure 3-11. It was selected due to its high extinction coefficient of 76500 $M^{-1}cm^{-1}$, which allows its release from the polymer NPs to be easily measured by UV-vis spectroscopy. In addition, it is soluble in $CHCl_3$, which allows it to be noncovalently encapsulated in the PEA NPs to provide a control system for comparison with the covalent system. However, it is also soluble in water, which enables its release from the NPs without the use of additional surfactant or other materials. To conjugate rhodamine **3** to PEA **2**, the polymer was first activated using DCC in the presence of DMAP and DPTS in dry dichloromethane, and then rhodamine **3** was added to the reaction mixture. The reaction was stirred for 24 h at room temperature, then the excess unreacted rhodamine and other reagents were removed by dialysis, affording the PEA-rhodamine conjugate **4**. UV-vis spectroscopy was used to determined the amount of coupled rhodamine, and it was determined that the coupling had proceeded in 71 % yield, resulting in a PEA conjugate containing 10 wt% of rhodamine.
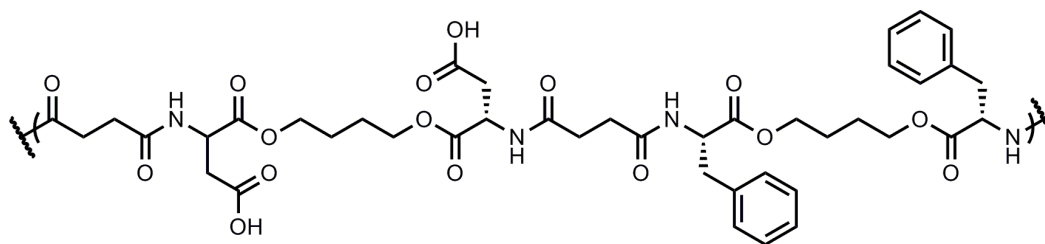
Figure 3-10: Chemical structure of PEA 2.
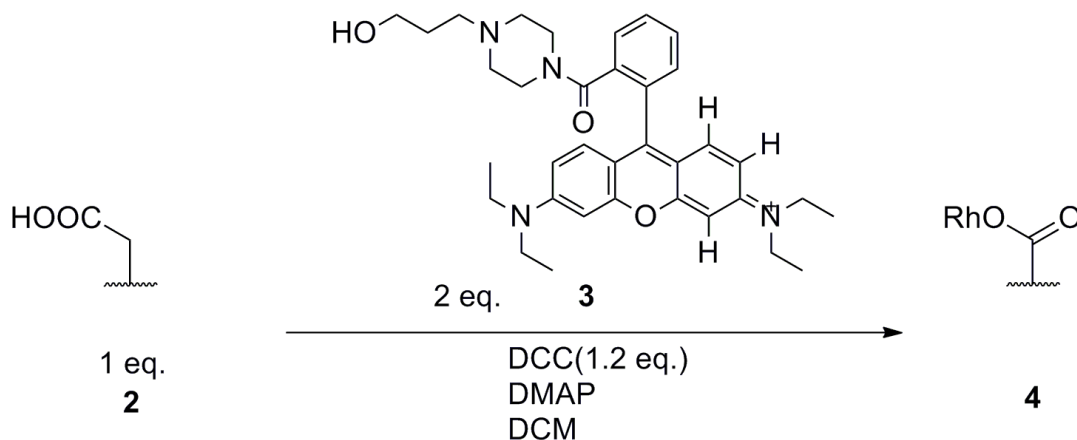
Figure 3-11: Synthesis of a PEA-rhodamine B conjugate 4.

NPs were prepared from PEA-rhodamine conjugate **4** using the optimized procedure described above via the emulsification-evaporation method using a ratio of 1:5 $CHCl_3:H_2O$, concentration of 5 mg/mL of PEA in $CHCl_3$, concentration of 18 mg/mL of PVA, and a sonication time of 2 minutes. Characterization of the NPs by DLS indicated that the particles had a Z-average diameter of 177 nm and polydispersity of 0.12. It is well known from the literature that hydrophobic drugs can be easily encapsulated during the emulsification-evaporation technique if they are soluble in the organic phase (Wischke and Schwendeman, 2008). Therefore, particles containing non-covalently encapsulated rhodamine B were prepared using the same procedure except that 2.5 mg of rhodamine was dissolved in the $CHCl_3$ layer along with the PEA. The loading efficiency was calculated by UV-visible spectroscopy in DMF (relative to a calibration curve of rhodamine piperazine amide) and was determined to be 91%, corresponding to 24 wt% rhodamine in the NPs.

3.3.3 Release of Rhodamine from PEA NPs

To study the release of rhodamine from the covalent and noncovalent PEA NPs, the NPs were placed inside a dialysis membrane with a 3.5 kg/mol MWCO and the membrane was placed in pH 7.4 phosphate buffer at 37º C with stirring. Rhodamine released from the NPs would be expected to diffuse easily across the membrane into the dialysate. Thus, the UV-vis absorbance of the dialysate at 565 nm was measured for each system at varying time points and the result was compared to a calibration curve of rhodamine in the same buffer in order to calculate the rhodamine concentration in the dialysate. The dialysate was replaced with fresh buffer at each time point. As shown in Figure 3-12, in the case of noncovalently encapsulated rhodamine, the release was rapid with about 30% of rhodamine released in first hour and about 50% after 2 hours. Almost 96% of the rhodamine was released in 8 hours. This rapid release can likely be attributed to the hydrophilicity of rhodamine, which favours its release into the buffer under sink conditions.
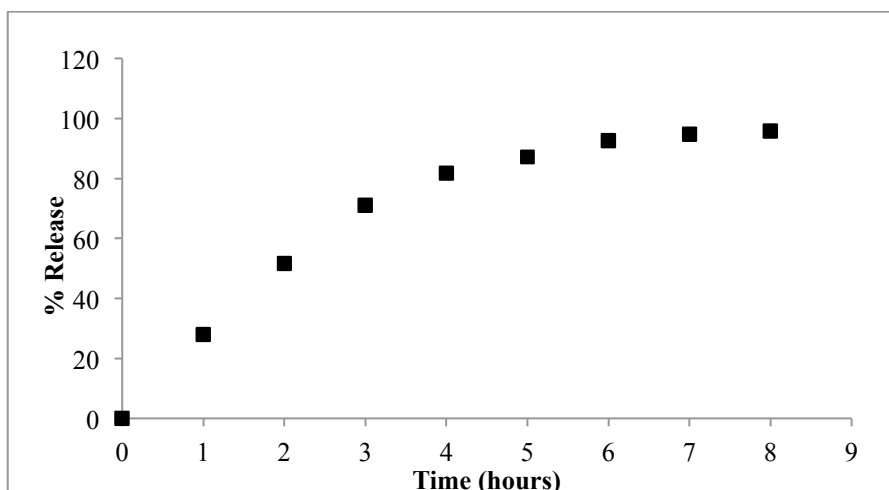
Figure 3-12: % Rhodamine release versus time for PEA NPs containing noncovalently encapsulated rhodamine (pH 7.4 phosphate buffer solution, 37° C).

As shown in Figure 3-13, release of the covalently conjugated rhodamine was much slower, with only 0.63% released in first 24 hours, 5.5% after 163 hours, and 20.7% after 715 hours. This can be attributed to the requirement for ester hydrolysis to occur in the hydrophobic core of the nanoparticle prior to release of the rhodamine. This may therefore be limited to the degradation rate of the PEA, as water penetration for hydrolysis would be slow or impossible in the intact particle. It should also be noted that while ester hydrolysis would be expected to be a pseudo-first-order process the appearance of the release curve in Figure 3-13 appears more zero order.
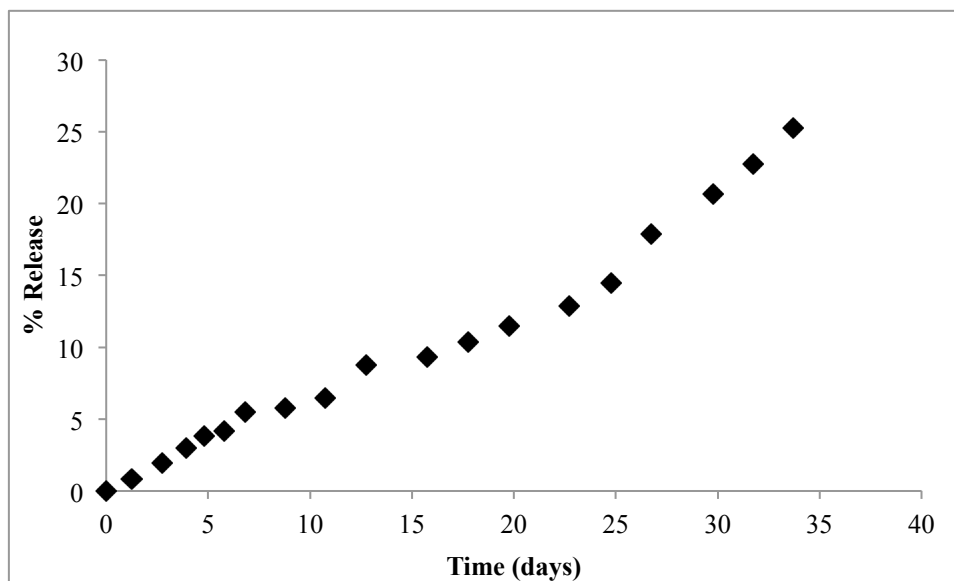
Figure 3-13: The release profile of rhodamine piperazine amide from the NPs prepared from PEA-rhodamine B conjugate 4 in pH 7.4 phosphate buffer solution as the release media.

This pseudo-zero order release is indeed desirable, as it implies that steady-state drug concentrations might be obtainable with this type of system *in vivo*. However, it should also be noted that as this study was only performed to ~20% rhodamine release, we cannot speculate on the release profile after this point.

3.3.4 Preparation of PEA NPs Containing Floxuridine

In this study, floxuridine was chosen as the drug molecule for covalent immobilization for several reasons. Floxuridine is an antimetabolite derivative of 5-fluorouracil that has been used in patients with metastatic colorectal and primary liver cancer. Floxuridine inhibits thymidylate synthase and consequently interferes with DNA replication (Andrea *et al.*, 2014). Its incorporation into a nanoparticle may reduce its toxicity and increase its chemotherapeutic effectiveness for the treatment by local, systemic, or oral administration. It has multiple hydroxyl groups that can be used for covalent attachment. In addition, floxuridine is highly hydrophilic. This means that it would be very challenging or impossible to encapsulate in NPs by a conventional emulsification-evaporation procedure. Its covalent immobilization addresses this issue. At the same time, its hydrophilicity will enable it to be released well from the NPs following cleavage of the ester linkage to the PEA.

Floxuridine (**5**) was coupled to PEA **2** using a similar procedure that used for the coupling of rhodamine, except that DMF was used as the solvent to dissolve the drug and (1-ethyl-3-(3-dimethylaminopropyl) carbodiimide) (EDC·HCl) was used as the coupling agent as it is more compatible with DMF (Figure 3-14). The product PEA-floxuridine conjugate **6** was again purified by dialysis. ^{1}H NMR spectra obtained confirmed the successful coupling of the drug. As shown in Figure 3-15, the spectrum contains peaks corresponding to floxuridine at $\delta =$ 11.81, 8.18, 6.08, and 2.07 ppm in DMSO-d_6. Based on integration of the peaks, ~60% of the pendant carboxylic acid groups were functionalized with drug.
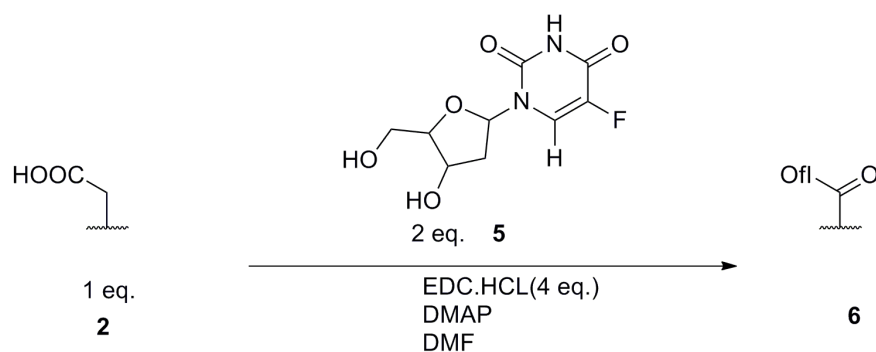
Figure 3-14: Synthesis of a PEA-floxuridine conjugate 6.
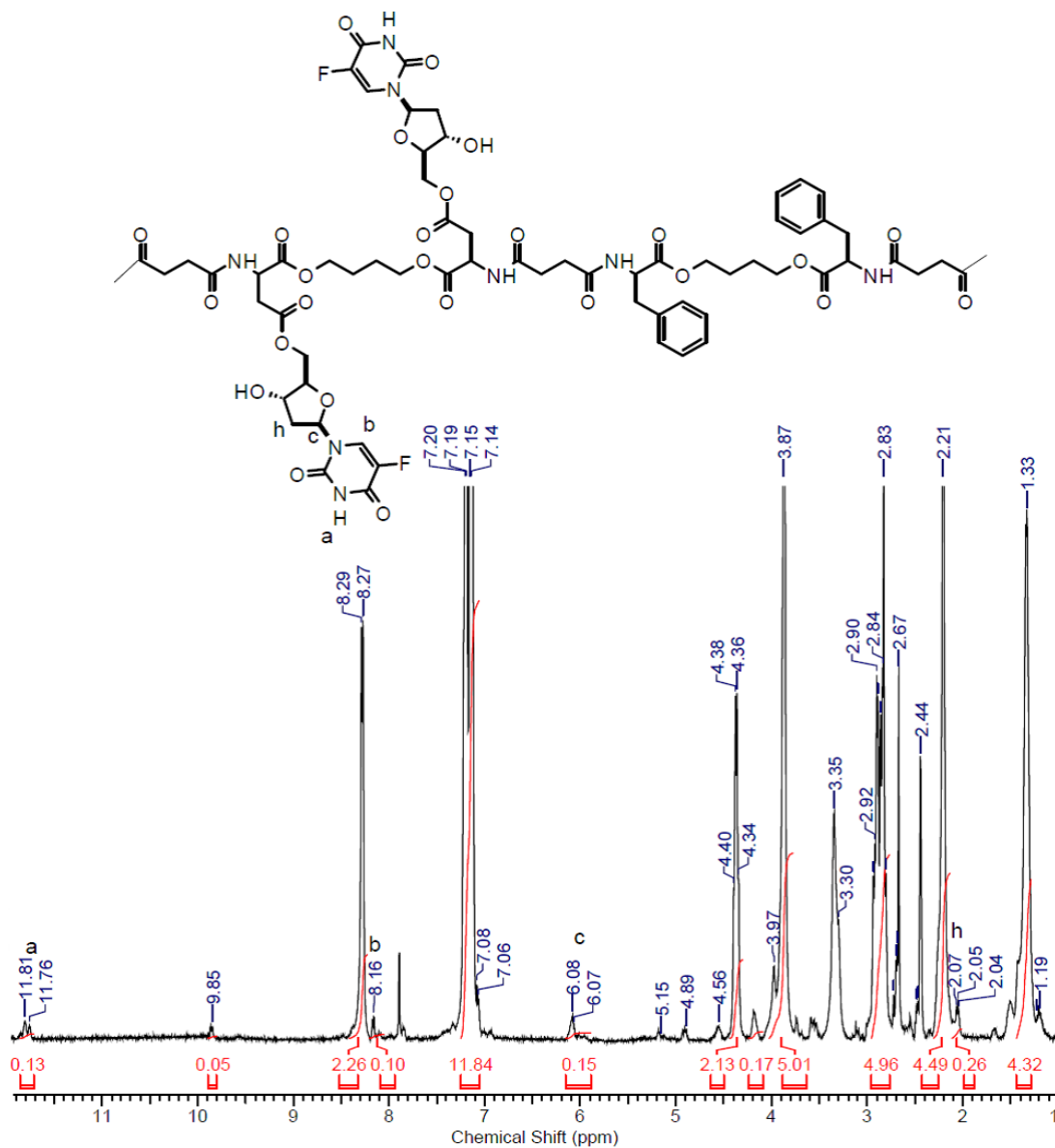
Figure 3-15: ^{1}H NMR spectrum of the floxuridine-PEA conjugate (DMSO-d_6, 400 MHz)

NPs were prepared from the PEA-floxuridine conjugate using the optimized emulsification-evaporation and salting-out procedures involving 14 mg/mL PVA. The resulting lyophilized

particles were then characterized by DLS, SEM, and TEM. DLS results showed that the NPs obtained via the emulsification-evaporation method had a Z-average diameter of 191±7 nm while those prepared using the salting-out procedure had a Z-average diameter of 180 nm (Figure 3-16). SEM and TEM confirmed the size and spherical morphology of the particles (Figure 3-17).
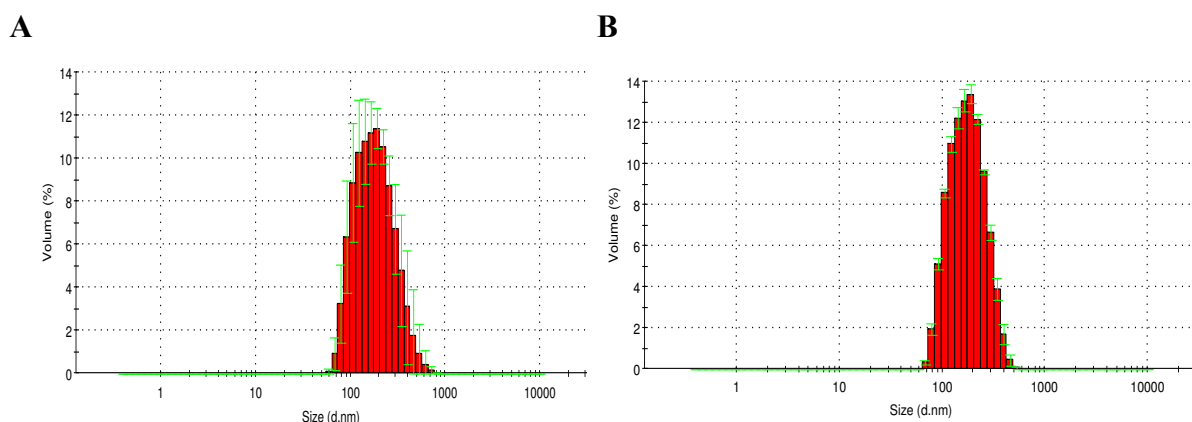
Figure 3-16: DLS traces for NPs prepared from the PEA-floxuridine conjugate using a) the emulsification-evaporation method and b) the salting-out procedure. The suspension was passed through a 0.2 μm syringe filter prior to measurement.
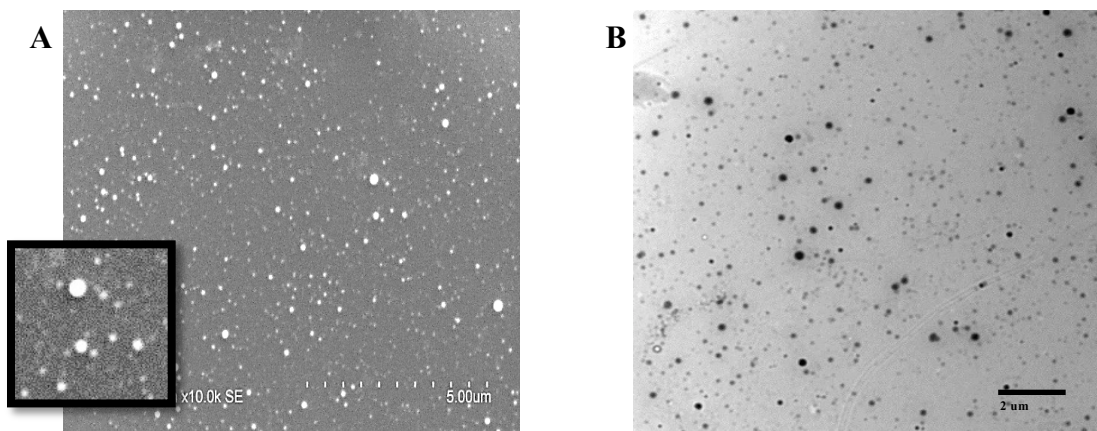
Figure 3-17: NPs prepared from a PEA-floxuridine conjugate using the emulsification-evaporation and imaged by a) SEM, and B) TEM images at different magnifications.

a) Release of floxuridine from the NPs

The release of floxuridine was studied by the dialysis method described above for rhodamine, except that the floxuridine concentration in the dialysate was monitored by HPLC. As shown in Figure 3-18, there was a small burst release of ~5% the drug over the first 6 h. The reason for this burst release is unclear as this effect was not observed for the rhodamine conjugate. However, this is still much less burst release than is observed in many non-covalent

nanoparticle systems (Yang *et al.*, 2010). This can likely be attributed to the hydrolysis of ester bonds at the nanoparticle surface and subsequent release of this drug. Following this, the release occurred in a slower, sustained manner, reaching about 9% of the total drug released over 11 days. This confirms the significant slowing of drug release that is achievable using the covalent conjugation strategy and is consistent with the results of the rhodamine release study.
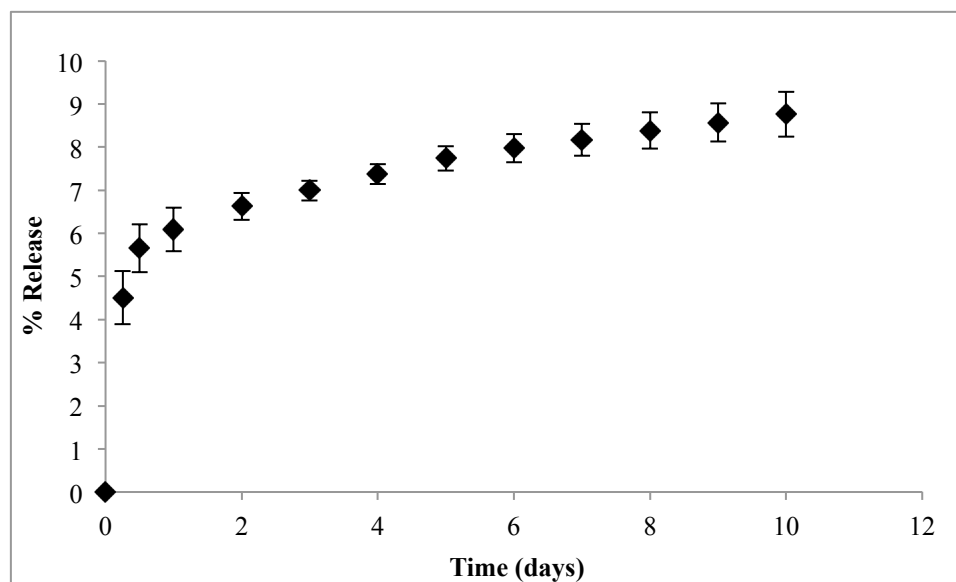
Figure 3-18: % Release of floxuridine over time for NPs prepared from the PEA-floxuridine conjugates 6.

3.4 Conclusion

This study investigated the use of emulsification-evaporation and salting-out methods for the preparation of NPs from biodegradable PEAs. By optimizing parameters such as the surfactant concentration, PEA concentration, and the ratio of organic to water phases, it was possible to prepare particles having Z-average diameters of less than 200 nm and reasonable polydispersities by both techniques. All of the prepared particles had negative zeta potentials and spherical morphologies as observed by SEM and TEM. It was also demonstrated that the pendant functional groups on a PEA could be used to conjugate a rhodamine B derivative. The optimized nanoparticle preparation conditions were used to prepare NPs from the rhodamine B conjugate and also to from control NPs in which rhodamine was physically encapsulated. The covalent conjugate afforded a much slower release than the noncovalent control suggesting that this approach is valuable for the elimination of the burst release effect. The approach was also extended to covalent immobilization of the anti cancer drug

floxuridine in NPs. This system also exhibited a small burst release of 5% of the drug, but this was followed by a slower, sustained release. Overall this work suggests the promise of using PEA NPs for drug delivery applications and in particular the use of PEAs with pendant functional groups for covalent conjugation of drugs. This affords NPs exhibiting slow and sustained drug release for applications where this is required.

3.5 References

[1] Acharya, S.; Sahoo, S. K., (2011). "PLGA nanoparticles containing various anti cancer agents and tumour delivery by EPR effect", Advanced Drug Delivery Reviews, 63, 170–183.

[2] Aftabrouchard, D.; Dorlker, E., (1992). "Preparation methods for biodegradable microparticles loaded with water-soluble drugs", STP Pharma Sciences, 2, 365 -380.

[3] Allémann, E.; Leroux, J.-C.; Gurny, R.; Doelker, E., (1993). "In Vitro Extended-Release Properties of Drug-Loaded Poly(DL-Lactic Acid) Nanoparticles Produced by a Salting-Out Procedure", Pharmaceutical Research,10,1732-1737.

[4] Anderson, J. M.; Shive, M. S., (1997). "Biodegradation and biocompatibility of PLA and PLGA microspheres", Advanced Drug Delivery Reviews, 28, 5–24.

[5] Andrea, C.; Michael, D.; Derek, P.; Marinela, C.; Alexandra, G.; Dina, P.; Peter, A.; Yuman, F.; Ronald, P. D.; William, R. J.; Nancy, E. K., (2014). Floxuridine Hepatic Arterial Infusion Associated Biliary Toxicity Is Increased by Concurrent Administration of Systemic Bevacizumab", Annals of Surgical Oncology 21:479–486.

[6] Atkins, K.; Lopez, D.; Knight, D.; Mequanint, K.; Gillies, E., (2009). " A versatile approach for the syntheses of poly(ester amide)s with pendant functional groups", Polymer Science: Part A: Polymer Chemistry, 47, 3757-3772.

[7] Bae, Y.; Kataoka, K., (2009). "Intelligent polymeric micelles from functional poly(ethylene glycol)-poly(amino acid) block copolymers":, Advanced Drug Delivery Reviews, 61, 768–784.

[8] Burgess, P.; Hutt, P. B.; Farokhzad, O. C.; Langer, R.; Minick, S.; Zale, S., (2010). "On firm ground: IP protection of therapeutic nanoparticles", Nature Biotechnology, 28, 1267–1270.

[9] Caldorera-Moore, M. E.; Liechty, W. B.; Peppas, N. A., (2011). "Responsive Theranostic Systems: Integration of Diagnostic Imaging Agents and Responsive Controlled Release Drug Delivery Carriers", Accounts of Chemical Research, 44, 1061–1070.

[10] Davis, M. E., (2009). The First Targeted Delivery of siRNA in Humans via a Self-Assembling, Cyclodextrin Polymer-Based Nanoparticle: From Concept to Clinic", Molecular Pharmaceutics. 6, 659–668.

[11] Desai, M.P.; Labhasetwar, V.; Amidon, G.L.; Levy R.J, (1996). Gastrointestinal Uptake of Biodegradable Microparticles: Effect of Particle Size", Pharmaceutical Research, 13, 1838–1845.

[12] Dhal, P. K.; Polomoscanik, S. C.; Avila, L. Z.; Holmes-Farley, S. R.; Miller, R. J., (2009). Functional polymers as therapeutic agents: Concept to market place", Advanced Drug Delivery Reviews, 61, 1121–1130.

[13] Drummond, D. C.; Meyer, O.; Hong, K.; Kirpotin D. B.; Papahadjopoulos, D., (1999). "Optimizing liposomes for delivery of chemotherapeutic agents to solid tumors", Pharmacological Reviews, 51, 691–743.

[14] Farokhzad, O. C.; Langer, R., (2006). "Nanomedicine: Developing smarter therapeutic and diagnostic modalities", Advanced Drug Delivery Reviews, 58, 1456–1459.

[15] Farokhzad, O. C.; Langer, R., (2009). "Impact of nanotechnology on drug delivery", ACS Nano, 3, 16–20.

[16] Galindo-Rodriguez, S.; Alle´mann, E.; Fessi, H.; Doelker, E., (2004). "Physicochemical Parameters Associated with Nanoparticle Formation in the Salting-Out, Emulsification-Diffusion, and Nanoprecipitation Methods", Pharmaceutical Research, 21, 1428-1439.

[17] Guo, K.; Chu, C. C., (2009). "Biodegradable and injectable paclitaxel-loaded poly(ester amide)s microspheres: Fabrication and characterization", Biomed Materials Research Part B,89B: 491–500.

[18] Guo, R.; Chu, C.-C., (2007). " Biodegradation of unsaturated poly(ester-amide)s and their hydrogels", Biomaterials, 28, 3284-3294.

[19] Horwitz, J.A.; Shum, K.M.; Bodle, J.C.; Deng, M.; Chu, C.C.; Reinhart-King, C.A., (2010). "Biological performance of biodegradable amino acid-based poly(ester amide)s: Endothelial cell adhesion and inflammation in vitro", Biomaterials Research A, 95, 371-380.

[20] Jokhadze, G.; Machaidze, M.; Panosyan, H.; CHU, C. C.; Katsarava, R., (2007). "Synthesis and characterization of functional elastomeric poly(ester amide) co-polymers",Biomaterials Science Polymer Edition,18, 411–438.

[21] Julienne, M.C.; Alonso, M.J.; Gomez Amoza, J.L.; Benoit, J.P., (1992). "Preparation of Poly(D,L-Lactide /Glycolide) Nanoparticles of Controlled Particles Size Distribution: Application of Experimental Designs", Drug Development And Industrial Pharmacy, 18, 1063-1077.

[22] Knight, D. K.; Gillies, E. R.; Mequanint, K., (2011). "Strategies in Functional Poly(ester amide) Syntheses to Study Human Coronary Artery Smooth Muscle Cell Interactions", Biomacromolecules, 12, 2475–2487.

[23] Moghimi, S. M.; Hunter, A. C.; Murray, J. C., (2001). "Long-circulating and target-specific nanoparticles: theory to practice", Pharmacological reviews, 53, 283–318.

[24] Nguyen, T.; Francis, M. B., (2003). "Practical Synthetic Route to Functionalized Rhodamine Dyes", Organic Letter, 5, 3245-3248.

[25] Shai, J.; Xiao, Z.; Kamaly, N.; Farokhzad, O. C., (2011). "Self-Assembled Targeted Nanoparticles: Evolution of Technologies and Bench to Bedside Translation", Accounts of Chemical Research, 44, 1123–1134.

[26] Wischke, C.; Schwendeman, S. P., (2008). "Principles of encapsulating hydrophobic drugs in PLA/PLGA microparticles", International Journal of Pharmaceutics, 364, 298–327.

[27] Yang, L.; Chen, L.; Zeng, R.; Li, C.; Qiao, R.; Hu, L.; Li, Z., (2010). "Synthesis, nanosizing and in vitro drug release of a novel anti-HIV polymeric prodrug: Chitosan-O-isopropyl-5′-O-d4Tmonophosphate conjugate", Bioorganic & Medicinal Chemistry, 18, 117–123.

[28] York, A. W., Kirkland, S. E., McCormick, C. L., (2008). Advances in the synthesis of

amphiphilic block copolymers via RAFT polymerization: Stimuli-responsive drug and gene delivery", Advanced Drug Delivery Reviews, 60, 1018–1036.

[29] Zauner, W.; Farrow, N.A.; Haines, A.M., (2001). "In vitro uptake of polystyrene micro-spheres: effect of particle size, cell line and cell density", Controlled Release 71, 39–51.

Chapter 4 Poly(ethyl glyoxylate) Nanoparticles

4.1 Introduction

In recent years, there has been a growing interest in using polymeric NPs for drug delivery (Dadwal, 2014; Maheshwara Rao *et al.*, 2014; Suresh and Sah, 2014). In particular, polyesters such as poly(lactic acid) (PLA), polycaprolactone (PCL), poly(3-hydroxybutyrate) (PHB), and poly(glycolic acid) (PGA) have been extensively investigated due to their biodegradability and biocompatibility (Matsumoto *et al.*, 1999; Venkatraman *et al.*, 2005; He *et al.*, 2007; Lassalle and Ferreira, 2007; Xie *et al.*, 2007). Nevertheless, these polyesters have some drawbacks. The non-enzymatic degradation rate in water and in the human body is not sufficiently fast for many applications as degradation can require months. Additionally, the build-up of acidic byproducts within the degrading polymer device can result in poor stability of encapsulated acid-labile molecules such as proteins. (Fu *et al.*, 2000; Zhu *et al.*, 2000; Zhou *et al.*, 2003).

Controlling the degradability of polyesters is of great interest. The degradability significantly changes upon synthesis of a copolymer. For example, the copolymerization of lactic acid (LA) and glycolic acid (GA) forms PLGA, which hydrolyzes much faster than PLA (Fu *et al.*, 2000, Zhu *et al.*, 2000). Decreasing the hydrophobicity and crystallinity of the polymers can also enhance the degradation rate. Additionally, the degradation rate of PLA can be altered by varying the relative stereochemistry of the LA monomers (Park *et al.*, 1992, Ibim *et al.*, 1997). Moreover, the synthesis of branched structures was found to increase the rate of degradation due to the lower the degree of crystallinity of the branched polymer (Pitt *et al.*, 1992).

An alternative approach to control the degradability of aliphatic polyesters is to blend them with other polymers that can effectively modify their properties. For example, in a past study, PLA was blended with non-degradable polymers such as poly(ethylene oxide) (PEO), poly(propylene oxide), (PPO) and poly(ethylene-vinyl acetate) in an effort to modify degradation and drug-release behaviors of PLA-based polymeric drug-delivery systems (Park *et al.*, 1992). Also, the degradability, miscibility and drug-release behavior of PLGA/polyphosphazene and PLGA/PVA blends were also studied (Pitt *et al.*, 1992; Ibim *et*

al., 1997). Mi *et al.*, (2002) used blends of PLGA and chitin, a natural biodegradable polymer, to synthesize microspheres for anti-cancer drug delivery. The characterization of the microparticles showed the occurrence of phase separation of the blend due to their incompatibility. Overall, the hydration, degradation, and morphological modifications of the microparticle system affect significantly the drug release profile.

Although numerous studies and promising results involving biodegradable polymers as drug carriers have been reported, new research has also focused on the use of stimuli-responsive polymers. These polymers have the ability to undergo significant changes in their chemical and physical properties upon exposure to variations in the environment such as light (Bansal and Zhang, 2014), heat (Strover *et al.*, 2008), and pH change (Yao et al, 2011). By using these materials, timing, dose and site of the release can be managed. Among the stimuli capable to trigger the release of therapeutics, light is a finely tunable external stimulus that is non-invasive and not affected by physiological parameters such as temperature, pH and ionic strength. Our group has successfully synthesized UV-triggerable self-immolative polyglyoxylates by the incorporation of a UV-responsive end-cap (nitroveratryl carbonate (NVOC)) onto the polymer terminus (Fan *et al.,* 2014). Upon UV light exposure, NVOC undergoes photolysis, allowing the polymer to undergo end-to-end depolymerization. The results showed that a 40 minute UV exposure was enough for complete cleavage of the NVOC group. After cleavage of the end cap, 50% of poly(ethyl glyoxylate) (PEtG) had depolymerized into ethyl glyoxylate hydrate (EtGH) within 3 h, then up to 70% within 24 h. In contrast, the non-irradiated end-capped PEtG was stable for 7 days. In addition, the degradation results of PEtG films upon UV light exposure illustrated that the degradation over the first 12 days likely occurred through a surface erosion mechanism characterized by a gradual decrease in the mass of the PEtG films. Micellar self-assemblies of PEO-PEtG-PEO triblock copolymers were synthesized and characterized before and after UV irradiation. Rapid degradation of 90% of PEtG block copolymers was observed just after irradiation and about 45% of EtGH underwent hydrolysis to glyoxylic acid hydrate and ethanol over 24 h at 37 °C.

This chapter describes a study to investigate the applicability of UV-responsive PEtG to formulate solid NPs. The objective of this study is to manipulate the degradation rate of the NPs and the release profile of a drug. In order to achieve this goal, PEtG/PLA blend NPs

were designed for triggered and controlled drug delivery, based on UV-triggered self-immolative PEtG and biodegradable PLA polymer. Letrazole was used in this study as a model hydrophobic drug. The effects of organic:aqueous ratio, sonication time, concentration and type of the surfactant on the size of PLA NPs were investigated. PEtG/PLA blend NPs were synthesized using the optimized conditions and characterized. Letrazole release performance from PEtG/PLA blend NPs of different ratios was studied with and without UV irradiation.

4.2 Materials and Methods

PEtG with an NVOC end-cap was prepared as previously reported (Bo *et al.*, 2014). It had an M_n of 53 kg/mol with dispersity of 1.7 based on size exclusion chromatography (SEC) relative to polystyrene standards. Poly(*D,L*-lactic acid) (PDLLA) was purchased from Sigma Aldrich with a molecular weight range of 18-28 kg/mol and with T_g 46-50 °C. PVA of $M_w =$ 31,000, 88% hydrolyzed. All chemicals were purchased from Sigma Aldrich and used without further purification unless otherwise specified. Letrazole was purchased from Ontario Chemicals. ^{1}H NMR spectra were record at 400 or 600 MHz and chemical shifts (δ) are reported in parts per million (ppm). The residual solvent peaks of acetonitrile (δ 1.94 ppm), deuterium oxide (δ 4.7 ppm), dimethyl sulfoxide (δ 2.5 ppm.

4.2.1 Optimization of nanoparticle preparation

The influence of organic solvent:aqueous ratio, sonication time, concentration and type of the surfactant on the diameters of the PLA NPs were evaluated and these parameters are summarized in Table 4-1, Table 4-2, Table 4-3, and Table 4-4. The emulsification-evaporation method described in below was used in each case, followed by a common purification procedure described below. Each preparation was performed in triplicate.

4.2.2 Fabrication of PEtG/PLA blend NPs

Sodium cholate was selected as the emulsifying agent. Solution blending was used in this study. Blends of PEtG /PDLLA were prepared by mixing different ratios of 100/0, 75/25, 50/50, 25/75, and 0/100, respectively) in CH_2Cl_2. The NPs were prepared using the polymer blend solution via the emulsification-evaporation technique. Briefly, 5 mL of CH_2Cl_2 containing 1 mg/mL of the blended polymers was added to 5 mL of an aqueous solution of 6

mg/mL sodium cholate. The two-phase solution was sonicated using a probe sonicator for 6 minutes: 30 seconds on and 10 seconds off (Branson 450 digital sonifier using an amplitude of 70%). Then, the organic solvent was evaporated using moderate stirring for 3 hours. The NPs were washed three times with distilled water to remove the excess surfactant using an Amicon® ultrafiltration cell using a Millipore® regenerated cellulose membrane of with a molecular weight cut-off (MWCO) of 50,000 g/mol.

4.2.3 Characterization of the NPs

a) Particle diameter

Nanoparticle diameter was measured by DLS using a Zetasizer Nano ZS instrument (Malvern Instruments). Values reported are the Z-average with the standard deviation, along with polydispersity. The analysis was performed at 25 ℃. Aliquot samples were prepared in deionized water (Millipore purification system) at a concentration of 0.1 mg/ mL in a glass cuvette. Each measurement was performed in triplicate.

b) Zeta potential

The zeta potentials of the particles were determined by using a Zetasizer Nano ZS instrument (Malvern Instruments). Measurements were performed in deionized water at neutral pH at a concentration of 0.5 mg/mL. Each measurement was performed in triplicate.

c) Transmission electron microscopy (TEM)

A drop (10 µL) of the nanoparticle suspension (0.01 mg/mL) was transferred onto a Formvar/carbon grid and left to completely dry. TEM images were obtained using a Philips CM10 microscope operating at 80 KV with a 40 µm aperture.

4.2.4 Thermal characterization of PEtG/PLA blends and polymer blend NPs

Thermal properties of freeze-dried PEtG/PLA blend NPs of different ratios of 100/0, 75/25, 50/50, 25/75, 0/100 PEtG/PLA were measured by thermogravimetry (TGA, on a Q600 SDT TA Instrument) and differential scanning calorimetry (DSC), on a Q20 DSC TA instrument). Thermogravimetric analyses were performed under a nitrogen atmosphere at a heating rate of 10 ℃/min. DSC was performed under a nitrogen atmosphere at a heating/cooling rate of 10

°C/min from -100 to 100 °C. The T_g was obtained from the second heating cycle.

4.2.5 Drug loading and encapsulation efficiency for PEtG/PLA blend NPs

Letrazole loaded NPs were prepared by the above described method except that letrazole (20-60% w/w relative to the polymer) was dissolved in the 5 mL of CH_2Cl_2 solution containing 1 mg/mL of PEtG/PLA blends. During washing of the NPs using the ultrafiltration technique, the washed solution was collected to determine the amount of the non-encapsulated drug using UV-visible (UV-vis) spectroscopy based on the absorption at 238 nm and a calibration curve for the free drug in water (Varian Cary 300 Bio UV-Visible Spectrophotometer). The amount of encapsulated drug was assumed to be the amount that was not detected in the wash. Non-encapsulated drug was subtracted from the initial amount to determine the mass of the drug in the NPs. In order to calculate the mass of recovered NPs, the washed NPs were lyophilized at 0.060 mBar and -80º C for 48 hours (LABCONCO Lyophilizer) and then weighed. The calculations of actual loading% and encapsulation efficiency% were done in triplicate from three different batches as illustrated in Equations 4.1 and 4.2, respectively.

$$\text{Actual loading\% (w/w)} = \frac{\text{mass of the drug in NPs}}{\text{mass of recovered NPs}} \times 100 \qquad \text{Equation (4.1)}$$

$$\text{Encapsulation Efficiency \%} = \frac{\text{mass of the drug in NPs}}{\text{mass of the drug used in the formulation}} \times 100 \qquad \text{Equation (4.2)}$$

4.2.6 Degradation of PEtG NPs studied by NMR spectroscopy

Letrazole loaded PEtG NPs were prepared by the method described above using 3:5 drug:polymer ratio in deuterated water (D_2O) without the washing step. The NP suspension was then transferred into two sets of NMR tubes. One set of tubes was exposed to different times of 20, 40, 60, and 80 minutes of UV light irradiation (wavelength: 300−350 nm, 5.3 mW cm^{-2}) to initiate the cleavage of the end-cap and thus depolymerization. The other set of NMR tubes was stored in a light-impermeable box over this time and used as controls. ^{1}H NMR spectra were then recorded at different time intervals to determine the required time for complete end-cap removal.

4.2.7 *In vitro* release study for letrazole

Letrazole loaded PEtG NPs were exposed to UV light in a quartz cuvette for 20 minutes and then put in a dialysis tube with MWCO of 6000-8000 g/mol, which was stirred in phosphate buffer (100 mM) solution of pH 7.4 at 37 $^{\circ}$C. At different time intervals, the dialysate was replaced with fresh phosphate buffer. The amount of released letrazole was assessed at various time points by UV-vis spectroscopy based on the absorbance at 238 nm versus a calibration curve prepared in the same buffer. The release profile for the irradiated NPs was compared with non-irradiated NPs.

4.2.8 Nile red encapsulation and release

0.1 mg of nile red was dissolved in 5 mL of CH_2Cl_2 containing PEtG (1 g/L). An aqueous solution of 6 g/L SC was then added to the organic solution and the resulting emulsion was sonicated for 6 minutes (30 seconds on and 10 seconds off) as described above. The organic solvent was then evaporated. The fluorescence intensity was obtained on a Varian CARY Eclipse Fluorescence spectrophotometer equipped with double excitation and emission monochromators. An excitation wavelength of 350 nm was used for nile red and the emission spectra were recorded from 400 to 700 nm. The fluorescence intensity was measured for non-irradiated PEtG NPs, and 20,40, and 60 minute irradiated PEtG NPs. The intensity measurements were taken for the same samples over 4 days.

4.3 Results and discussion

In the current work, we investigated the influence of different preparation variables on basic characteristics of letrazole loaded NPs prepared by the emulsification-evaporation method. Letrazole, an oral non-steroidal aromatase inhibitor intended for treatment of hormonally responsive local and metastatic breast cancer was selected as the drug (Cohen *et al.*, 2002; Long *et al.*, 2004). Its hydrophobic-hydrophilic balance was expected to allow it to be incorporated into the NPs by the emulsification-evaporation method while its modest solubility in water would allow its loading and release to be readily detected by UV-vis spectroscopy. Letrazole-loaded NPs and microparticles have been shown to provide controlled release, significantly higher tumor uptake, and enhanced therapeutic efficacy (Mondal *et al.*, 2008; Dey *et al.*, 2009; Mondal *et al.*, 2010). However, the stimulus-induced release of letrazole has not previously been investigated and may lead to more selective

delivery of the drug, further enhancing its efficacy and decreasing its toxicity.

4.3.1 Optimization of PLA nanoparticle preparation

Particle size must be controlled, particularly for intravascular delivery. Because the estimated diameter of the smallest blood capillaries in the human body is 4 – 7 mm (Kreuter, 1996; Gorner *et al.*, 1999), the particle size should ideally be less than 100 nm to prevent capillary occlusion. Additionally, it was reported that the size of a NP is a major factor in the fate of a particle inside the body (Harashima *et al.*, 1994). There is a strong correlation between the size of the particles and opsonization and consequent macrophage recognition through phagocytosis (Fang *et al.*, 2006; Vonarbourg *et al.*, 2006; Alexis *et al.*, 2008). Thus, the diameter of drug carriers is a crucial parameter affecting on the circulation and their biodistribution profile (Moghimi *et al.*, 1993, 2001). Therefore, finely tunable particle size is important to achieve of an effective drug delivery carrier. In this study, the NPs were prepared by the emulsification-evaporation method that was also used in Chapter 3. Using this method, the size can be controlled by adjusting parameters such as type and amount of the surfactant, the concentrations and viscosity of organic and aqueous phase, as well as other parameters (Tice and Gilley, 1985). CH_2Cl_2 was chosen as the organic phase in this study because it is a good solvent for PEtG, PLA, and letrazole. The results of this study showed that the size of non-loaded PLA NPs is influenced by several formulation variables including the organic:aqueous ratio, sonication time, and the concentration and type of the surfactant.

a) Effect of organic:aqueous ratio

To determine the effect of the organic:aqueous ratio on the particle size, fixing the amount of PLA at 5 mg, the PLA was dissolved in 1, 2.5, or 5 mL of CH_2Cl_2 and the organic phase was added to 5 mL of 18 mg/mL PVA in water solution. The resulting emulsion was subjected to 2 minutes of sonication (30 seconds on and 10 seconds off). As shown in Table 4-1, The results demonstrated that the smallest particle diameter was obtained by using the ratio of 1:1 CH_2Cl_2:water, with a Z-average diameter of 236±5. Additionally, the polydispersity index (PDI) was a relatively low value of 0.12±0.03. Thus, this ratio was used to further optimization of NPs. This result might be attributed to the viscosity of the organic phase. At a fixed amount of the polymer, a small volume of the organic phase leads to an increase in polymer concentration and a more viscous organic phase that provides a high mass transfer

resistance (Galindo-Rodriguez *et al.*, 2004) and low stirring efficiency (Guo and Chu, 2009). Consequently, the diffusion of the organic phase into the aqueous phase is reduced resulting in larger particle size. In contrast, a decrease in the viscosity of the organic phase by increasing the volume of the organic phase at fixed polymer amount leads to an increase in the distribution efficiency of the polymeric phase into external aqueous phase, forming smaller droplet size.

Table 4-1: Influence of different ratios of CH_2Cl_2:water on the Z-average diameter and diameter polydispersity of NPs prepared by the emulsification-evaporation method using 5 mg PLA, concentration of 18 mg/ mL of PVA, and sonication time of 2 minutes.

CH_2Cl_2:water ratio (mL/mL)	Z-average diameter[*](nm)	PDI[*]
1:5	327±10	0.24±0.02
1:2	274±5	0.21±0.4
1:1	236±5	0.12±0.03

[*]Average ± SD

b) Effect of the sonication time

The effect of different sonication times of 2, 4, or 6 minutes on the nanoparticle diameter was investigated, using a fixed concentration of 1 mg/mL of PLA in 5 mL of CH_2Cl_2 and 5 mL of 18 mg/mL of PVA aqueous solution optimized above. In general, an increase in sonication time from 2 to 6 minutes led to a decrease in particle diameter from 236± 5 to 207± 4 nm as illustrated in Table 4-2. This reduction can be explained by a reduction in the adhesion between the polymeric droplets, which is induced by sonication. Thus, a 6-minute sonication time was used for further optimization of the NPs.

Table 4-2: Influence of the sonication time on the Z-average diameter and polydispersity of NPs prepared by the emulsification-evaporation method using 5mg of PLA, concentration of 18 mg/ mL of PVA, and 1:1 CH_2Cl_2:water layer.

Sonication time (minutes)	Z-average diameter[*] (nm)	PDI[*]
2	236±5	0.12±0.03
4	218±4	0.15±0.02
6	207±4	0.17±0.02

[*]Average ± SD

c) Effect of PVA concentration in the aqueous layer

Using the optimized conditions consisting of a sonication time of 6 minutes, 1:1 CH_2Cl_2:water ratio, and a fixed concentration of 1 mg/mL of PLA in 5 mL of CH_2Cl_2, the effect of PVA concentration in aqueous layer on the nanoparticle diameter was studied. As demonstrated in Table 4-3, an increase in the concentration of PVA in the aqueous phase from 10 to 18 mg/mL led to a decrease in the diameter and PDI from 288± 62 to 204± 4 and from 0.53± 0.15 to 0.17± 0.02, respectively, while a further increase in the concentration up to 40 mg/mL resulted in an increase in the diameter and PDI to 419± 50 and 0.51± 0.02, respectively. These results show that 10 g/L PVA solution was not sufficient to cover the polymeric droplets during the formulation, leading to coalescence of the small droplets to form large ones, while 40 mg/mL was more than enough and may lead to an increase in the viscosity of the aqueous layer, resulting in a lowering of the efficiency of the sonication process.

Table 4-3: Influence of PVA concentration in the aqueous layer on Z-average diameter and diameter polydispersity for NPs prepared by an emulsification-evaporation method using 5 mg PLA, 1:1 CH_2Cl_2:aqueous layer, and sonication time of 6 minutes.

Amount of PVA (mg/mL)	Z-average diameter[*] (nm)	PDI[*]
10	288±62	0.53±0.15
18	207±4	0.17±0.02
40	419±50	0.51±0.02

[*]Average ± SD

d) Effect of sodium cholate as a surfactant

The influence of using of sodium cholate (SC) as a surfactant instead of PVA on the particle diameter was also investigated by using the optimized conditions of 1 mg/mL of PLA in 5 mL of CH_2Cl_2, 5 mL of water, and sonication for 6 minutes. SC is an ionic surfactant and suitable for particle preparation (Sahli *et al.*, 1997) owing to its natural origin, its biocompatibility, and its interfacial properties. The stability of the particle suspension is due to formation of a strong negative charge on the surface of the particles.

As shown in Table 4-4, SC provided a substantial decrease in the particle diameter when the

other variables were held constant at 1:1 CH_2Cl_2:aqueous ratio and 6 minutes of sonication time. Moreover, the size of PLA NPs decreased slightly when SC concentrations increased. The particle diameter dropped from 107± 5 to 88± 0.4 upon increasing the SC concentration from 3 mg/mL to 6 mg/mL. The significant reduction in the particle diameter upon using SC compared to PVA is attributed to the difference in molecular structures of the two surfactants where SC molecules are much smaller than the PVA chains, resulting in an increase in the viscosity of the aqueous phase in case of PVA, which leads to reduction of the shear stress during the homogenization process. Additionally, it was found that PVA has a high affinity for the aqueous phase and the PVA chains are favorably directed towards the aqueous phase (Murakami *et al.*, 1999). Based on these optimization experiments, 1:1 CH_2Cl_2:water, sonication for 6 minutes, and 6 mg/ mL SC aqueous solution were the optimized conditions used for PLA NPs of particle diameter of less than 100 nm and would be used for subsequent experiments.

Table 4-4: Influence of SC concentration in the aqueous layer on Z-average diameter and diameter polydispersity of NPs prepared by an emulsification-evaporation method using 5 mg PLA, 1:1 CH_2Cl_2:aqueous layer, and sonication time of 6 minutes.

Concentration of SC (mg/mL)	Z-average diameter[*] (nm)	PDI[*]
3	107±5	0.16±0.01
6	88±0.4	0.16±0.02

[*]Average ± SD

4.3.2 The size and zeta potential of PEtG/PLA blend NPs

Using the previously optimized conditions, NPs were prepared using PEtG/PLA blend solutions of different ratios of 100:0, 75:25, 50:50, 25:75, and 0:100 using the SC surfactant. Table 4-5 shows the results of particle size and zeta potential measurements on the particles. The results showed that all particle diameters were in the range of 85± 1.1 nm to 92± 1.1nm. The zeta potentials of all NPs prepared by SC ranged from – 28.7 mV to -39.9 mV indicating that the negatively charged SC surfactant was incorporated in the surface of polymeric droplets during the preparation (Lamprecht *et al.*, 2001). Also, the TEM results confirmed the DLS results as shown in Figure 4-1, Figure 4-2, Figure 4-3, Figure 4-4, and Figure 4-5.

Table 4-5: Z-average diameters and zeta potentials for PEtG/PLA blend NPs.

NPs PEtG:PLA	Z-average* (nm)	Zeta potential (mV)
100:0 NPs	86±1.4	-35
75:25 NPs	86±2.3	-28.7
50:50 NPs	85±1.1	-38.9
25:75 NPs	92±1.1	-29.4
0:100 NPs	88±0.4	-39.9

*Average ± SD
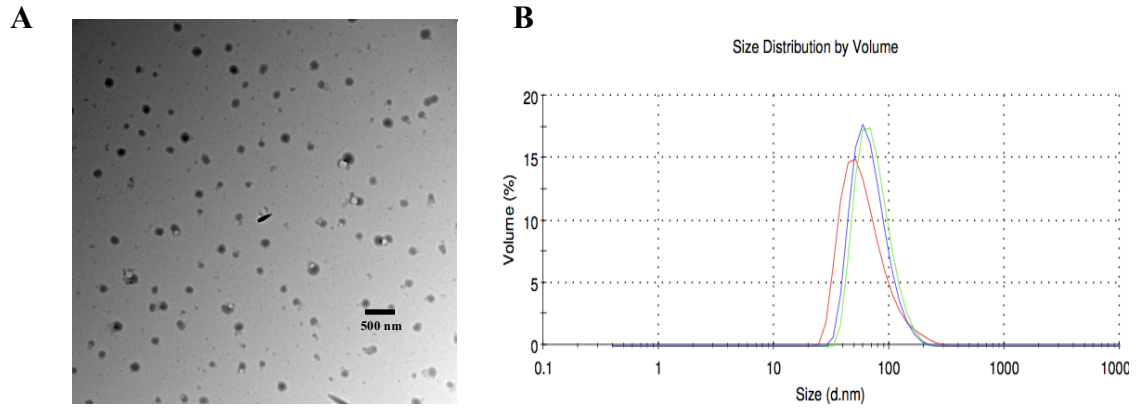
A   B

Figure 4-1: A) TEM image and B) DLS traces of 100 PEtG NPs from different batches.
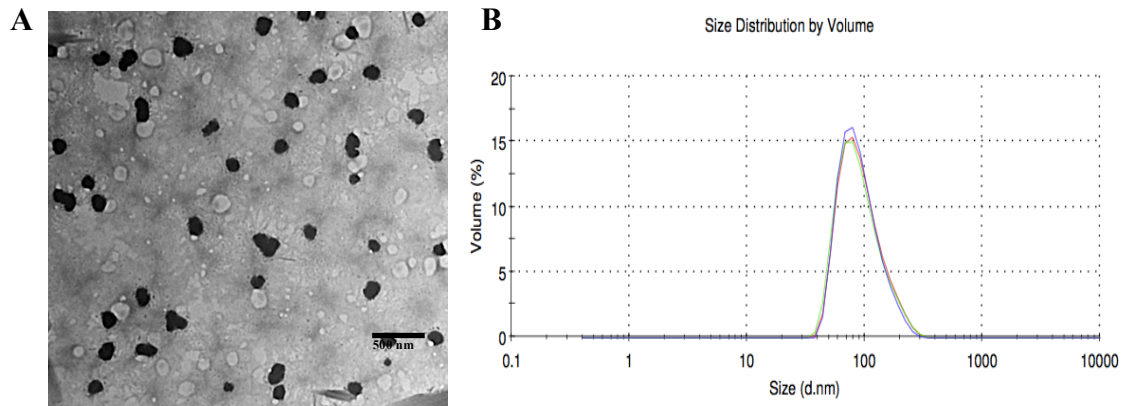
A   B

Figure 4-2: A) TEM image and B) DLS traces of 75 PEtG: 25PLA NPs from different batches.
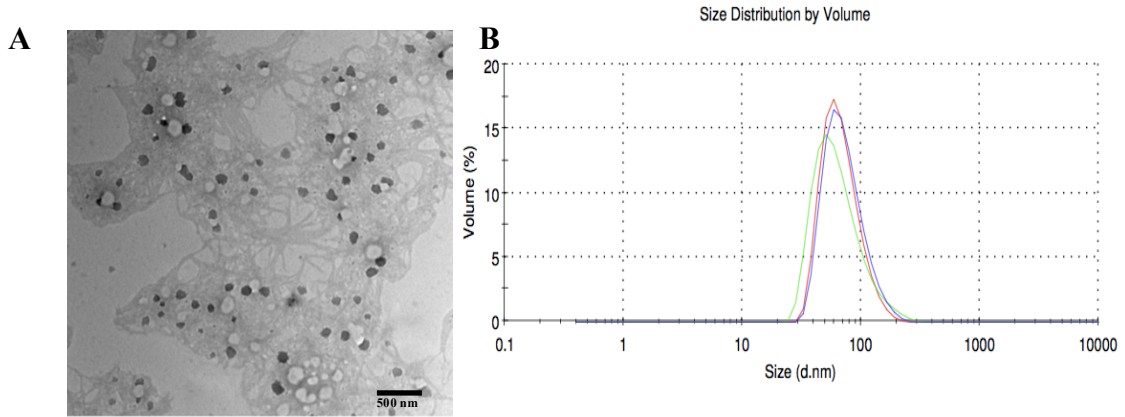
Figure 4-3: A) TEM image and B) DLS traces of 50PEtG: 50PLA NPs from different batches.
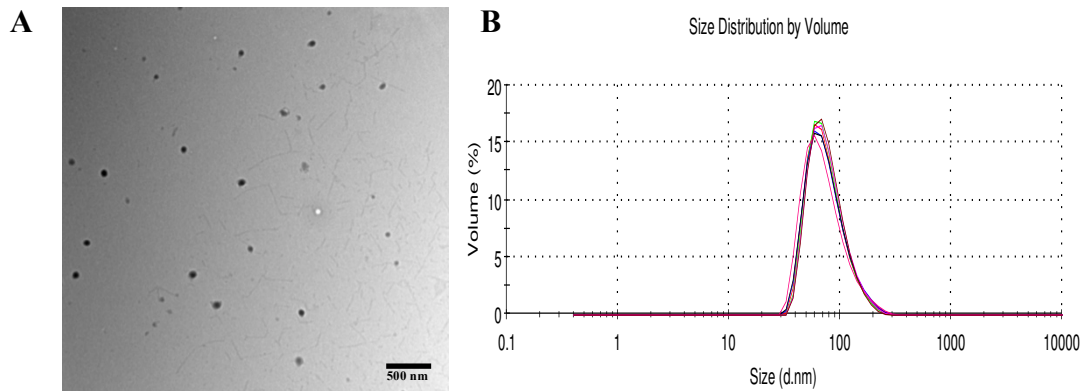
Figure 4-4: A) TEM image and B) DLS traces of 25PEtG: 75PLA NPs from different batches.
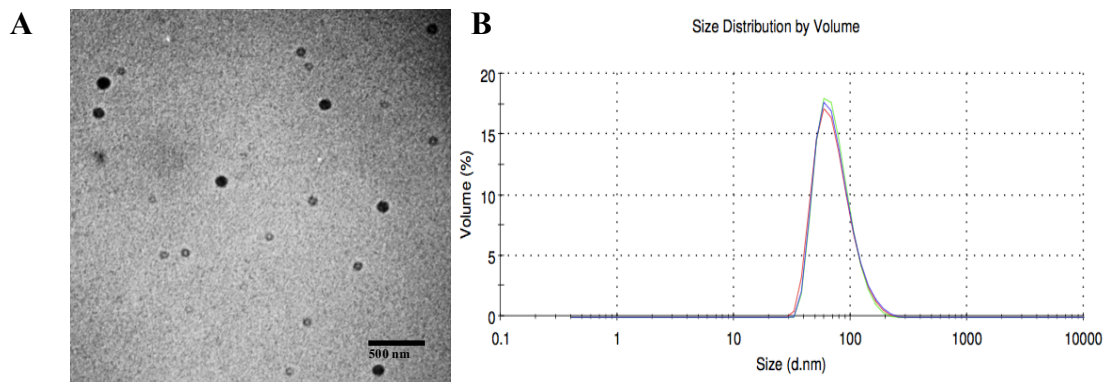
Figure 4-5: TEM image and DLS trace of 100PLA NPs.

4.3.3 Thermal characterization of PEtG/PLA blends and PEtG/PLA NPs

TGA was performed first to determine the decomposition temperatures of PEtG/PLA blend NPs. All NPs underwent decomposition in multiple stages, which can likely be attributed to the different components including the PEtG which degrades between ~150-200 °C, the PLA

which degrades between 200-250 °C, and the SC coating which is stable up to 350 °C. The physical compatibilities between the two polymers were determined by DSC in the temperature range of -100 - 100 °C. The results from Table 4-6 and Appendix A show that PEtG and PLA are both amorphous polymers with T_gs of -12 °C and 44 °C respectively. Blending of these polymers at the molecular level would lead to a single new $T_g$, which would be expected to be intermediate between the T_gs of these two polymers. However, at all blend ratios two T_gs with values similar to those of the two polymers were observed. In each case, the T_g of PEtG was slightly increased through incorporation into the NPs, while that of PLA was slightly decreased, which is likely due to a very small degree of mixing between the two polymers. However, the results suggest that the NPs existed in a primarily phase-separated form, at least at the nanoscale. It should also be noted that DSC did not reveal any thermal transitions for SC. In its crystalline form, it is known to have a T_m= 198 °C but this exceeds the temperature range of our experiment, which was limited by the poor stability of the PEtG at higher temperatures.

Table 4-6: Glass transition temperatures of pure polymers, PEtG/PLA blend, and PEtG/PLA blend NPs of different ratios.

Sample	PLA	PLA NPs	25/75 NPs	50/50 NPs	75/25 NPs	PEtG NPs	PEtG
T_g(°C)	44	40	2, 39	3, 47	2, 39	2	-12

4.3.4 Loading % and encapsulation efficiency of PEtG and PLA NPs:

The effects of different ratios of letrazole:polymer on loading % and encapsulation efficiency of PEtG and PLA NPs were investigated. As illustrated in Table 4-7, in the case of PEtG NPs, the results showed that the encapsulation and the loading increased gradually with an increasing ratio of letrazole:PEtG. By using different letrazole:polymer ratios of 1:5, 2:5, and 3:5 (w/w), the drug loading in PEtG NPs were 9.8± 1.1%, 17.8±6.8%, and 29.8± 5.1%, and the encapsulation efficiencies were 62.2± 9.1, 73.2± 14.6, and 86.5± 8.0 respectively. Additionally, in case of PLA, the encapsulation efficiency and loading % increased by increasing the ratio of letrazole:PLA.

The loading % increased from 11.1±5.5 to 28.4±1.6% and encapsulation efficiency increased from 66.9±3.2 to 75.7±7.7 upon increasing the letrazole to polymer ratio from 1:5 to 3:5.

This might be due to the low solubility of the drug in the aqueous phase (0.078 g/L) and the high partition coefficient of the drug to the polymeric matrix relative to the aqueous phase. Overall, the results showed good encapsulation and loading efficiencies of letrazole in PEtG and PLA NPs. Also, DLS results of the PEtG and PLA NPs using different ratios of letrazole:polymer indicated that there was no significant increase in the particle diameter as shown in Table 4-8.

Table 4-7: Drug loading and encapsulation efficiency of PEtG and PLA NPs using different letrazole:polymer ratios.

Letrazole: polymer		Drug Loading[*] % (w/w)	Encapsulation Efficiency[*] %
PEtG NPs	1:5	9.8±1.1	62.2±9.1
	2:5	17.8±5.8	73.2±14.6
	3:5	29.8±5.1	86.5±8.0
PLA NPs	1:5	11.1±5.5	66.9±3.2
	2:5	22.3±4.9	78.2±2.2
	3:5	28.4±1.6	75.7±7.7

[*]Average ± SD

Table 4-8: Influence of different ratios of letrazole:polymer on Z-average diameter and diameter distribution of NPs prepared by an emulsification-evaporation method.

Letrazole: polymer		Z-Average diameter[*] (nm)	PDI
PEtG NPs	1:5	86.2±1.4	0.06±0.04
	2:5	92.4±5.8	0.09±0.03
	3:5	91.3±3.3	0.09±0.04
PLA NPs	1:5	84.4±2.8	0.16±0.02
	2:5	100.2±6.1	0.19±0.04
	3:5	89.9±3.2	0.12±0.03

[*]Average ± SD

4.3.5 UV-responsive degradation of PEtG NPs.

Letrazole loaded PEtG NPs were prepared using 3:5 letrazole:polymer ratio (~30 wt% drug) in order to study UV-responsive degradation of PEtG in form of NPs. First, a UV stability test for letrazole was performed to ensure that the drug was not degraded upon UV

irradiation. This assessment was done using ^{1}H NMR spectroscopy by dissolving letrazole in CD$_3$CN, acquiring an initial spectrum of the drug, irradiating the drug for 1 hour with a UV light source and then acquiring another spectrum of the drug. The results showed that letrazole was stable upon UV irradiation as demonstrated in Figure 4-6 as no changes in the NMR spectrum of the drug were observed.
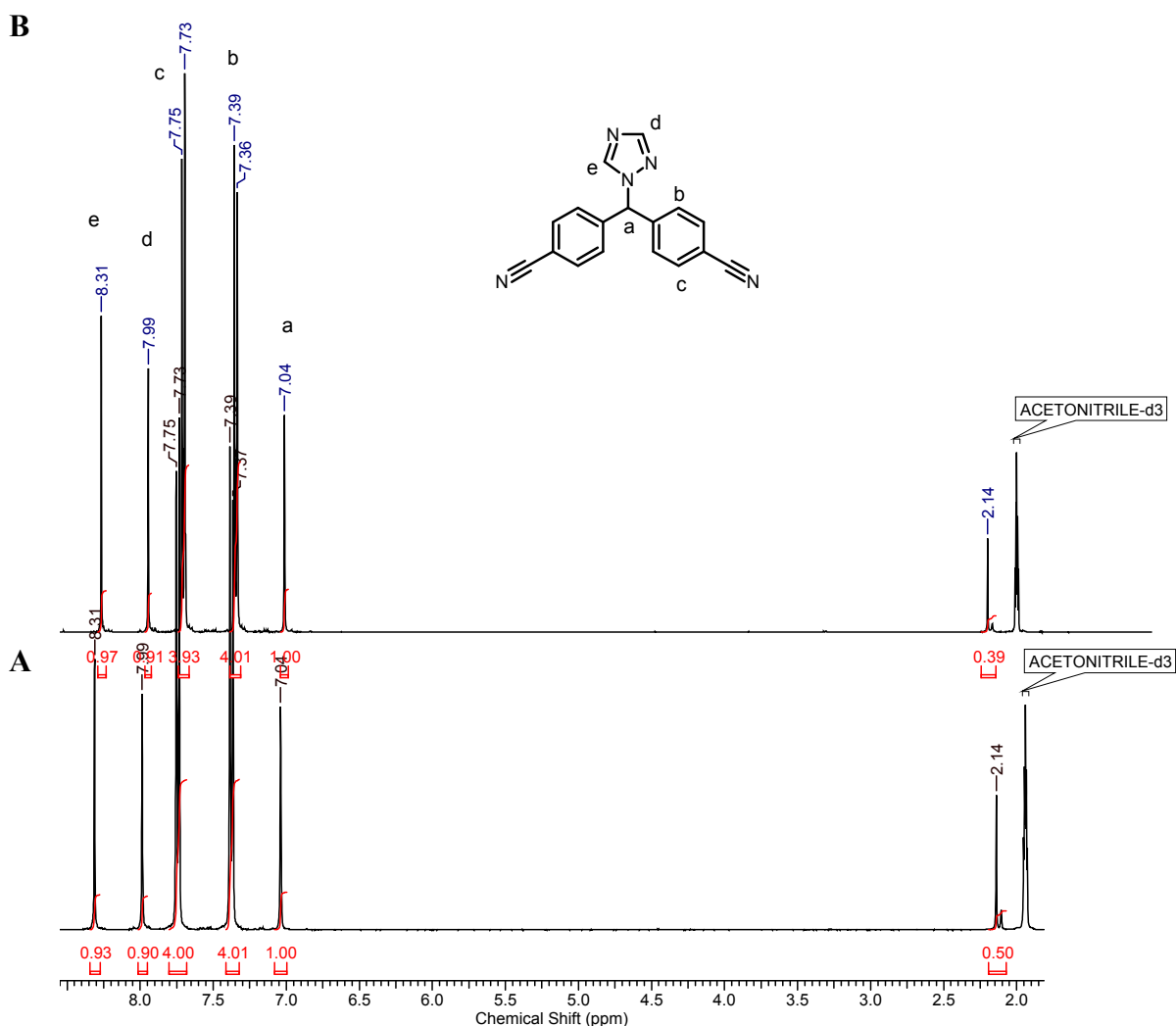

Figure 4-6: ^{1}H NMR spectra showing UV Stability of letrazole in CD$_3$CN: A) before UV irradiation and B) after UV irradiation.

The PEtG-letrazole NPs (~30 wt% drug) were prepared in D$_2$O and exposed to different irradiation times of 20, 40, 60, and 80 minutes to determine the required irradiation time for NVOC cleavage. It was found that 20 minutes was sufficient to complete removal of the NVOC end-cap. Because PEtG is insoluble in water, only the surfactant and water-soluble degradation byproducts were detected in the ^{1}H NMR spectra. After irradiation, sharp peaks

at 1.16, 4.13, and 5.2 ppm corresponding to the expected degradation product of EtGH emerged as EtG in water forms immediately its hydrate form. No significant difference in the intensities of these peaks was observed with different irradiation times as illustrated in Figure 4-7. Moreover, because letrazole has a low limit solubility in water (0.078 mg/mL), it peaks did not show up in the ^{1}H NMR spectra.
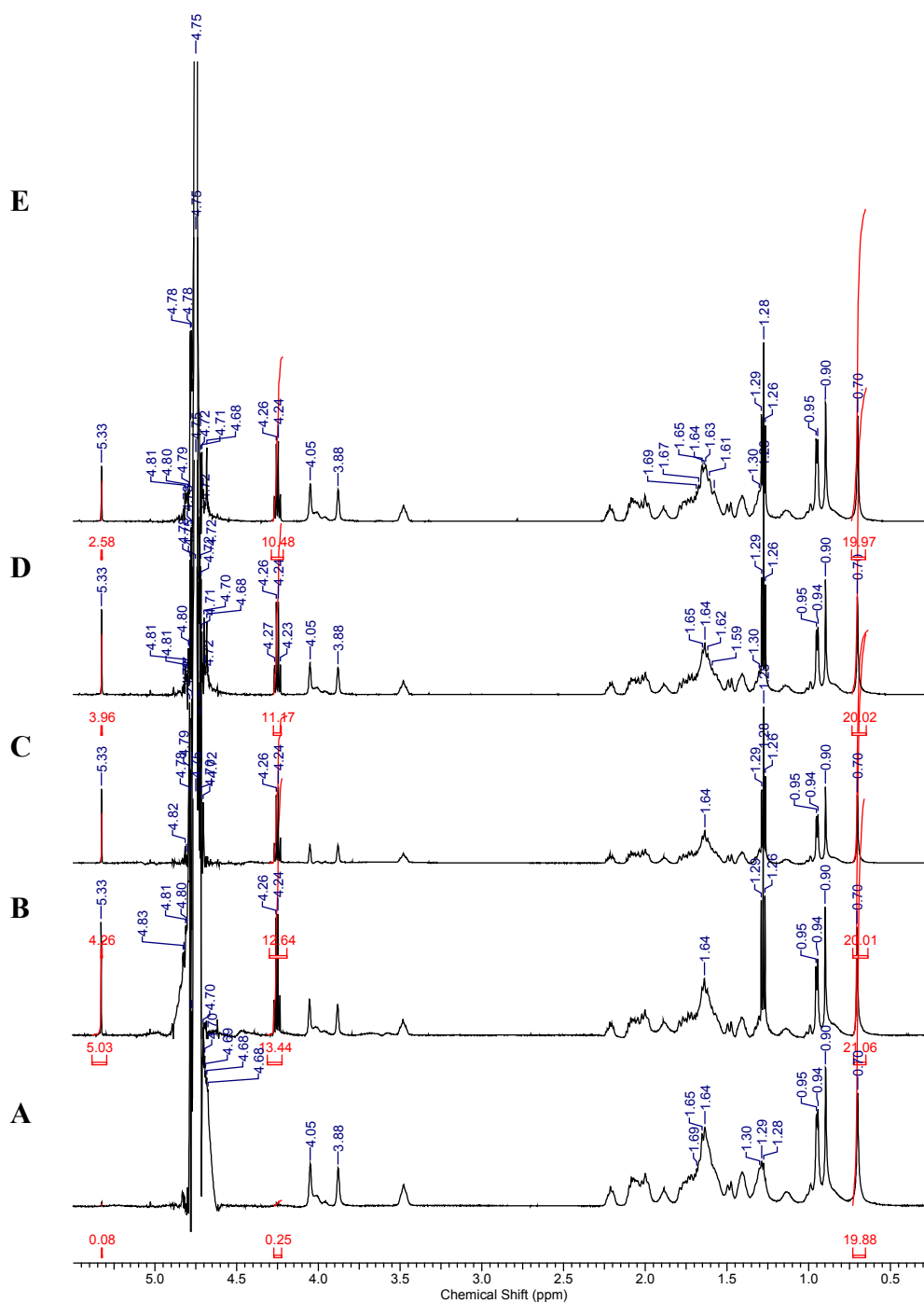

Figure 4-7: ^{1}**HNMR spectra of loaded NPs a) before irradiation, b) after 20, c) after 40, d) 60, and e) 80 minute UV irradiation but with incubation at 25°C in D₂O.**

4.3.6 *In vitro* release study

a) Letrazole release performance with different drug loading values without UV irradiation

Letrazole loaded PEtG and PLA NPs prepared with 1:5, 2:5, and 3:5 letrazole:polymer ratios were placed in a dialysis membrane with a 6000 to 8000 g/mol MWCO and these were stirred in pH 7.4 phosphate buffer at 37 °C in order to study the release profiles of the NPs without UV irradiation. As shown in Figure 4-8 and Figure 4-9, the release pattern of letrazole from PEtG and PLA NPs was biphasic, involving first a burst effect, followed by a slower release. The burst effect for the drug likely resulted from the release of the drug near the surface of the particles. However, the drug at the centers of the NPs took longer to diffuse out of the polymer matrix, or to be released upon polymer degradation.

The results revealed that the NPs with high loading content (3:5 letrazole:polymer) showed the lowest burst effect in both PEtG and PLA NPs. In contrast, the NPs with the lowest letrazole content showed a pronounced burst effect as shown in Figure 4-8 and Figure 4-9. This might be explained by the fact that at low drug content, the drug was concentrated on the surfaces of the particles, while by increasing drug amount during preparation, letrazole became more distributed though the polymer matrix, resulting in a decrease in the burst effect.

It is also noteworthy that the burst effect from PLA NPs was more pronounced than from PEtG NPs, which might be attributed to more compact nanostructure of PEtG than PLA due to the difference in molecular weight (Ravivarapu *et al.*; 2000; Duvvuri *et al.*, 2006). Moreover, the short chains of PLA means more carboxylate free ending that leads to more water penetration and more release thereafter (Zambaux *et al.*, 1999). Because the NPs from PEtG and PLA were in the same size range, the drug release kinetics cannot be attributed to differences in size.
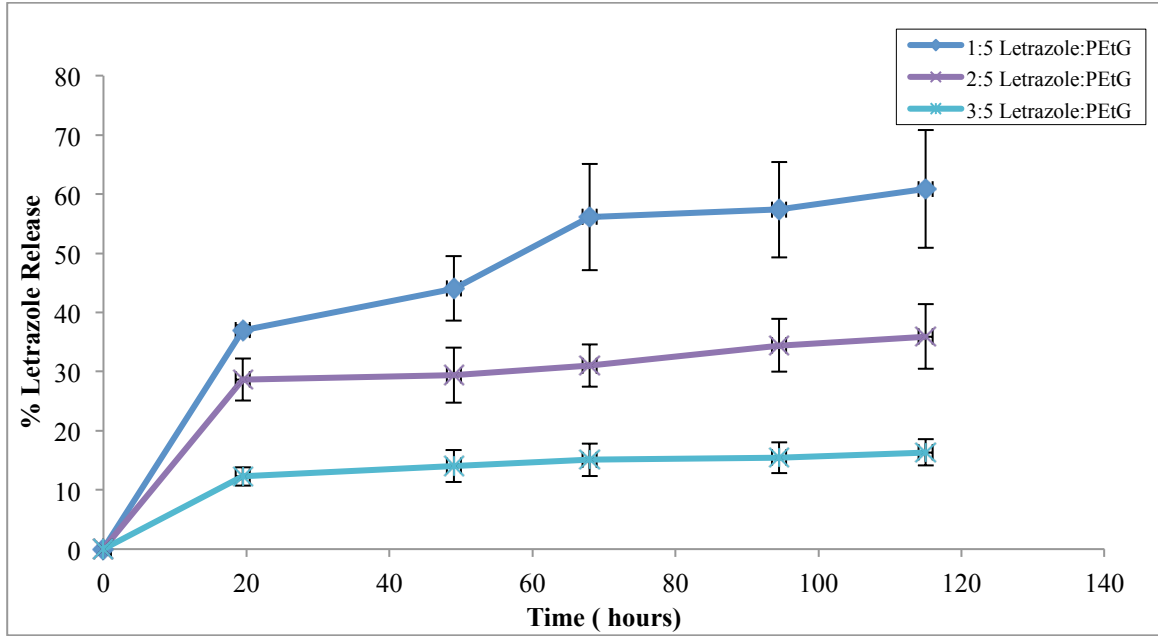
Figure 4-8: Letrazole release profile from PEtG NPs using different loadings of 1, 2, and 3 mg of letrazole per 5mg of PEtG in pH 7.4 PBS at 37 °C.
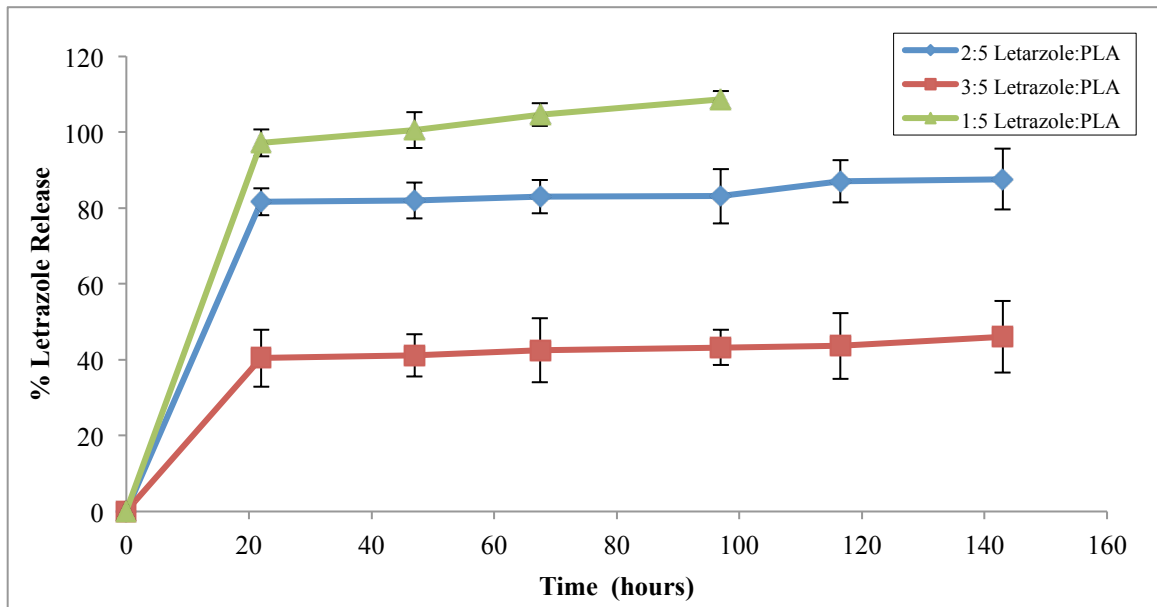

Figure 4-9: Letrazole release profile from PLA NPs using different loadings of 1, 2, and 3 mg of letrazole per 5 mg of PLA in pH 7.4 PBS at 37 °C.

b) Letrazole release performance from PEtG/PLA blend NPs without UV irradiation

PEtG/PLA blend NPs were synthesized with 3:5 letrazole:polymer ratio to study the effect of

different polymer ratios on the release profile in PBS of 7.4 pH at 37 °C. The results were consistent with the previous results using 100% PLA and 100% PEtG NPs. Increasing the PLA content in the NP formulation led to increasing burst release as shown in Figure 4-10 and Table 4-9.

Table 4-9: Drug loading, encapsulation efficiency, and initial burst effect of PEtG/PLA blend NPs of different ratios using 3:5 letrazole:polymer ratio.

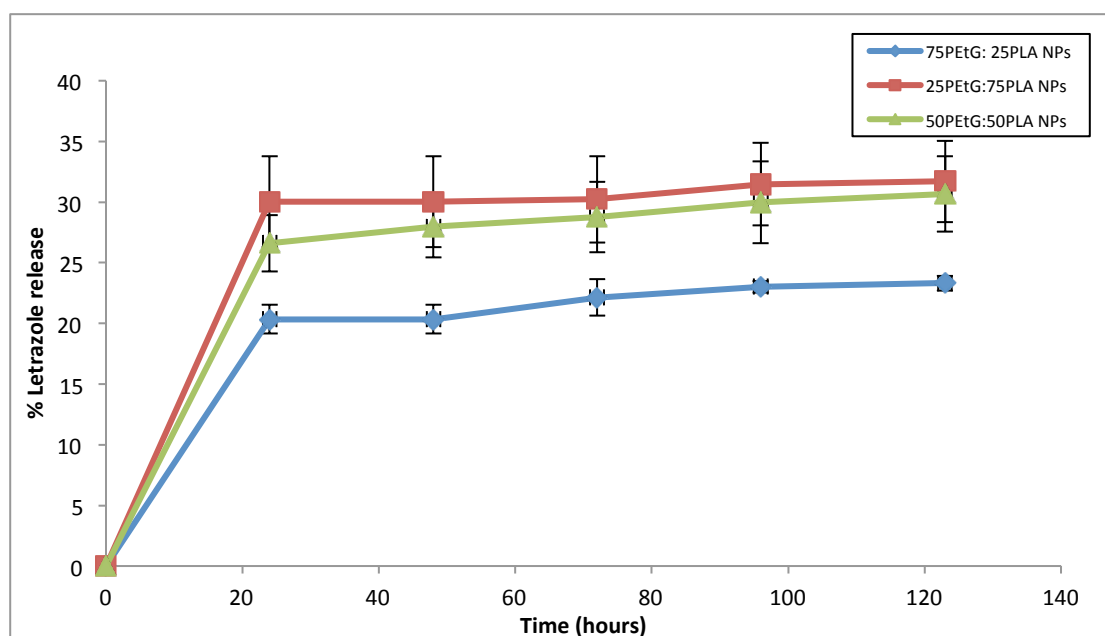| NPs PEtG:PLA	Drug Loading[*] % (w/w)	Encapsulation Efficiency[*] %	Initial burst release[*] %
100:0	29.8±5.1	86.5±8.0	12.3±1.6
75:25	26.4±2.3	72.6±3.0	20.3±1.2
50:50	20.8±6.0	76.4±0.1	26.6±2.3
25:75	24.2±1.8	71.9±4.7	30.0±3.7
0:100	28.4±1.6	75.7±7.7	40.4±3.4

[*]Average ± SD

Figure 4-10: Letrazole release profile from 75PEtG:25PLA, 50PEtG:50PLA, and 25PEtG:75PLA NPs using 3:5 letrazole:polymer ratio in pH 7.4 PBS at 37 °C.

c) Letrazole release from PEtG NPs upon UV irradiation

An *in vitro* study was performed using drug loaded PEtG NPs without irradiation (control test) and with 20 minute UV irradiation in phosphate buffer solution of pH 7.4 at 37 °C. The letrazole release profile was not expected as UV irradiation was expected to lead to a very

rapid release of letrazole upon UV induced depolymerization of PEtG. However, the release of the drug from irradiated NPs was only slightly higher than the non-irradiated NPs as shown in Figure 4-11. This experiment was repeated several times to confirm this unexpected result.
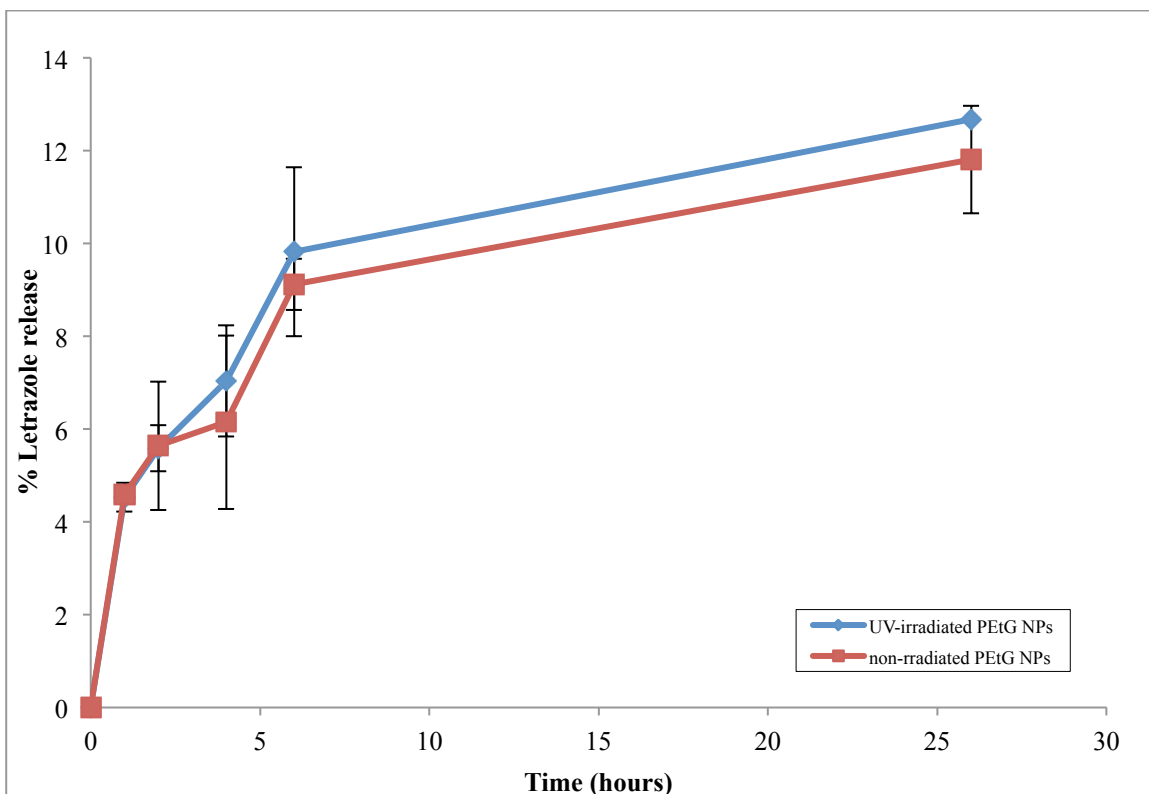

Figure 4-11: Letrazole release profile from UV-irradiated and non-irradiated PEtG NPs using 3:5 letrazole to polymer ratio in pH 7.4 PBS at 37 °C.

As shown in Figure 4-12, ^{1}H NMR spectra illustrated that non-degraded PEtG remained within the dialysis tube in the case of the non-irradiated NPs, explaining the expected slow release of letrazole in this case. However, in the case of the irradiated PEtG NPs, no undegraded PEtG or PEtG degradation products were detected, confirming that the polymer was successfully degraded and released into the release media through the dialysis membrane. At this stage, it was hypothesized that the slow release resulted in the poor solubility of letrazole.

A

AV 300
1D Proton Spectrum
Sample 1
Sept. 22, 2014.

5.5　5.0　4.5　4.0　3.5　3.0　2.5　2.0　1.5　1.0　0.5　ppm

0.78　　1.63　　19.13　1.73　2.56　3.00　0.36
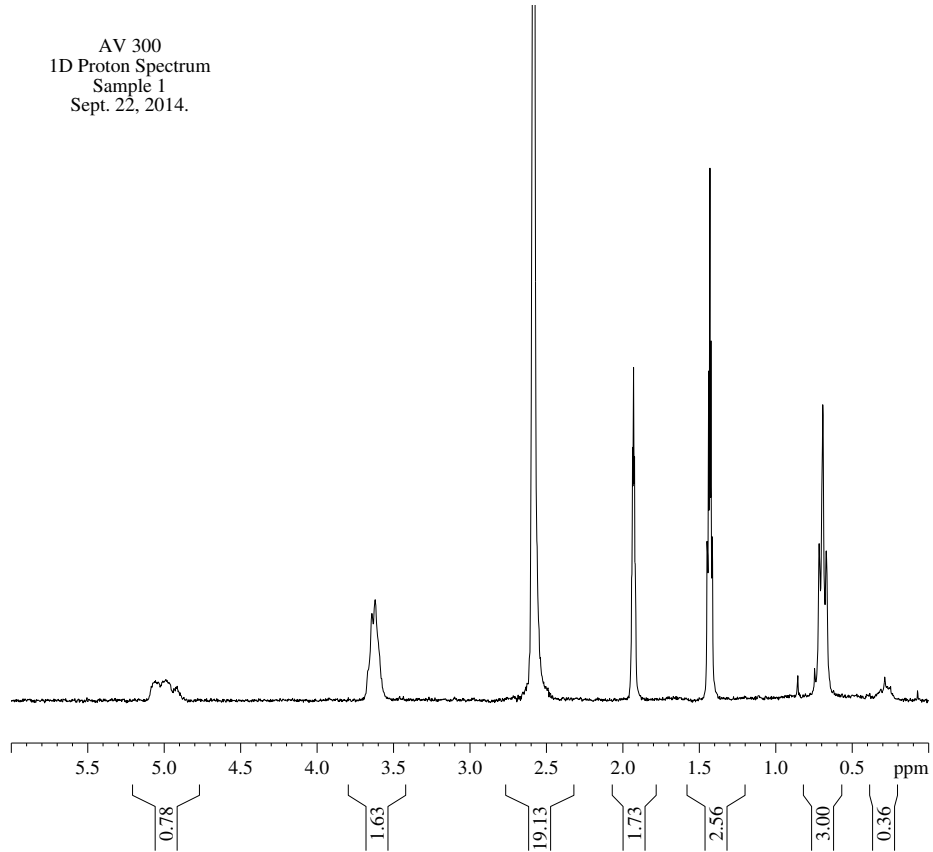
B

AV 300
1D Proton Spectrum
Sample 2
Sept. 22, 2014.

5.5　5.0　4.5　4.0　3.5　3.0　2.5　2.0　1.5　1.0　0.5　ppm
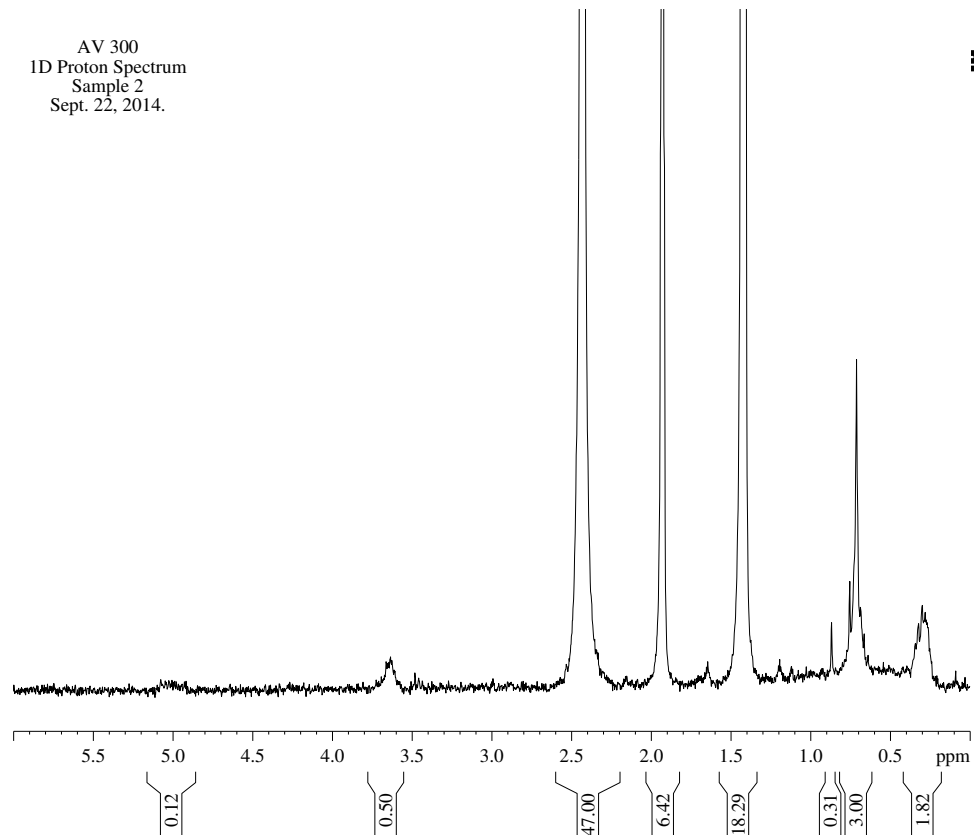
0.12　　0.50　　47.00　6.42　18.29　0.31 3.00　1.82

Figure 4-12: ^{1}HNMR spectra of the dialysate after 1 day dialysis a) non-irradiated and b) UV-irradiated.

Several experimental designs were investigated in order to determine the reason for the slow release from irradiated NPs. Tween 20 was used in 0.1% v/v in the release media as a solubilizing agent with irradiated and non-irradiated PEtG NPs in order to compare the release performance. The results showed again that the release from the irradiated NPs was only slightly higher than the non-irradiated NPs. Another attempt was performed was to prepare rhodamine B loaded PEtG NPs (more water soluble dye) and apply sonication after UV irradiation, and then the results were compared with a control test of non-irradiated NPs. The results showed that the rhodamine release from non-irradiated NPs was slightly higher than the irradiated NPs, likely due to photobleaching in the case of the irradiated particles. The results also showed that the sonication after UV irradiation decreased the rhodamine release in case of the irradiated NPs and, while the sonication increased the rhodamine release from the non-irradiated NPs as illustrated in Figure 4-13. It is important to mention that these trials were done once, but none of them showed the expected triggered release. At this stage, it was proposed that the slow release might be attributed to the remaining cholic acid that traps the probe/drug within a nanoaggregate even after PEtG depolymerization.
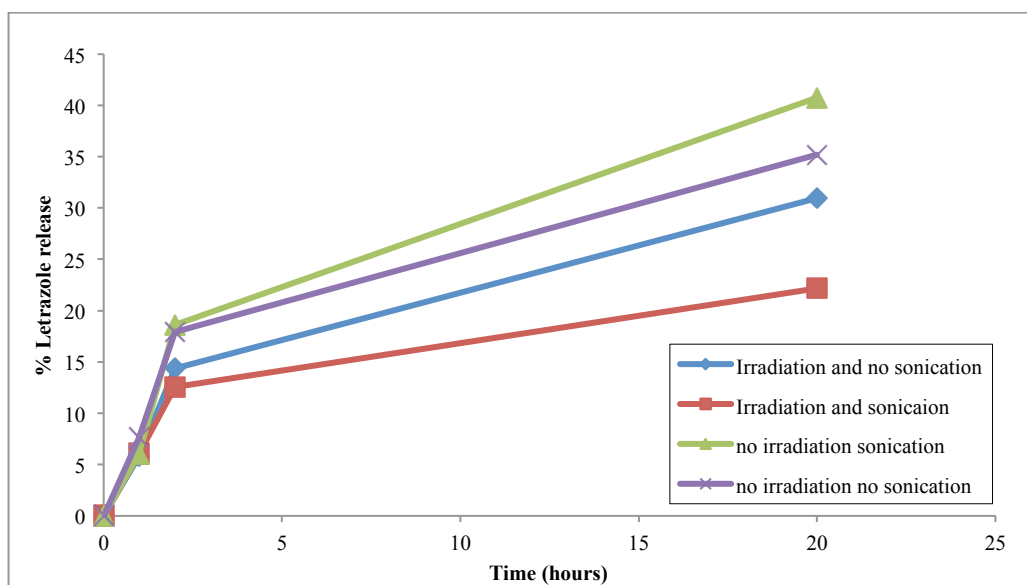

Figure 4-13: The profile of Rhodamine release from (green) non-irradiated and sonicated PEtG NPs; (purple) non-irradiated and non-sonicated PEtG NPs; (blue) irradiated and non-sonicated PEtG NPs, and (red) irradiated and sonicated PEtG NPs.

d) Nile red encapsulation

To further probe the NP degradation and potential drug release, Nile red was encapsulated in the PEtG NPs. Nile red exhibits high fluorescence when it is encapsulated into the hydrophobic core of a NP, but low solubility and extensive aggregation in an aqueous

solution where it displays negligible fluorescence. Therefore, it is a useful direct probe of its environment because it does not need to be released through a dialysis membrane to be probed. For non-irradiated NPs, the fluorescence intensity was high; however, the intensity decreased by 50% upon irradiation for 20, 40, 60, and 80 minutes (all of the same intensity), confirming the ^{1}H NMR results that PEtG depolymerized, leaving the nile red in a more polar environment (Figure 4-14). No further decrease in fluorescence was observed for any of these samples over the next 4 days, suggesting that depolymerization had already reached completion at the first measurement. However, approximately 50% of the initial fluorescence still remained, even at the long time points. This is consistent with some or all of the nile red remaining encapsulated within SC aggregates (Figure 4-14 and Figure 4-15).
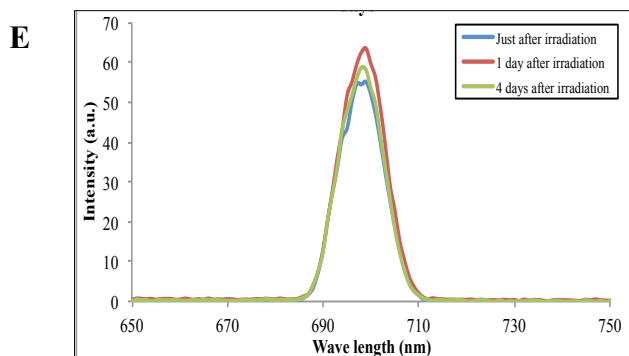
E
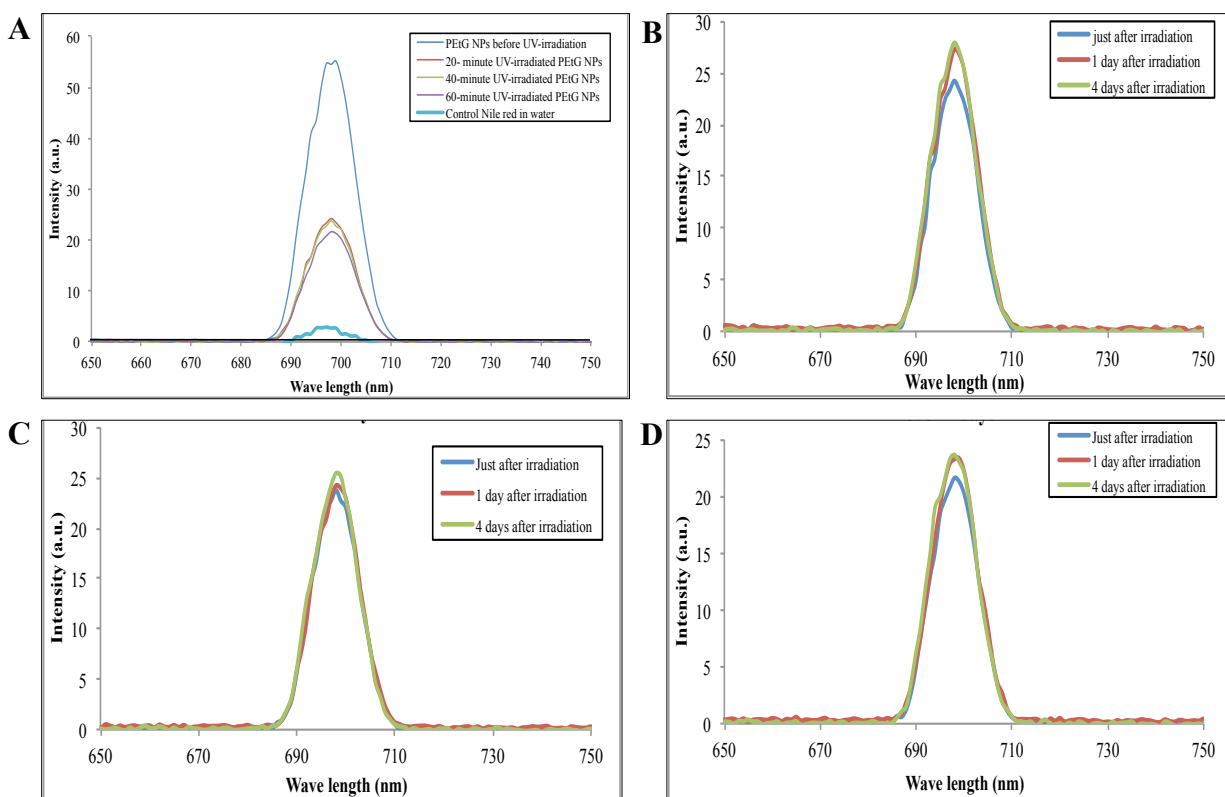
Figure 4-14: A) Change of fluorescence intensity of Nile red encapsulated on PEtG NPs before and after irradiation for 20,40, and 60 minutes; B) change in the fluorescence intensity of 20 minute, C) 40 minute, D) 60 minutes irradiated, and E) non irradiated PEtG NPs over 4 days.
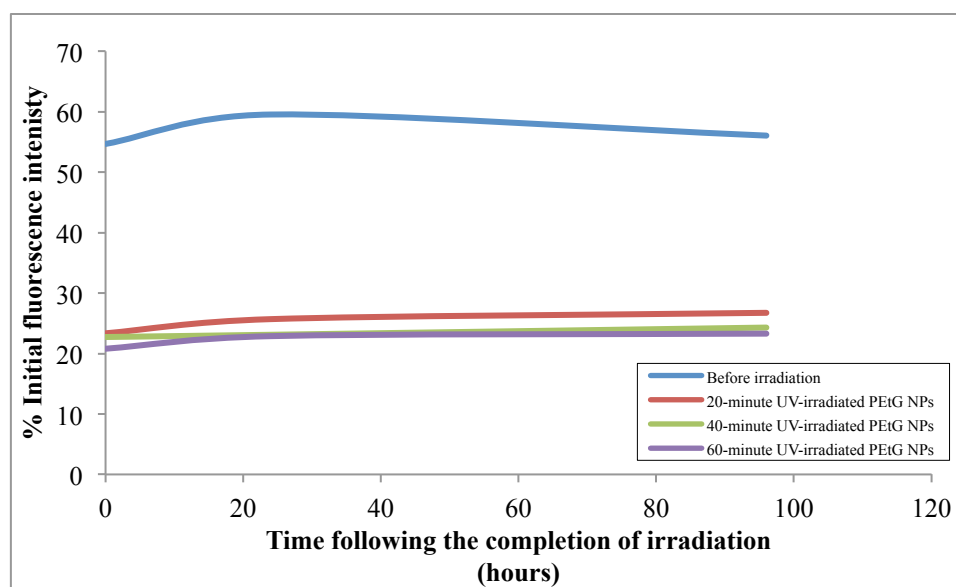

Figure 4-15: Percent initial fluorescence of nile red intensity over 4 days.

4.4 Conclusions

This study investigated the use of an emulsification-evaporation method for the preparation of PEtG/PLA blend NPs with PEtG designed to impart stimuli responsive properties to the NPs, for the release of drug to be triggered. The influence of several experimental parameters such as the organic to aqueous ratio, sonication time, and type and concentration of the surfactant on the particle diameter of PLA NPs were investigated. By using the optimized PLA nanoparticle preparation conditions, it was possible to prepare PEtG/PLA blend NPs having Z-average diameters of less than 100 nm and reasonable polydispersities. All of the prepared particles had negative zeta potentials due to remaining cholic acid on the surface of the NPs. The thermal characterization of the polymer blend NPs demonstrated that the two polymers exhibited phase separation as the amorphous regions maintained their original

properties, and thus two T_gs were observed. It was possible to encapsulate the drug letrazole into the NPs with good efficiencies, leading to high drug content. The extent of burst release from the NPs depended on the ratio of PLA:PEtG, with more PLA leading to more burst release. Unfortunately, the UV light irradiated NPs exhibited unexpectedly slow release, which occurred at the same rate as release from the non-irradiated NPs. Investigations were performed and the results suggested that even though the PEtG breaks down rapidly under the conditions of the experiment, the drug may remain encapsulated in aggregates formed by the surfactant SC. Additional research will be required to address this issue.

4.5 References

[1] Alexis, F.; Pridgen, E.; Molnar, L.K.; Farokhzad, O.C., (2008). "Factors affecting the clearance and biodistribution of polymeric nanoparticles", Molecular Pharmaceutics, 5,505–515.

[2] Bansal, A.; Zhang, Y., (2014). "Photocontrolled Nanoparticle Delivery Systems for Biomedical Applications", Accounts of Chemical Research, 47, 3052–3060

[3] Cohen, M.H.; Johnson, J.R.; Li, N.; Chen, G.; Pazdur, R., (2002). "Approval summary: letrozole in the treatment of postmenopausal women with advanced breast cancer", Clinical Cancer Research, 8, 665–669.

[4] Dadwal, M.; (2014). "Polymeric nanoparticles as promising novel carriers for drug delivery: an overview", Advanced Pharmacy Education & Research, 4, 20-30.

[5] Dey, S. K.; Mandal, B.; Bhowmik, M.; Ghosh L. K., (2009). "Development and in vitro evaluation of Letrozole loaded biodegradable nanoparticles for breast cancer therapy", Brazilian Pharmaceutical Sciences, 45, n. 3.

[6] Duvvuri, S.; Janoria, K. G.; Mitra, A. K., (2006). "Effect of Polymer Blending on the Release of Ganciclovir from PLGA Microspheres", Pharmaceutical Research, 23, 215-223.

[7] Fan, B.; Trant, J. F.; Wong A. D.; Gillies, E. R., (2014). "Polyglyoxylates: A Versatile Class of Triggerable Self-Immolative Polymers from Readily Accessible Monomers", Journal of the American Chemical Society, 136, 10116−10123.

[8] Fang, C.; Shi. B.; Pei, Y.Y.; Hong, M.H.; Wu, J.; Chen, H.Z., (2006). "In vivo tumor targeting of tumor necrosis factor-α-loaded stealth nanoparticles: Effect of MePEG molecular weight and particle size", European Journal of Pharmaceutical Sciences, 27:27–36.

[9] Fu, K.; Pack, D.W.; Klibanov, A.M.; Langer, R., (2000). "Visual evidence of acidic environment within degrading poly(lactic-co-glycolic acid) (PLGA) microspheres", Pharmaceutical Research;17:100–6.

[10] Galindo-Rodriguez , S.; Alle´mann, E.; Fessi, H.; Doelker, E., (2004). "Physicochemical Parameters Associated with Nanoparticle Formation in the Salting-out, Emulsification-Diffusion, and Nanoprecipitation Methods", Pharmaceutical Research, 21, 1428-1439.

[11] Go¨ïner, T.; Gref, R.; Michenot, D.; Sommer, F.; Tran, M.N.; Dellacherie, E., (1999). "Lidocaine-loaded biodegradable nanospheres. I. Optimization of the drug incorporation into the polymer matrix", Control Release 57, 259–268.

[12] Guo, K.; Chu, C. C., (2009). "Biodegradable and Injectable Paclitaxel-Loaded Poly(ester amide)s Microspheres: Fabrication and Characterization", Biomedical Materials Research Part B: Applied Biomaterials, 89B, 491-500.

[13] Harashima, H.; Sakata, K.; Funato, K.; Kiwada, H., (1994). "Enhanced hepatic uptake of liposomes through complement activation depending on the size of liposomes", Pharmaceutical Research, 11:402–6.

[14] He, G.; Lwin Ma L.; Pan, J.; Venkateraman, V., 2007. "ABA and BAB type triblock copolymers of PEG and PLA: A comparative study of drug release properties and stealth particle characteristics", International Journal of Pharmaceutics", 334:48–55.

[15] Huang, J.; Wigent, R. J.; Bentzley, C. M.; Schwartz J. B., (2006). "Nifedipine solid dispersion in microparticles of ammonio methacrylate copolymer and ethylcellulose binary blend for controlled drug delivery Effect of drug loading on release kinetics", International Journal of Pharmaceutics, 319, 44–54

[16] Ibim, S.E.M.; Ambrosio, A.M.A.; Kwon, M.S.; El-Amin, S.F.; Allcock, H.R.; Laurencin, C.T., (1997). "Novel polyphosphazene/poly(lactide-co-glycolide) blends: miscibility and degradation studies", Biomaterials;18:1565–9.

[17] Journal of Control Release;86:195–205.

[18] Kim, J.K.; Garripelli, V. K.; Jeong, U.H.; Park, J.S.; Repka, M. A.; Jo, S., (2010). "Novel pH-sensitive polyacetal-based block copolymers for controlled drug delivery", International Journal of Pharmaceutics, 401, 79–86.

[19] Kreuter, J., (1996). "Nanoparticles and microparticles for drug and vaccine delivery", Journal of Anatomy. 189, 503–505.

[20] Lamprecht, A.; Ubrich, N.; Yamamoto, H.; Schafer, U.; Takeuchi, H.; Lehr, C.-M.; Maincent, P.; Kawashima, Y., (2001). "Design of rolipram-loaded nanoparticles: comparison of two preparation methods", Controlled Release 71 297–306

[21] Lassalle, V.; Ferreira, M.L., (2007). "PLA nano-and microparticles for drug delivery: An overview of the methods of preparation", Macromolecular Bioscience, 7, 767–83.

[22] Long, B.J.; Jelovac, D.; Handratta, V., (2004). "Therapeutic strategies using the aromatase inhibitor letrozole and tamoxifen in a breast cancer model". Journal of National Cancer Institute (Bethesda), 96, 456–465.

[23] Maheshwara Rao, J.; Shyam Sunder, R.; Krishna, S. A., (2014). "Formulation characterization and optimization of process variables of chitosan nanoparticles containing sulfasalazine", Journal of Chemical and Pharmaceutical Sciences, 7, 67-72.

[24] Matsumoto, J.; Nakada, Y., Sakurai, K.; Nakamura. T.; Takahashi, Y., (1999). "Preparation of nanoparticles consisted of poly(L-lactide)–poly(ethylene glycol)–poly(L-lactide) and their evaluation in vitro", International Journal of Pharmaceutics, 185, 93–101.

[25] Mi, F.; Lin, Y. M.; Wu, Y.B.; Shyu, S.S.; Tsai, Y.H., (2002). "Chitin/PLGA blend microspheres as a biodegradable drug-delivery system: phase-separation, degradation and release behavior", Biomaterials", 23, 3257–3267.

[26] Moghimi, S.M.; Hedeman, H.; Muir, I.S.; Illum, L.; Davis, S.S., (1993). "An investigation of the filtration capacity and the fate of large filtered sterically-stabilized microspheres in rat spleen", Biochimica et Biophysica Acta, 1157, 233–240.

[27] Mondal, N.; Halder, K. K.; Kamila, M. M.; Debnath, M. C.; Pal, T. K.; Ghosal, S. K.; Sarkar, B. R.; Ganguly S., (2010). "Preparation, characterization, and biodistribution of letrozole loaded PLGA nanoparticles in Ehrlich Ascites tumor bearing mice" International Journal of Pharmaceutics, 397, 194–200.

[28] Mondal, N.; Pal, T. K.; Ghosal S. K., (2008). "Development, physical characterization,

micromeritics and in vitro release kinetics of letrozole loaded biodegradable nanoparticles", Pharmazie, 63, 361–365.

[29] Murakami, H.; Kobayashi, M.; Takeuchi, H.; Kawashima, Y., (1999). "Preparation of poly(DL-lactide-co-glycolide) nanoparticles by modified spontaneous emulsification solvent diffusion method", International Journal of Pharmaceutics, 187, 143–152.

[30] Park, T.C.; Cohen, S.; Langer, R., (1992). "Poly(l-lactic acid)/pluronic blends: characterization of phase separation behavior, degradation, and morphology and use as protein-releasing matrices", Macromolecules, 25, 116–22.

[31] Pitt, C.G.; Cha, Y.; Shah, S.S.; Zhu, K.J., (1992). "Blends of PVA and PLGA: control of the permeability and degradability of hydrogels by blending", Controlled Release, 19, 189–200.

[32] Ravivarapu, H. B.; Burton, K.; DeLuca, P. P., (2000). "Polymer and microsphere blending to alter the release of a peptide from PLGA microspheres", European Journal of Pharmaceutics and Biopharmaceutics, 50, 263-270.

[33] Sahli, H.; Tapon Bretaudiere, J.; Fischer, A.M.; Sternberg, C.; Spenlehauer, G.; Verrecchia, T.; Labarre, D., (1997). "Interactions of poly(lactic acid) and poly(lactic acid-co-ethylene oxide) nanoparticles with the plasma factors of the coagulation system", Biomaterials, 18, 281–288.

[34] Stover, T. C.; Kim, Y. S.; Lowe, T. L.; Kester, M., (2008). "Thermoresponsive and biodegradable linear-dendritic nanoparticles for targeted and sustained release of a pro-apoptotic drug", Biomaterials, 29, 359–369.

[35] Suresh, P. K.; Sah, A. K., (2014). "Nanocarriers for ocular delivery for possible benefits in the treatment of anterior uveitis: focus on current paradigms and future directions", Expert Opinion on Drug Delivery, 11, 1747-1768.

[36] Tice, T.R.; Gilley, R.M., (1985). "Preparation of injectable controlled-release microcapsules by solvent-evaporation process", Journal of Control Release, 2, 343 -352.

[37] Venkatraman, S.S.; Jie, P.; Min, F.; Chiang Freddy, B.Y.; Leong-Huat, G., (2005). "Micelle-like nanoparticles of PLA–PEG–PLA triblock copolymer as chemothera-peutic carrier", International Journal of Pharmaceutics, 32, 219–298.

[38] Vonarbourg, A.; Passirani, C.; Saulnier, P.; Benoit, J.P., (2006). "Parameters influencing the stealthiness of colloidal drug delivery systems", Biomaterials, 27:4356–73.

[39] Xie, Z.; Lu, T.; Chen, X.; Lu, C.H.; Zheng. Y.; Jing, X., (2007). "Triblock poly(lactic acid)-b-poly(ethylene glycol)-b-poly(lactic acid)/paclitaxel conjugates: Synthesis, micellization, and cytotoxicity". Applied Polymer Science, 105, 2271–9.

[40] Yao, J.; Ruan, Y.; Zhai, T.; Guan, J.; Tang, G.; Li, H.; Dai, S., (2011). "ABC block copolymer as "smart" pH-responsive carrier for intracellular delivery of hydrophobic drugs", Polymer, 52, 3396-3404.

[41] Zambaux, M.F.; Bonneaux, F.;Gref, R.;Dellacherie, E.; Vigneron C., (1999). "Preparation and characterization of protein C-loaded PLA nanoparticles", Controlled Release, 60, 179–188.

[42] Zhu, G.Z.; Mallery, S.R.; Schwendeman, S. P., (2000). "Stabilization of proteins

encapsulated in injectable poly (lactide-co-glycolide)", Nature Biotechnology, 18, 52–7.

Chapter 5 : Conclusions and Recommendations

5.1 Conclusions

The following findings summarize the major outcomes of this research:

- The use of poly(ester amide)s (PEA)s containing pendant functional groups for preparation of drug delivery NPs was investigated. By using emulsification-evaporation and salting-out methods and running a series of optimization experiments to investigate the effects of varying the surfactant concentration, PEA concentration and the ratio of organic to water phases, it was possible to prepare particles having Z-average diameters of less than 200 nm and reasonable polydispersities by both techniques.

- The pendant functional groups on a PEA could be used for the covalent immobilization of drug molecules. First an alcohol functionalized rhodamine B derivative as a model drug was conjugated via an ester linkage with a coupling efficiency of ~40% prior to nanoparticle preparation. The optimized NP preparation conditions were used to prepare NPs from the PEA-rhodamine B conjugate and also from control NPs in which rhodamine B was physically encapsulated. The covalent conjugate afforded a much slower release than the noncovalent control suggesting that this approach is valuable for the elimination of the burst release effect. The approach was also extended to covalent immobilization of the hydrophilic anti cancer drug floxuridine in NPs. This system also exhibited a high coupling efficiency of 60% for the hydrophilic drug, a small burst release effect of 5%, and small Z-average diameters of less than 200 nm. This initial burst was followed by a slower, sustained release. Overall this work suggests the promise of using PEA NPs for drug delivery applications and in particular the use of PEAs with pendant functional groups for covalent conjugation of drugs. This affords NPs exhibiting slow and sustained drug release for applications where this is required.

- In order to overcome the problem of nonspecific release of drug throughout the body, which can be expected for most NP systems, stimuli responsive NPs were investigated. Drug delivery NPs based on stimuli responsive polymers were prepared using PEtG. PEtG is UV responsive self-immolative polymer that undergoes end-to-

end depolymerization upon UV irradiation. This study investigated the use of an emulsification-evaporation method for the preparation of PEtG/PLA blend NPs with PEtG designed to impart stimuli responsive properties to the NPs, for the release of drug to be triggered.

- The effect of several optimization experiments such as the organic to aqueous ratio, sonication time, and type and concentration of the surfactant on the particle diameter of PLA NPs were investigated. By using the optimized preparation conditions, it was possible to prepare PEtG/PLA blend NPs having Z-average diameters of less than 100 nm and reasonable polydispersities. All of the prepared particles had negative zeta potentials due to remaining cholic acid on the surface of the NPs. The thermal characterization of the polymer blend NPs demonstrated that the two polymers exhibited phase separation as the amorphous regions maintained their original properties, and thus two T_gs were observed. These NPs showed good efficiencies to encapsulate the hydrophobic drug letrazole. The results showed that the burst effect from the NPs depended on the ratio of PLA:PEtG, with more PLA leading to more burst release. Unfortunately, the UV light irradiated NPs exhibited unexpectedly slow release, which occurred at the same rate as release from the non-irradiated NPs. Investigations were performed and the results suggested that even though the PEtG breaks down rapidly under the conditions of the experiment, the drug may remain encapsulated in aggregates formed by the surfactant SC. Additional research will be required to address this issue. NPs based on PEtG might be an appropriate tool for site-specific and time-controlled drug delivery.

5.2 Recommendations

In order to further improve some of the aforementioned shortcomings, the following recommendations are proposed:

- For NPs prepared from PEA-floxuridine conjugates, cell toxicity and cell uptake study should be investigated, followed by detailed *in vivo* studies in animal models.
- Letrazole PEtG interaction requires more investigation using DSC technique that may describe the physical state of the drug and internal structure of the NPs in order to explain the decrease in the burst effect with increase the loading of the dug.

- Using another drug with different solubility may solve the problem of slow release.

- Assuming that the surfactant is forming micelles and that the drug may remain trapped inside these assemblies after degradation of the PEtG, new approaches require investigation. Formulation of nano-micelles through copolymer self-assembly may solve this problem. The hydrophilicity/hydrophobicity can be managed using copolymer self-assembly where the hydrophilic polymers only attach the two ends of the hydrophobic polymer, and the molecular weight can be selected.

Appendixes

A   Appendix A

A.1. DSC thermograms
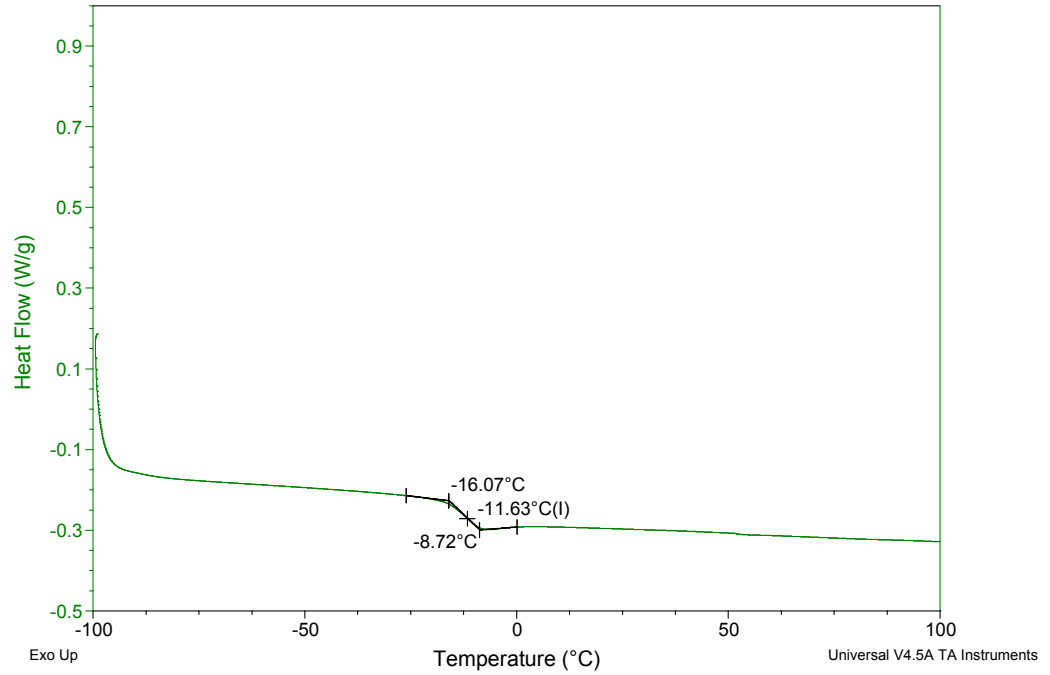
Figure A-1: DSC of PEtG polymer.
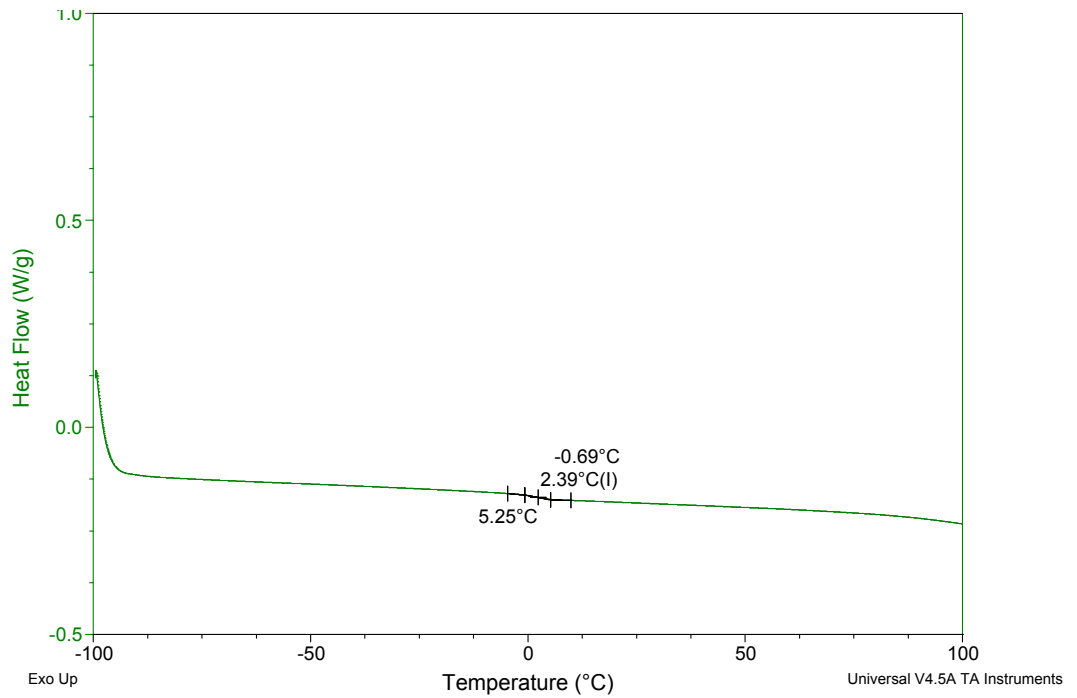
Figure A-2: DSC of PEtG NPs.
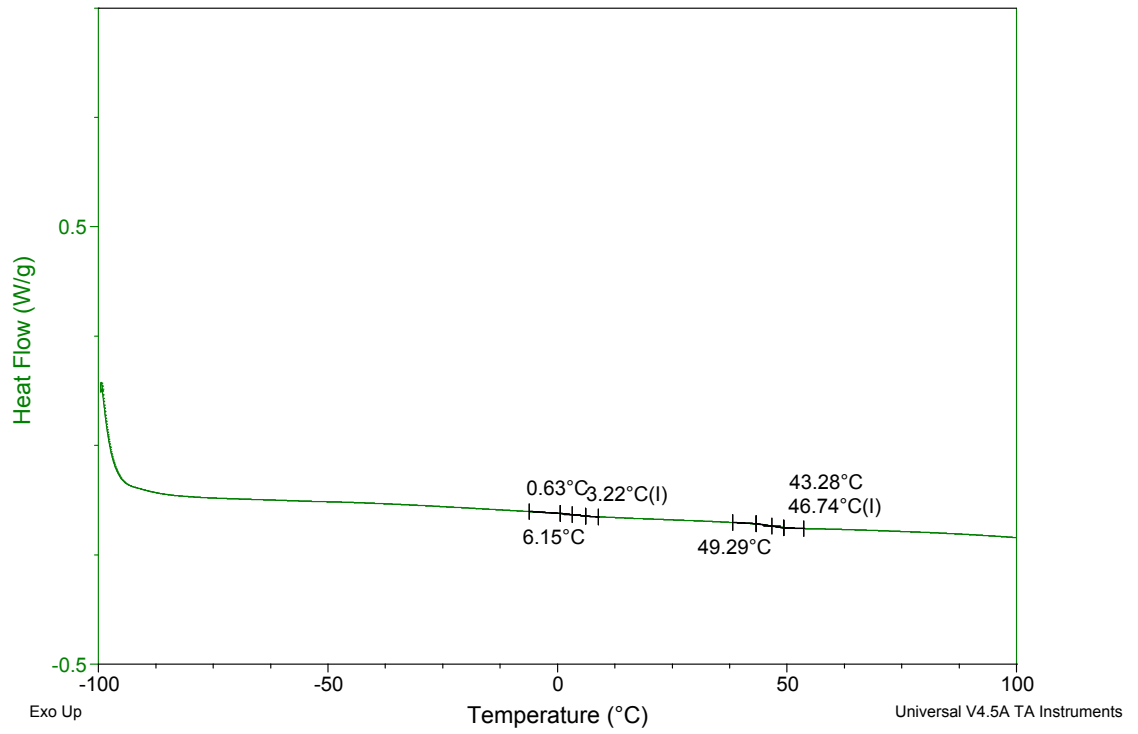
Figure A-3: DSC of 50:50 PEtG:PLA blend NPs.
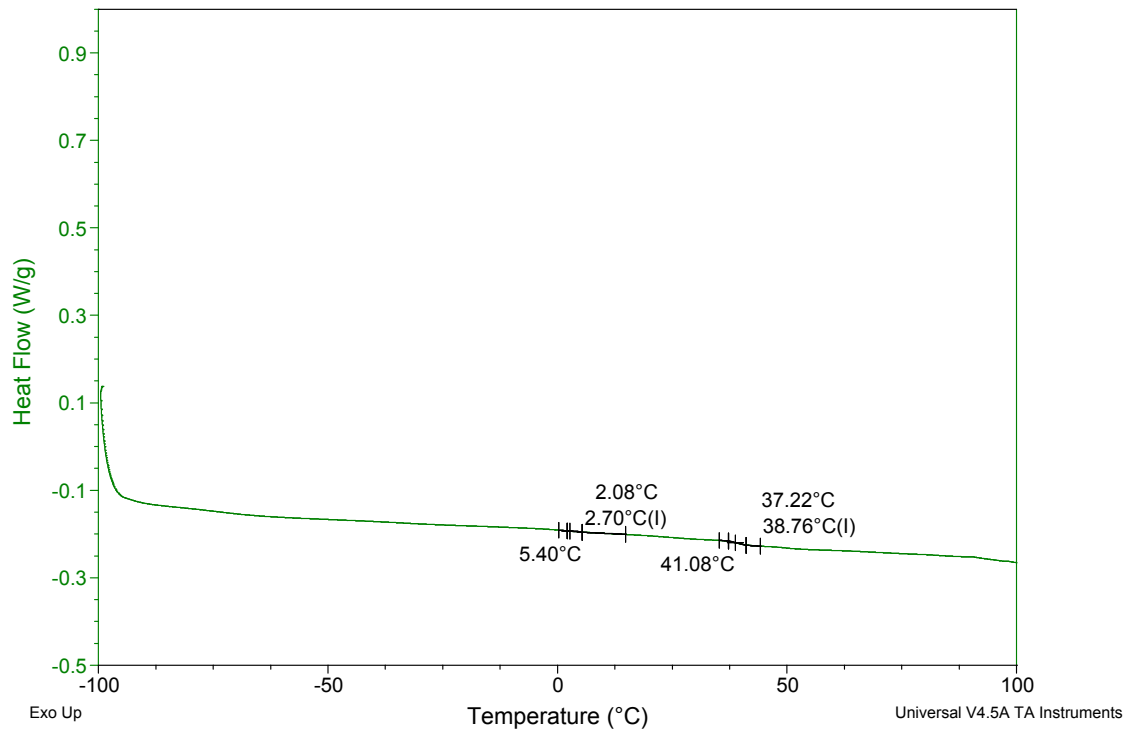
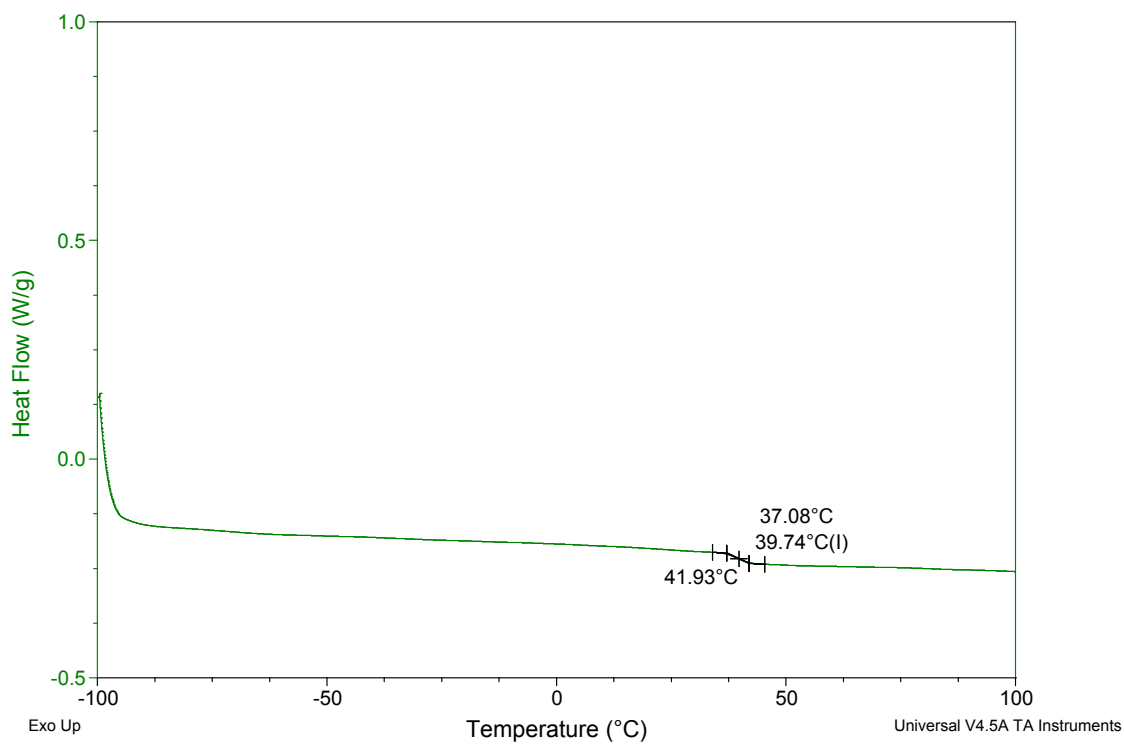**Figure A-4: DSC of 25:75 PEtG:PLA blend NPs.**

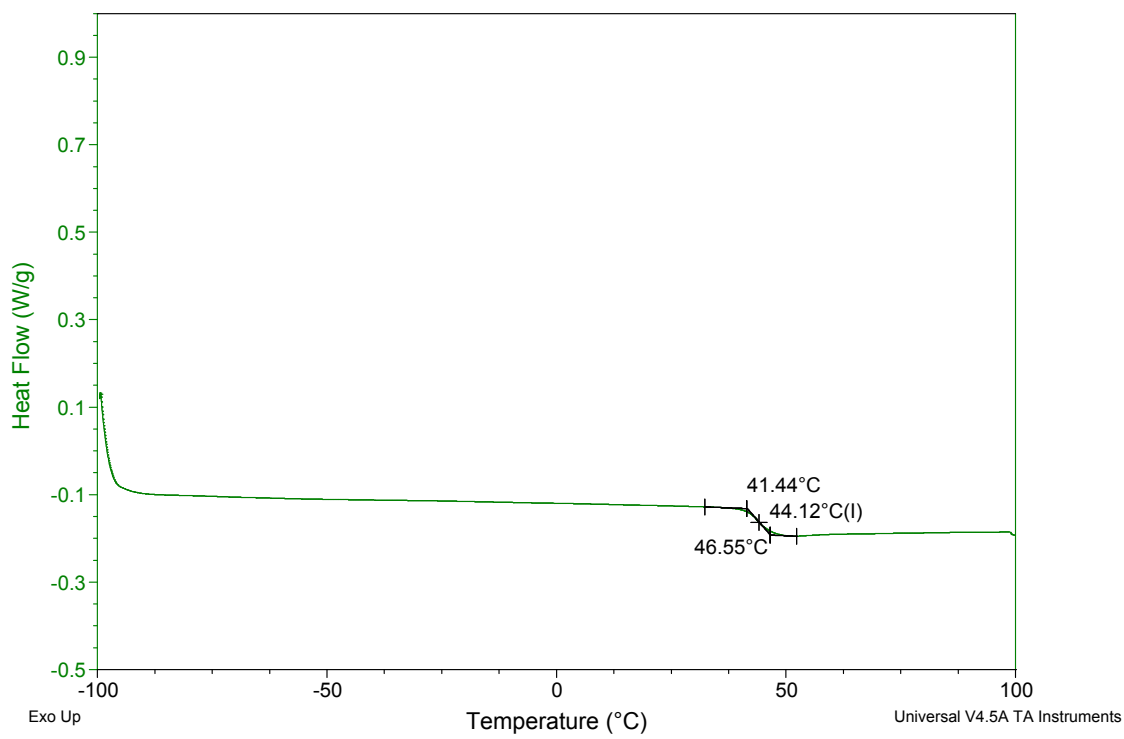**Figure A-5: DSC of PLA NPs.**

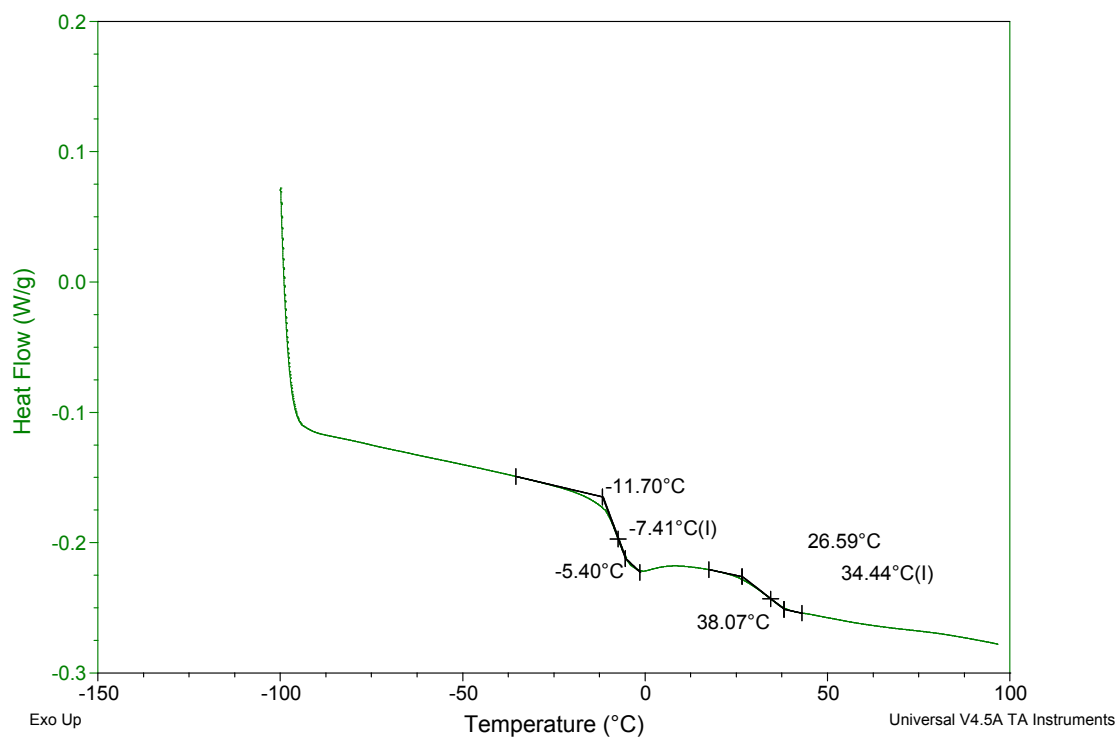
Figure A-6: DSC of PLA polymer.

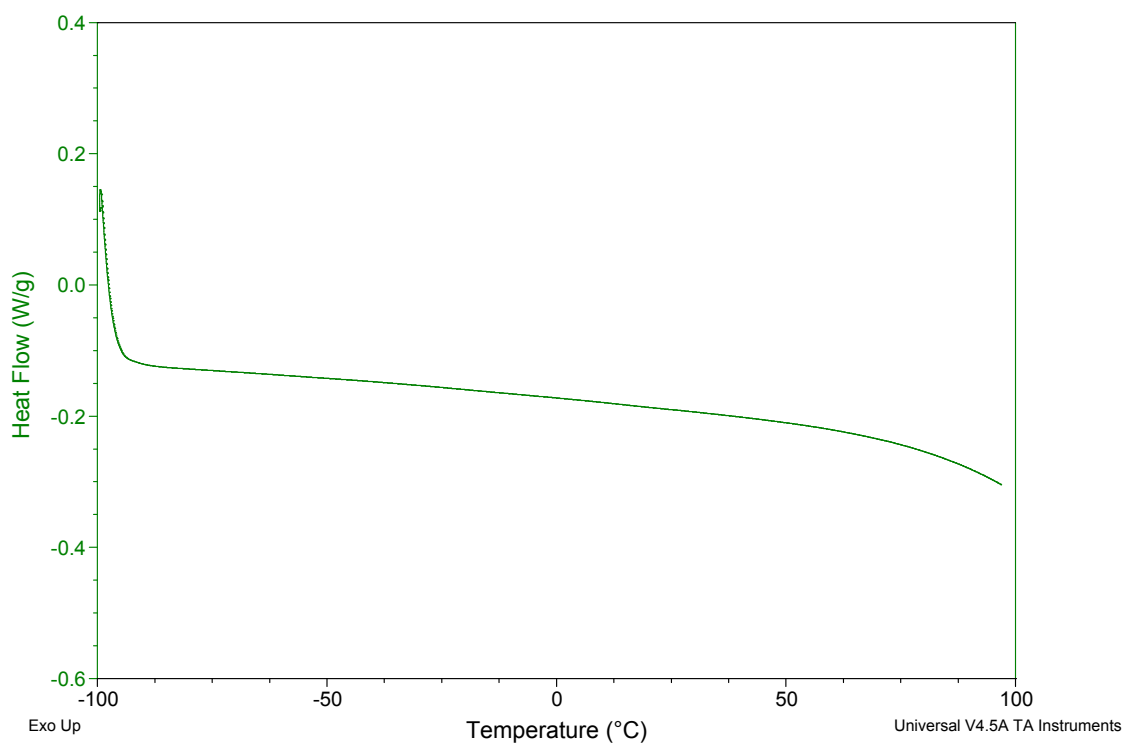**Figure A-7: DSC of PEtG/PLA blend.**

Figure A-8: DSC of sodium cholate.
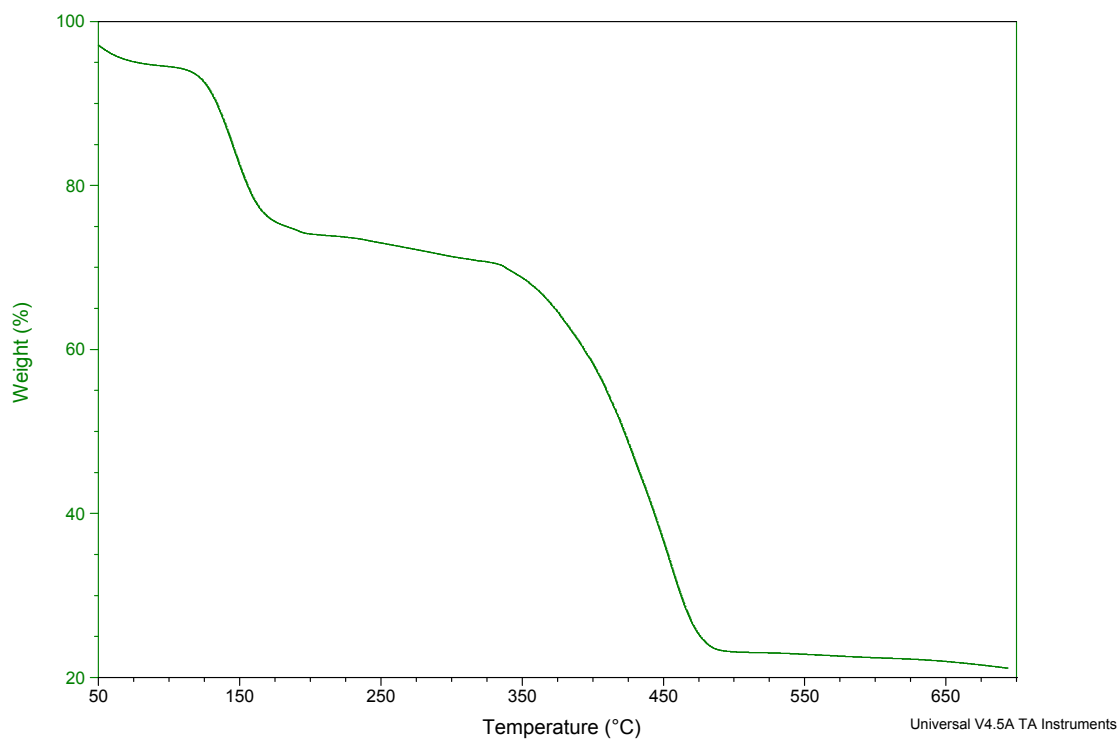
A.2.   TGA curves

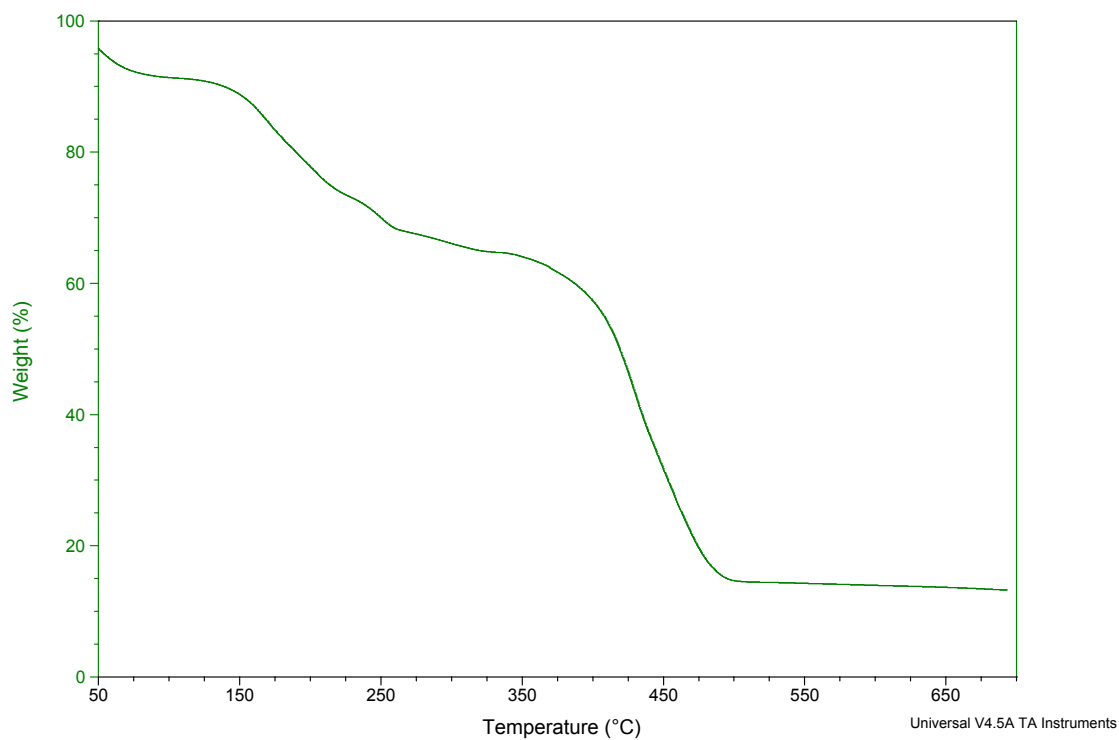

Figure A-9: TGA curve for PEtG NPs.

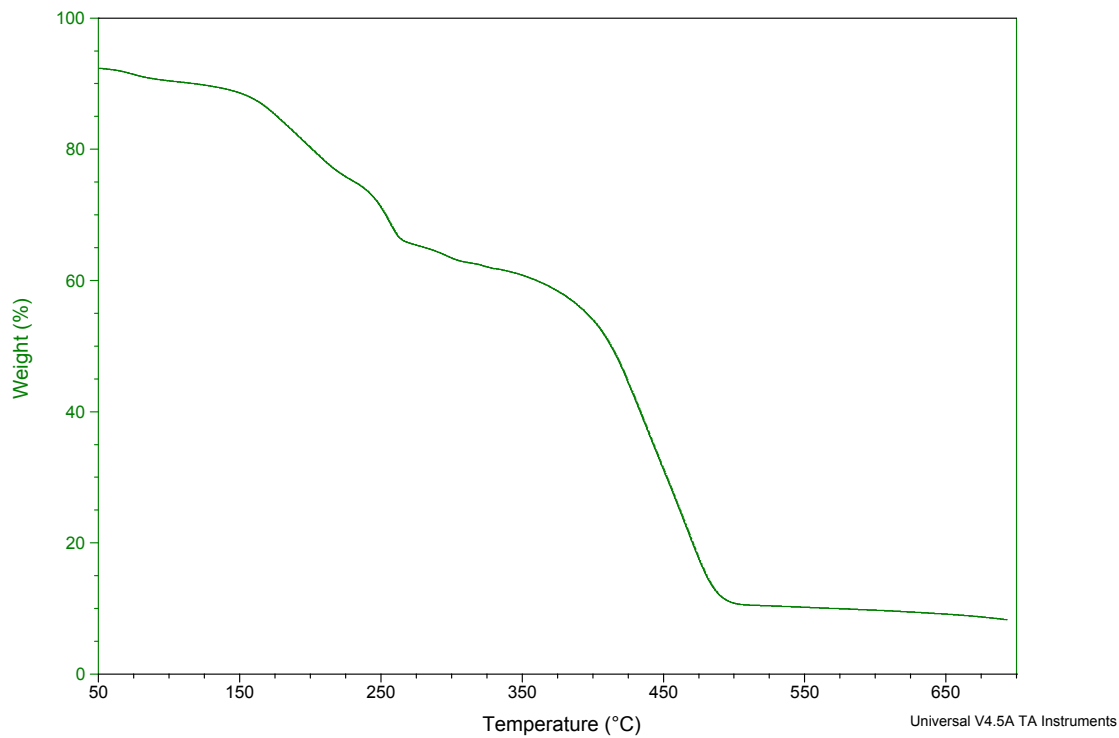**Figure A-10: TGA curve for 75:25 PEtG:PLA blend NPs.**
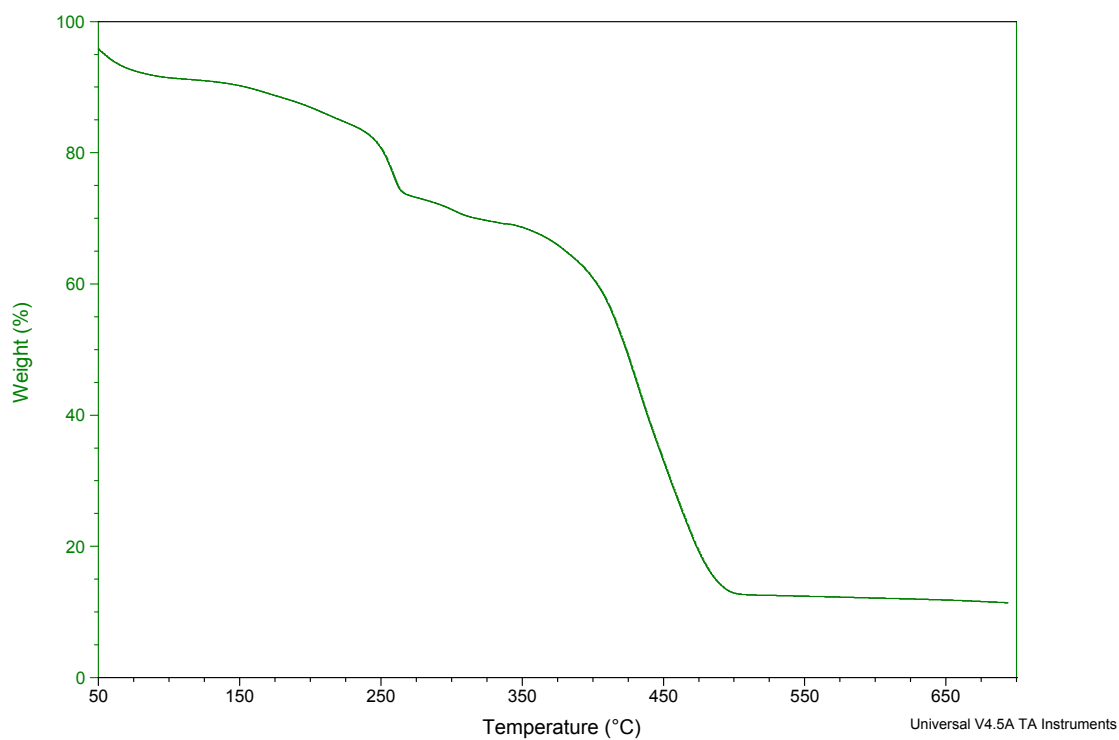
Figure A-11: TGA curve for 50:50 PEtG:PLA blend NPs.

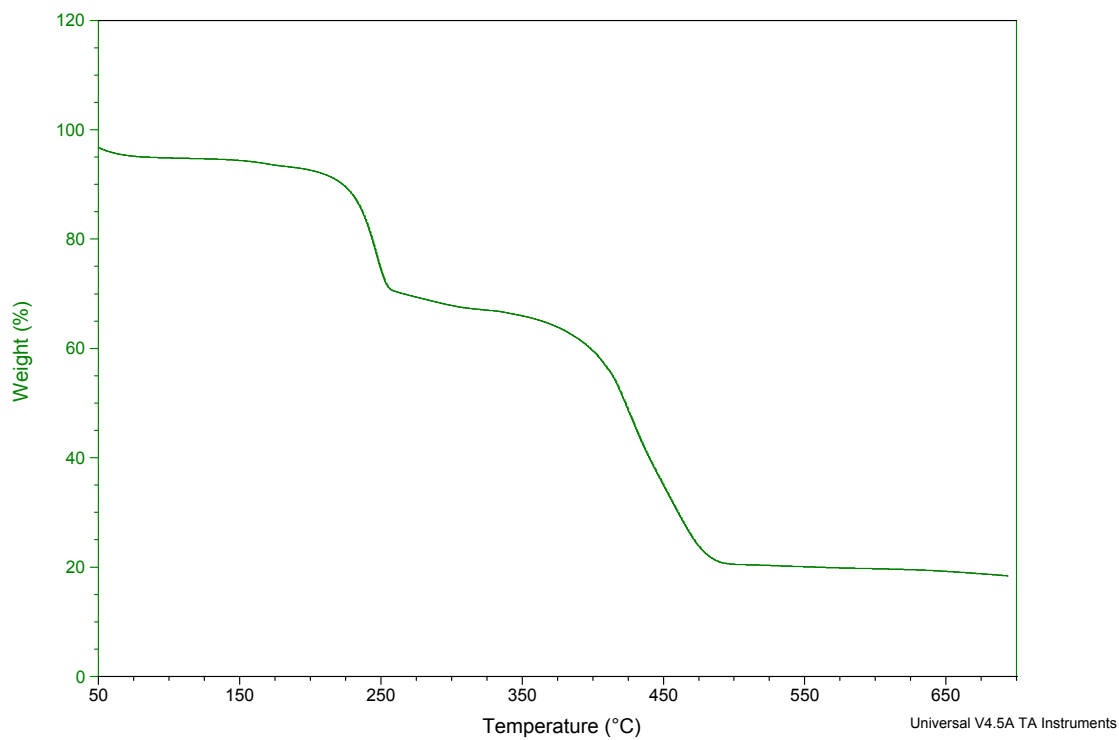**Figure A-12: TGA curve for 25:75 PEtG:PLA blend NPs.**
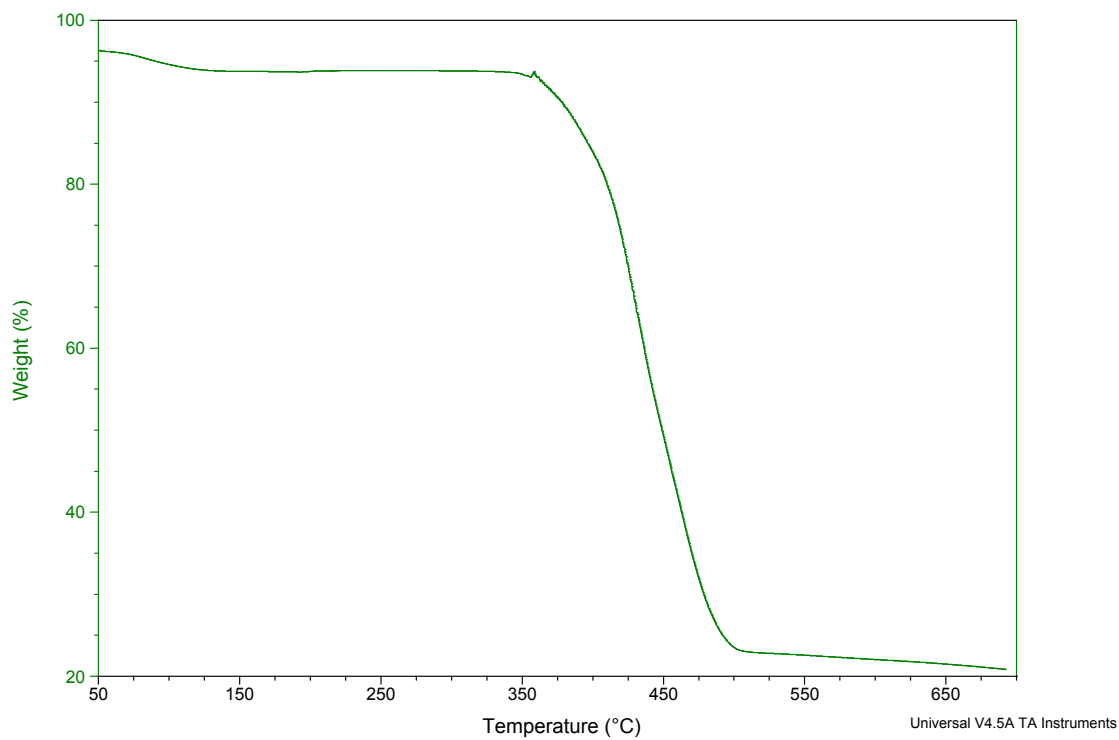
Figure A-13: TGA curve for PLA NPs.

Figure A-14: TGA curve for sodium cholate.
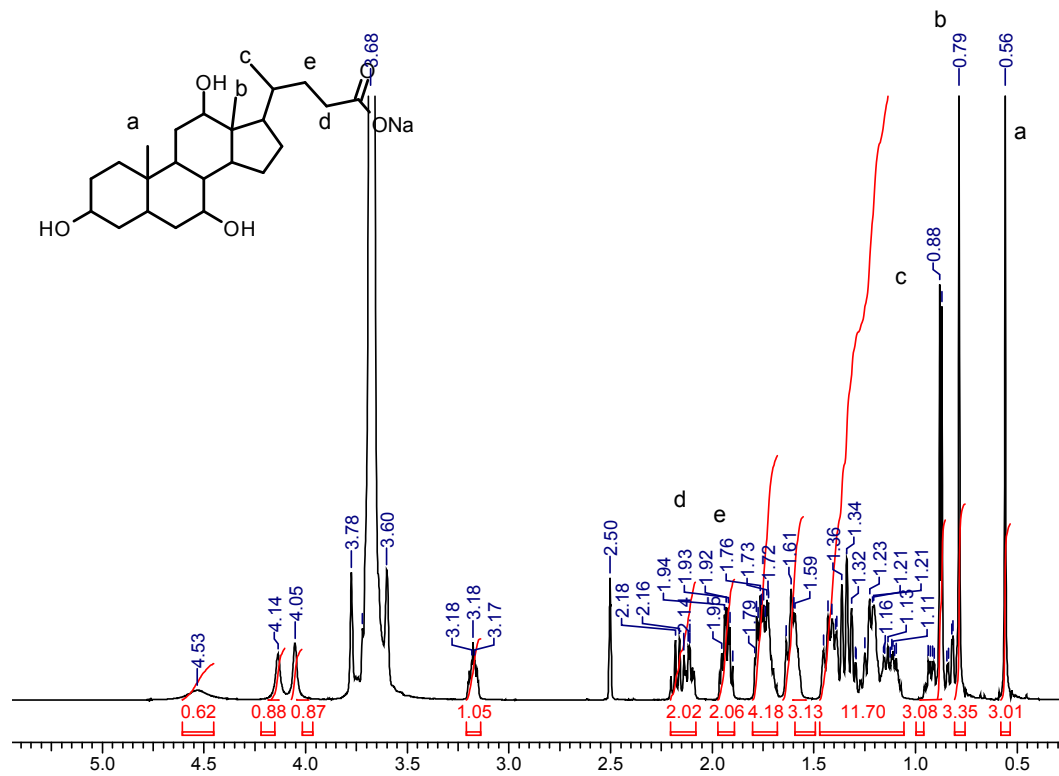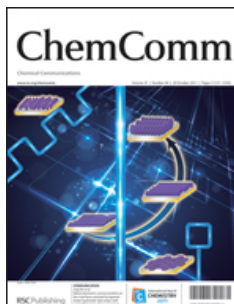
A.3. NMR spectra

Figure A-15: Representative ^{1}HNMR spectrum of Sodium cholate in DMSO-d_6.

Copyright Clearance Center

RightsLink®

Home   Account Info   Help   Live Chat

ChemComm

Chemical Communications

RSC Publishing

Title:	High-density doxorubicin-conjugated polymeric nanoparticles via ring-opening metathesis polymerization
Author:	Paul A. Bertin,DeeDee Smith,SonBinh T. Nguyen
Publication:	Chemical Communications (Cambridge)
Publisher:	Royal Society of Chemistry
Date:	Jul 4, 2005

Copyright © 2005, Royal Society of Chemistry

Logged in as:
Amira Moustafa
Account #:
3000853627

LOGOUT

Order Completed

Thank you very much for your order.

This is a License Agreement between Amira Moustafa ("You") and Royal Society of Chemistry. The license consists of your order details, the terms and conditions provided by Royal Society of Chemistry, and the payment terms and conditions.

Get the printable license.

License Number	3507400814415
License date	Nov 13, 2014
Licensed content publisher	Royal Society of Chemistry
Licensed content publication	Chemical Communications (Cambridge)
Licensed content title	High-density doxorubicin-conjugated polymeric nanoparticles via ring-opening metathesis polymerization
Licensed content author	Paul A. Bertin,DeeDee Smith,SonBinh T. Nguyen
Licensed content date	Jul 4, 2005
Issue number	30
Type of Use	Thesis/Dissertation
Requestor type	non-commercial (non-profit)
Portion	figures/tables/images
Number of figures/tables/images	2
Distribution quantity	5
Format	print and electronic
Will you be translating?	no
Order reference number	None
Title of the thesis/dissertation	Polymeric Nanoparticles for drug release
Expected completion date	Nov 2014
Estimated size	112
Total	0.00 CAD

Copyright Clearance Center
RightsLink®

Home | Account Info | Help | Live Chat

American Association for Cancer Research

Title:	Therapeutic Nanoparticles for Drug Delivery in Cancer
Author:	Kwangjae Cho, Xu Wang, Shuming Nie et al.
Publication:	Clinical Cancer Research
Publisher:	American Association for Cancer Research
Date:	March 1, 2008

Copyright © 2008, American Association for Cancer Research

Logged in as:
Amira Moustafa
Account #:
3000853627

LOGOUT

Order Completed

Thank you very much for your order.

This is a License Agreement between Amira Moustafa ("You") and American Association for Cancer Research ("American Association for Cancer Research"). The license consists of your order details, the terms and conditions provided by American Association for Cancer Research, and the payment terms and conditions.

Get the printable license.

License Number	3507401212490
License date	Nov 13, 2014
Licensed content publisher	American Association for Cancer Research
Licensed content publication	Clinical Cancer Research
Licensed content title	Therapeutic Nanoparticles for Drug Delivery in Cancer
Licensed content author	Kwangjae Cho, Xu Wang, Shuming Nie et al.
Licensed content date	March 1, 2008
Volume number	14
Issue number	5
Type of Use	Thesis/Dissertation
Requestor type	non-commercial (non-profit)
Format	print and electronic
Portion	figures/tables/illustrations
Number of figures/tables/illustrations	1
Will you be translating?	no
Circulation	5
Territory of distribution	North America
Title of your thesis / dissertation	Polymeric Nanoparticles for drug release
Expected completion date	Nov 2014
Estimated size (number of pages)	112
Total	0.00 CAD

ORDER MORE... | CLOSE WINDOW

Copyright Clearance Center

RightsLink®

Home | Account Info | Help | Live Chat

ACS Publications
Most Trusted. Most Cited. Most Read.

Title: A New Design for Light-Breakable Polymer Micelles

Author: Jinqiang Jiang, Xia Tong, Yue Zhao

Publication: Journal of the American Chemical Society

Publisher: American Chemical Society

Date: Jun 1, 2005

Copyright © 2005, American Chemical Society

Logged in as:
Amira Moustafa
Account #:
3000853627

LOGOUT

BACK | CLOSE WINDOW

Copyright Clearance Center

RightsLink®

Home | Account Info | Help | Live Chat

ACS Publications Most Trusted. Most Cited. Most Read.

Title:	Redox-Sensitive Disassembly of Amphiphilic Copolymer Based Micelles
Author:	Ja-Hyoung Ryu, Raghunath Roy, Judy Ventura, et al
Publication:	Langmuir
Publisher:	American Chemical Society
Date:	May 1, 2010
	Copyright © 2010, American Chemical Society

Logged in as:
Amira Moustafa
Account #:
3000853627

LOGOUT

PERMISSION/LICENSE IS GRANTED FOR YOUR ORDER AT NO CHARGE

This type of permission/license, instead of the standard Terms & Conditions, is sent to you because no fee is being charged for your order. Please note the following:

- Permission is granted for your request in both print and electronic formats, and translations.
- If figures and/or tables were requested, they may be adapted or used in part.
- Please print this page for your records and send a copy of it to your publisher/graduate school.
- Appropriate credit for the requested material should be given as follows: "Reprinted (adapted) with permission from (COMPLETE REFERENCE CITATION). Copyright (YEAR) American Chemical Society." Insert appropriate information in place of the capitalized words.
- One-time permission is granted only for the use specified in your request. No additional uses are granted (such as derivative works or other editions). For any other uses, please submit a new request.

If credit is given to another source for the material you requested, permission must be obtained from that source.

BACK | CLOSE WINDOW

**ELSEVIER LICENSE
TERMS AND CONDITIONS**

Nov 02, 2014

This is a License Agreement between Amira Moustafa ("You") and Elsevier ("Elsevier") provided by Copyright Clearance Center ("CCC"). The license consists of your order details, the terms and conditions provided by Elsevier, and the payment terms and conditions.

All payments must be made in full to CCC. For payment instructions, please see information listed at the bottom of this form.

Supplier	Elsevier Limited The Boulevard,Langford Lane Kidlington,Oxford,OX5 1GB,UK
Registered Company Number	1982084
Customer name	Amira Moustafa
Customer address	
License number	3500910838653
License date	Nov 02, 2014
Licensed content publisher	Elsevier
Licensed content publication	Biomaterials
Licensed content title	Thermoresponsive and biodegradable linear-dendritic nanoparticles for targeted and sustained release of a pro-apoptotic drug
Licensed content author	Thomas C. Stover,Young Shin Kim,Tao L. Lowe,Mark Kester
Licensed content date	January 2008
Licensed content volume number	29
Licensed content issue number	3
Number of pages	11
Start Page	359
End Page	369
Type of Use	reuse in a thesis/dissertation
Intended publisher of new work	other
Portion	figures/tables/illustrations

Number of figures/tables/illustrations	3
Format	both print and electronic
Are you the author of this Elsevier article?	No
Will you be translating?	No
Title of your thesis/dissertation	Polymeric Nanoparticles for drug release
Expected completion date	Nov 2014
Estimated size (number of pages)	112
Elsevier VAT number	GB 494 6272 12
Permissions price	0.00 CAD
VAT/Local Sales Tax	0.00 CAD / 0.00 GBP
Total	0.00 CAD

Terms and Conditions

INTRODUCTION

1. The publisher for this copyrighted material is Elsevier. By clicking "accept" in connection with completing this licensing transaction, you agree that the following terms and conditions apply to this transaction (along with the Billing and Payment terms and conditions established by Copyright Clearance Center, Inc. ("CCC"), at the time that you opened your Rightslink account and that are available at any time at http://myaccount.copyright.com).

GENERAL TERMS

2. Elsevier hereby grants you permission to reproduce the aforementioned material subject to the terms and conditions indicated.
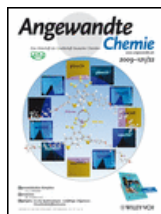
3. Acknowledgement: If any part of the material to be used (for example, figures) has appeared in our publication with credit or acknowledgement to another source, permission must also be sought from that source. If such permission is not obtained then that material may not be included in your publication/copies. Suitable acknowledgement to the source must be made, either as a footnote or in a reference list at the end of your publication, as follows:

"Reprinted from Publication title, Vol /edition number, Author(s), Title of article / title of chapter, Pages No., Copyright (Year), with permission from Elsevier [OR APPLICABLE SOCIETY COPYRIGHT OWNER]." Also Lancet special credit - "Reprinted from The Lancet, Vol. number, Author(s), Title of article, Pages No., Copyright (Year), with permission from Elsevier."

4. Reproduction of this material is confined to the purpose and/or media for which

Copyright Clearance Center   **RightsLink®**   Home   Account Info   Help   Live Chat

Title:	Paclitaxel-Initiated, Controlled Polymerization of Lactide for the Formulation of Polymeric Nanoparticulate Delivery Vehicles
Author:	Rong Tong, Jianjun Cheng
Publication:	Angewandte Chemie
Publisher:	John Wiley and Sons
Date:	May 19, 2008

Copyright © 2008 WILEY-VCH Verlag GmbH & Co. KGaA, Weinheim

Order Completed

Thank you very much for your order.

This is a License Agreement between Amira Moustafa ("You") and John Wiley and Sons ("John Wiley and Sons"). The license consists of your order details, the terms and conditions provided by John Wiley and Sons, and the payment terms and conditions.

Get the printable license.

License Number	3507410007982
License date	Nov 13, 2014
Licensed content publisher	John Wiley and Sons
Licensed content publication	Angewandte Chemie
Licensed content title	Paclitaxel-Initiated, Controlled Polymerization of Lactide for the Formulation of Polymeric Nanoparticulate Delivery Vehicles
Licensed copyright line	Copyright © 2008 WILEY-VCH Verlag GmbH & Co. KGaA, Weinheim
Licensed content author	Rong Tong, Jianjun Cheng
Licensed content date	May 19, 2008
Start page	4908
End page	4912
Type of use	Dissertation/Thesis
Requestor type	University/Academic
Format	Print and electronic
Portion	Figure/table
Number of figures/tables	2
Original Wiley figure/table number(s)	Figure 2, figure 3
Will you be translating?	No
Title of your thesis / dissertation	Polymeric Nanoparticles for drug release
Expected completion date	Nov 2014
Expected size (number of pages)	112
Total	0.00 CAD

Copyright Clearance Center **RightsLink®**   Home | Account Info | Help | Live Chat

ACS Publications
Most Trusted. Most Cited. Most Read.

Title: Traceable Multifunctional Micellar Nanocarriers for Cancer-Targeted Co-delivery of MDR-1 siRNA and Doxorubicin

Author: Xiao-Bing Xiong, Afsaneh Lavasanifar

Publication: ACS Nano

Publisher: American Chemical Society

Date: Jun 1, 2011

Copyright © 2011, American Chemical Society

Logged in as:
Amira Moustafa
Account #:
3000853627

LOGOUT

PERMISSION/LICENSE IS GRANTED FOR YOUR ORDER AT NO CHARGE

This type of permission/license, instead of the standard Terms & Conditions, is sent to you because no fee is being charged for your order. Please note the following:

- Permission is granted for your request in both print and electronic formats, and translations.
- If figures and/or tables were requested, they may be adapted or used in part.
- Please print this page for your records and send a copy of it to your publisher/graduate school.
- Appropriate credit for the requested material should be given as follows: "Reprinted (adapted) with permission from (COMPLETE REFERENCE CITATION). Copyright (YEAR) American Chemical Society." Insert appropriate information in place of the capitalized words.
- One-time permission is granted only for the use specified in your request. No additional uses are granted (such as derivative works or other editions). For any other uses, please submit a new request.

If credit is given to another source for the material you requested, permission must be obtained from that source.

BACK   CLOSE WINDOW

**ELSEVIER LICENSE
TERMS AND CONDITIONS**

Nov 02, 2014

This is a License Agreement between Amira Moustafa ("You") and Elsevier ("Elsevier") provided by Copyright Clearance Center ("CCC"). The license consists of your order details, the terms and conditions provided by Elsevier, and the payment terms and conditions.

All payments must be made in full to CCC. For payment instructions, please see information listed at the bottom of this form.

Supplier	Elsevier Limited The Boulevard,Langford Lane Kidlington,Oxford,OX5 1GB,UK
Registered Company Number	1982084
Customer name	Amira Moustafa
Customer address	
License number	3500910318916
License date	Nov 02, 2014
Licensed content publisher	Elsevier
Licensed content publication	Polymer
Licensed content title	ABC block copolymer as "smart" pH-responsive carrier for intracellular delivery of hydrophobic drugs
Licensed content author	Jia Yao,Yuelei Ruan,Tao Zhai,Jun Guan,Guping Tang,Haoran Li,Sheng Dai
Licensed content date	7 July 2011
Licensed content volume number	52
Licensed content issue number	15
Number of pages	9
Start Page	3396
End Page	3404
Type of Use	reuse in a thesis/dissertation
Portion	figures/tables/illustrations
Number of	3

figures/tables/illustrations	
Format	both print and electronic
Are you the author of this Elsevier article?	No
Will you be translating?	No
Title of your thesis/dissertation	Polymeric Nanoparticles for drug release
Expected completion date	Nov 2014
Estimated size (number of pages)	112
Elsevier VAT number	GB 494 6272 12
Permissions price	0.00 CAD
VAT/Local Sales Tax	0.00 CAD / 0.00 GBP
Total	0.00 CAD

Terms and Conditions

INTRODUCTION

1. The publisher for this copyrighted material is Elsevier. By clicking "accept" in connection with completing this licensing transaction, you agree that the following terms and conditions apply to this transaction (along with the Billing and Payment terms and conditions established by Copyright Clearance Center, Inc. ("CCC"), at the time that you opened your Rightslink account and that are available at any time at http://myaccount.copyright.com).

GENERAL TERMS

2. Elsevier hereby grants you permission to reproduce the aforementioned material subject to the terms and conditions indicated.

3. Acknowledgement: If any part of the material to be used (for example, figures) has appeared in our publication with credit or acknowledgement to another source, permission must also be sought from that source. If such permission is not obtained then that material may not be included in your publication/copies. Suitable acknowledgement to the source must be made, either as a footnote or in a reference list at the end of your publication, as follows:

"Reprinted from Publication title, Vol /edition number, Author(s), Title of article / title of chapter, Pages No., Copyright (Year), with permission from Elsevier [OR APPLICABLE SOCIETY COPYRIGHT OWNER]." Also Lancet special credit - "Reprinted from The Lancet, Vol. number, Author(s), Title of article, Pages No., Copyright (Year), with permission from Elsevier."

4. Reproduction of this material is confined to the purpose and/or media for which permission is hereby given.

RightsLink®

Copyright Clearance Center

Home | Account Info | Help | Live Chat

ACS Publications
Most Trusted. Most Cited. Most Read.

Title: Polyglyoxylates: A Versatile Class of Triggerable Self-Immolative Polymers from Readily Accessible Monomers

Author: Bo Fan, John F. Trant, Andrew D. Wong, et al

Publication: Journal of the American Chemical Society

Publisher: American Chemical Society

Date: Jul 1, 2014

Copyright © 2014, American Chemical Society

Logged in as:
Amira Moustafa
Account #:
3000853627

LOGOUT

PERMISSION/LICENSE IS GRANTED FOR YOUR ORDER AT NO CHARGE

BACK | CLOSE WINDOW

Curriculum Vitae

Name: Amira M. Moustafa

Post-secondary Education and Degrees:	Masters of Science in Biochemical/Biomaterials Engineering Western University, London, Canada	**Jan 2012 – Dec 2014**
	Bachelor of Science in Pharmaceutical Sciences Mansoura University, Mansoura, Egypt.	**Sep 2000-May 2005**
Honours and Awards:	Western Graduate Research Scholarship Engineering Western University	**2012-2014**
	Annual undergraduate scholarship for top students Mansoura University	**2000-2005**
Related Work Experience	Research Assistant, Biochemical/Biomaterials Engineering Western University, London, Canada	**2012-2014**
	Professional pharmacist (Full-Time) Nephrology and Urology Center, Mansoura University, Mansoura, Egypt	**2006-2008**
	Pharmacist (Part-Time) Eltarshopy Inc., Mansoura University, Mansoura, Egypt	**2006-2008**

Publications:

Moustafa, A.; Gillies, E.R. "Synthesis, optimization, characterization and drug release profile of Floxuridine covalently attached nanoparticles using poly(ester amide)s, under preparation